

Assessing the potential of rAAV9 systemic gene therapy for GM2 gangliosidoses using a Sandhoff mouse model

By

Naderah Altaieb

A thesis submitted to the Faculty of Graduate Studies in partial
fulfilment of the requirements for the degree of
Master of Science

Department of Biochemistry and Medical Genetics
College of Medicine
Faculty of Health Science
University of Manitoba
Winnipeg, Manitoba

01/ 2015

© Copyright

2015, Altaieb

Abstract

The infantile GM2 gangliosidoses are severe neurodegenerative disorders, caused by a defect in the β -hexosaminidase system. They are characterized by lysosomal accumulation of the substrate, GM2 ganglioside, which results in severe neuronal damage and death in the early years of life. Sandhoff mice deficient in both major hexosaminidase isozymes, Hex A and Hex B, mimic the disease severity in the human condition including the motor deterioration, histopathological findings, and premature death. To investigate the utility of systemic adeno-associated virus 9 (AAV9)-based gene delivery in treating GM2 gangliosidoses, we evaluated the therapeutic outcome of a single intravenous injection of recombinant AAV9 encoding the complementing *Hexb* gene in a Sandhoff mouse model. We showed prolonged survival, preserved motor function, and reduced GM2 ganglioside accumulation as well as inflammation when systemic AAV9 therapy was administered to 1-2 days old mice. However, the formation of liver or lung tumours accompanied the positive therapeutic effect.

Acknowledgments

Mouse monitoring and follow-up procedures including genotyping, vector injection, open field testing, serum sample collection, monitoring, euthanization and organ harvesting were carried out by Jagdeep Walia, Christa Kruck, Biswajit Chowdhury, Henry Heng, Barbara Triggs-Raine and Richard Hemming. Vector construction was done by Christa Kruck. Alexander Bello from Microbiology National Lab in Winnipeg carried out the PCR for the determining vector genome copy number in brain and liver, and Matthew C. LaFave and Gaurav Kumar Varshney at NIH performed the analysis of AAV9 insertion sites.

Dedication

To Ali, Hesham, and Hussain.

To my two sisters, Bayan and Naba, without whom I wouldn't reach here.

To my beautiful sister in law, Omnia, because you care.

To my big family, you don't have any idea how much I want to replace everyone of you.

To all stubborn girls, way to go.

To every woman and child, I only have hopes.

When your dreams get you lost, remember how lucky you are to have dreams.

Contents

Preface

Contents	v
List of Tables	viii
List of Figures	ix
List of Symbols	xi
List of Appendices.....	xiv

1	Introduction	1
1.1	The lysosome	2
1.2	Lysosomal Storage Diseases (LSDs)	5
1.3	GM2 Gangliosidoses	8
1.3.1	Historical view	8
1.4	The β -hexosaminidase system	13
1.5	Classification of GM2 gangliosidoses	18
1.6	Molecular genetics and epidemiology of GM2 gangliosidoses	21
1.6.1	Mutations in the α -subunit gene	22
1.6.2	Mutations in the β -subunit gene	24
1.6.3	Mutations in the GM2A activator gene	24

1.7	Mouse models of GM2 gangliosidoses	25
1.8	Treatment approaches	27
1.8.1	Cross correction phenomena of lysosomal enzymes	28
1.8.2	Therapeutic strategies	28
1.9	Gene therapy	33
1.9.1	Definition	34
1.9.2	Adeno-associated viruses AAVs	38
1.9.2.1	Neutralizing antibodies	40
2	Hypothesis	43
2.1	Hypothesis	44
2.2	Rationale	44
2.3	Experimental design	44
3	Materials and Methods	47
3.1	Experimental animals	48
3.2	Analysis of motor function	49
3.3	Construction of rAAV2/9 viral vectors	49
3.4	Intravenous injection of rAAV9	50
3.5	Tissue and serum processing	50
3.6	Determination of vg number	51
3.7	β -Hexosaminidase assay	51
3.8	Protein Assay	52
3.9	Ganglioside analysis	53
3.10	Histology and microscopy	53
3.11	Semi-quantitative histology scoring	54

3.12	Analysis of AAV9 insertion sites.....	54
3.13	Statistical analyses.....	56
4	Results	57
4.1	Impact of AAV9-HexB on survival	58
4.2	Impact on motor activity of SD mice	61
4.3	Effect of AAV9-HexB treatment on GM2 ganglioside storage	66
4.4	β -Hexosaminidase analyses	72
4.5	Inflammation in the brains of AAV9-HexB treated mice	78
4.6	Copy number in the brain and liver of rAAV9 treated mice	80
4.7	Tumour pathology in rAAV9 treated mice	82
5	Supplementary	88
5.1	Statistical analysis.....	89
6	Discussion and future directions	92
6.1	Discussion.....	93
6.2	Future directions	99
6.2.1	Eliminating obstacles.....	99
6.2.2	Timing of intervention.....	101
6.2.3	Transduction and expression efficiency.....	103
6.2.4	Potential risk	106

List of Tables

Table 1- The GM2 ganglioside and the hexosaminidase system.....	14
Table 2- Experimental design.....	46
Table 3- Insertion sites with highest confidant.	86
Table 4- Statistical comparisons of control groups that are merged within figures	89
Table 5- Statistical comparisons of vector genome copy number in male vs. female.	91

List of Figures

Figure 1- GM2 ganglioside	12
Figure 2- GM2 ganglioside degradation pathways and genetic disorders	17
Figure 3- Gene therapy	35
Figure 4- Adeno-associated virus.....	39
Figure 5- Survival of rAAV9-injected mice.	60
Figure 6- Evaluation of motor cortex function	63
Figure 7- Evaluation of motor coordination	64
Figure 8- Evaluation of muscle strength	65
Figure 9- Histological assessment of GM2 ganglioside accumulation.....	68
Figure 10- Semi-quantitative analysis of cellular vacuolization	69
Figure 11- HPTLC analysis of ganglioside content.	70
Figure 12- Densitometry-based quantification of GM2 ganglioside in the brain.....	71
Figure 13- Serum β -hexosaminidase enzyme activity	74
Figure 14- β -hexosaminidase activity levels in control groups.....	75
Figure 15- 4-MUG brain β -hexosaminidase enzyme activity.....	76

Figure 16- 4-MUGS brain β -hexosaminidase enzyme activity.....	77
Figure 17- Brain inflammation	79
Figure 18- AAV9 vg copy number	81
Figure 19- Histological analysis of tumor tissues.....	84
Figure 20- AAV9 Integration Sites.....	85

List of Symbols

AAV9, adeno-associated virus serotype 9

BBB, blood-brain barrier

BMT, bone marrow transplant

Cb, cerebellum

CD63, cluster of differentiation 63

Cer, ceramide

CI-M6PR, cation-independent M6P receptor

CNS, central nervous system

Cx, cerebral cortex

ER, endoplasmic reticulum

ERAD, ER-associated degradation pathway

GA2, a neutrally charged glycosphingolipid

Gal, galactose

GalCer, galactosylceramide

GalNAc, N-acetyl-galactosamine

Glc, glucose

GlcCer, glucosylceramide

GM2, monosialo-ganglioside 2

GSL, glycosphingolipid

HEK, human embryonic kidney

Hex A, β -hexosaminidase A

Hex B, β -hexosaminidase B

Hex, β -hexosaminidase

Hip, hippocampus

HSCT, hematopoietic stem cell therapy

Hy, hypothalamus

Kb, kilobases

LAMP, lysosome-associated-membrane protein

LIMP2, lysosomal integral membrane protein 2

LSD lysosomal storage disease

LSD, lysosomal storage diseases

M6P, mannose-6-phosphate

M6PR, M6P receptors

Md, medulla

Mid, midbrain

ML, mucopolipidosis

MPSII, mucopolysaccharidosis II

MR, mannose receptor

mTOR, mammalian target of rapamycin

mTORC1, mammalian target of rapamycin complex 1

MUG, 4-methylumbelliferyl-2-acetamido-2-deoxy- β -D-glucopyranoside

MUGS, 4-methylumbelliferyl-6-sulfo-2-acetamido-2-deoxy- β -D-glucopyranoside

OA, olfactory bulb

OMIM, online Mendelian inheritance in man

Po, Pons

SA, sialic acid

SD, Sandhoff disease

Sep, septum

TB, toluidine blue

TFEB, transcription factor that recognizes the enhancer box

Th, thalamus

vg, vector genomes

wks, weeks

List of Appendices

Supplementary	88
5.1 Statistical analysis	89

Introduction

1.1 The lysosome

The lysosome is a membrane-bound compartment found within eukaryotic cells. Initially considered a simple digestive sack, the lysosome is now recognized as a cellular organelle that plays a crucial role in maintaining cellular homeostasis. It is involved in many cellular processes, including the degradation of intra- and extracellular material, cellular membrane repair, cholesterol homeostasis, energy production and cell death; all of this occurs in a dynamic adaptive and interactive process with the cellular environment^{1,2}.

Lysosomes appear as dense bodies that vary in shape and size^{3,4}, and are mostly seen in the preinuclear area of the cytosol⁵. The catabolic activity of lysosomes is owed to the presence of approximately 60 hydrolases in its acidic lumen, including nucleases, proteases, glycosidases, phosphatases, sulfatases, and lipases⁶. They allow the lysosome to hydrolyze a vast range of substrates. Molecules reach the lysosome after endocytosis via the endosome-lysosome pathway^{7,8}, or after autophagy via lysosomal invagination, chaperone-mediated internalization, or autophagosome formation⁹⁻¹¹. The pH of the lysosome lumen is maintained at 4.6–5.0 by proton-pumping vacuolar ATPases¹² that are separated from the rest of the cell by a single 7-10 nm protein-rich cholesterol-poor phospholipid-bilayer⁴. This bilayer contains about 215 lysosomal membrane proteins membrane-associated proteins among which lysosome-associated membrane proteins LAMP-1 and-2, lysosomal integral membrane protein LIMP-2, and CD63 are the most

1.1 The lysosome

abundant^{4,13}. Lysosomal membrane proteins are heavily glycosylated at their luminal domains, forming a glycocalyx layer that protects the lysosomal membrane from being degraded by the aggressive luminal contents. Further, they form a functional and regulatory part of the sorting, digesting, secreting and signaling components of the lysosome⁴.

When acid hydrolases and lysosomal membrane proteins are newly synthesized, they are directed to the lysosome by several pathways¹⁴. The most recognized pathway for targeting soluble hydrolases is the mannose-6-phosphate acquired in the cis-Golgi^{14,15}. Lysosomal membrane proteins require phosphorylation and lipid modifications, as regulatory signals, in addition to dileucine and tyrosine-based motifs that act as sorting signals in their cytosolic domains¹⁶.

Cells strictly rely on the lysosome for the turnover of cellular components through autophagy, a process that would accelerate from its basal level under a range of cellular stress inducing conditions, e.g. starvation and infection, allowing the generation of new cellular components and ATP from degrading oxidized lipids, aggregated protein, damaged organelles and pathogens^{17,18}. The fate of the degraded molecules is decided based on the cell nutrition state, energy and activity.

1.1 The lysosome

The lysosome is involved in cellular exocytosis. Controlled by the intracellular Ca^{+2} concentration¹⁹, the lysosomal membrane fuses with the plasma membrane, which allows the lysosome to secrete its content into the extracellular matrix, and mediates membrane repair²⁰⁻²³, pathogen clearance by immune response²⁴⁻²⁷, coagulation process²⁸, pigmentation²⁹, bone resorption, the release of spermatozoa during fertilization³⁰, and cell signaling^{31,32}.

Lysosomes also mediate cellular apoptosis through many pathways, most notably is the release of its hydrolase content -practically cathepsins, while rupture of lysosome induces necrosis^{1,33}.

Lysosome biogenesis and activity are regulated by the interaction between the coordinated lysosomal expression and regulation (CLEAR) network that includes genes encoding lysosomal membrane proteins, enzymes and the V-ATPase complex^{2,34}, the transcription factor that recognizes the enhancer box (TFEB) promoter sequence 5'-GTCACGTGAC-3' in the CLEAR network³⁵, and the kinase mammalian target of rapamycin complex 1 (mTORC1) that senses the cell nutrition state and regulates its growth^{36,37}. Under normal physiological condition, mTORC1 co-localizes with TFEB on the surface of the lysosomal membrane³⁸⁻⁴⁰, preventing its nuclear translocation and keeping autophagy at a basal rate^{18,41}. Under physiological stress, the interaction between mTORC1 and TFEB is interrupted leading to nuclear translocation of TFEB and induction

1.2 Lysosomal Storage Diseases (LSDs)

of autophagy by positive transcriptional regulation of lysosomal genes and proteins required for autophagy³⁹. Such interactions guarantee lysosomal adaptation to meet the cell's needs for degradation capacity and energy production, a machinery referred to as lysosome nutrient sensing (LYNUS)².

As much as the lysosome is essential in cellular homeostasis, its dysfunction is known to cause lysosomal storage diseases and has been associated with aging¹⁰, neurodegenerative diseases⁴², cardiovascular diseases⁴³, cytoskeletal abnormalities^{44,45}, immune diseases^{31,32,46}, and cancer⁴⁷.

1.2 Lysosomal Storage Diseases (LSDs)

Lysosomal storage diseases are hereditary disorders characterized by aberrant, excessive accumulation of cellular material in lysosomes. They are commonly caused by mutations in genes encoding lysosomal components⁴⁸. LSDs include those diseases caused by mutations in genes involved in modifying, processing, transporting or targeting lysosomal proteins, or any lysosome-related organelle⁴⁸. For examples, in Niemann-Pick type C, the primary defect causes the accumulation of unesterified cholesterol in the late endosome which consequently impairs the whole endosome-lysosomal system⁴⁹.

1.2 Lysosomal Storage Diseases (LSDs)

Since the initial identification of the lysosome in 1955 by Christian de Duve, nearly 60 LSDs have been identified, most of which are inherited as autosomal recessive diseases. Exceptions include Fabry disease, a form of sphingolipidosis caused by a deficiency in alpha galactosidase A, and Hunter disease, known as mucopolysaccharidosis II (MPSII) and caused by a deficiency in iduronate-2-sulfatase; both are X-linked recessive disorders, whereas Danon disease, caused by a mutation in *LAMP2*, is an X-linked dominant disorder. Collectively, LSDs affect 1 in every 5000-live births, but some are more prevalent in specific ethnicities or backgrounds⁴⁸.

The genetic defect in LSDs initially causes lysosomal accumulation followed by a gradual impairment of lysosomal function. This impairment is characterized by disturbed calcium homeostasis in the lysosome and endoplasmic reticulum (ER), abnormal cellular trafficking and signaling, impaired autophagy, protein aggregation, cell stress, apoptosis, and mounting an inflammatory response that impacts multiple body systems to a differing extent. The most affected organs are those with a high tissue/cellular level, high turnover rate, and/or particular sensitivity to the primary accumulated substrate. In addition to the tissues and organs displaying the disease-specific clinical manifestations, two thirds of LSDs exhibit neuronal pathology. Neurons entirely rely on autophagy for maintenance and repair, to ensure correct propagation of action potentials, neuronal connectivity and prolonged viability. The build up of undegraded substances, followed by dysregulated autophagy, disrupts the synaptic

1.2 Lysosomal Storage Diseases (LSDs)

architecture, neuronal transmission and signaling, and causes cytotoxic disturbances that activate microglia, the brain macrophages. Whereas in other diseases the activation of the innate immune response is dampened by clearing the insult, the inflammatory process in LSDs is potentiated by the continuous cytotoxic accumulation, ultimately leading to neuronal death. The same process is taking place in other organs and cell types, but the very limited regenerative capacity of neurons and their reliance on autophagy for prolonged survival, make the central nervous system (CNS) more vulnerable to such assault. The degree of neuronal involvement in any LSD depends also on the nature of the primary accumulated substrate, its concentration and rate of turnover in neurons⁵⁰⁻⁵².

LSDs are typically classified based on the nature of the major accumulating substrate; specifically mucopolysaccharidoses (MPS), mucopolipidosis (ML), sphingolipidoses, lipidoses, oligosaccharidoses, glycoproteinoses, glycogen storage diseases, and others⁵³. While the severity and onset of symptoms vary from one disease to another, the central nervous, peripheral nervous, reticuloendothelial, skeletal, respiratory, and cardiac system, as well as the liver are most effected in LSDs.

1.3 GM2 Gangliosidoses

The GM2 gangliosidoses are a group of autosomal recessive disorders caused by a defect in the lysosomal degradation of GM2 ganglioside. They belong to the sphingolipidoses and present as a severe neurodegenerative illness.

1.3.1 Historical view

The first description of GM2 gangliosidoses was documented late in the nineteenth century. A British ophthalmologist, *Warren Tay*, reported the presence of a peculiar cherry red macular (spot in the retina) degeneration in an infant with symptoms and signs of progressive central nervous system deterioration, and two more infants from the same family a few years later^{54,55}. He also reported a fourth patient from a different family in 1888 (although the patient was examined in 1885)⁵⁶.

In 1887, the American neurologist *Bernard Sachs*, apparently unaware of Tay's reports, described a pattern of early blindness, profound retardation, and early childhood death, presenting the first detailed clinical picture of the pathology in this disease.⁵⁷

The connection between Tay's cases and all other case reports between 1881 and 1892, including Sachs's detailed report from 1887, was made by the neurologist *E. Kingdon*. Kingdon who noticed the uniform nature of the disease in these reports, which

1.3 GM2 Gangliosidosis

included an apparently healthy child at birth but marked and debilitating muscle weakness at 3 to 4 months of age, apathy, loss of sight, and mental deterioration, all increasing in severity and culminating in death between one to two years of age. These led him to conclude “I believe that the foregoing records warrant us in concluding that we have to deal with a well-defined disease, which presents distinctive clinical and diagnostic signs”⁵⁸. Kingdon also was first to describe the autopsy of the brain and eye of an infant that had died of the disease.⁵⁸ After this, other physicians started comparing the macular changes, as usual as the physical and mental deterioration of their own patients to what they called “Warren Tay-Sachs amaurotic idiocy” cases.

Continuing his work, Dr. Sachs noticed the familial nature of the disease. Several of the affected children that he was treating occurred in families with Eastern European Jewish ancestry, many of which were from consanguineous marriages, and so called it amaurotic familial idiocy⁵⁹. The name Tay-Sachs amaurotic familial idiocy was then used to refer to the infantile forms of the severe neurodegenerative disease, mostly if not all seen among families of Ashkenazi Jewish descent.

In 1905, and after post-mortem studies on six infants with Tay-Sachs disease in Hungary, the neuroanatomist *Karl Schaffer*, recognized the neuronal and glial swelling present throughout the entire central nervous system as the basic pathology of Tay-Sachs disease. He attributed the swelling of these cells to abnormal accumulation of

1.3 GM2 Gangliosidosis

lipid, and classified the disease to the group of “Aufbrauch krankheiten,” or wasting diseases⁶⁰.

By 1929, Sachs managed to publish 4 additional papers on this disorder, each showing further understanding of the disease and concluded its cause as a defect in the “fermentation” (metabolism) in these cells⁶¹, and he ultimately described it as a disorder of cerebral lipidosis⁶².

In the years following Sachs’s first report, research was focused not only on the area of histopathology and chemistry, but also on genetic epidemiology. *Slome* was the one who identified the autosomal recessive inheritance pattern in Tay-Sachs disease⁶³, based on studies of more than 120 affected children in about 80 Ashkenazi Jewish families. This led to preliminary estimations of the gene frequencies among Ashkenazi Jewish, Sephardic Jewish, as well as non-Jewish individuals living in the US⁶⁴⁻⁶⁷.

The chemical composition of the lipid accumulated in the brain of Tay-Sachs disease was unknown until the German biochemist, *Ernst Klenk*, found an orcinol-reactive sugar-containing lipid in brain extracts of children who had died of Niemann-Pick⁶⁸ and Tay-Sachs disease⁶⁹. Klenk established that the new glycolipid was comprised of fatty acids, sphingosine, galactose and glucose⁶⁹, as well as its acidic sugar component named “neuraminic acid”, which was responsible for the orcinol positive reaction^{70,71}.

1.3 GM2 Gangliosidoses

This glycolipid was found to be highly concentrated in ganglion cells, and was therefore named “ganglioside”⁷². At the same time, the Swedish biochemist *Gunnar Blix* identified the acetylated galactosamine, and the orcinol- reactive sugar, which he later named “sialic acid”, as parts of the glycolipid extracted from bovine brain^{73,74}. In 1962, Svennerholm identified GM2 as the specific ganglioside accumulated in Tay-Sachs disease⁷⁵. The structure of GM2 ganglioside (**Fig. 1**) and other monoasialogangliosides of mammalian brain were established the following year by *Kuhn and Wiegandt* (1963)⁷⁶ and *Ledeen and Salsman* (1965)⁷⁷.

1.3 GM2 Gangliosides

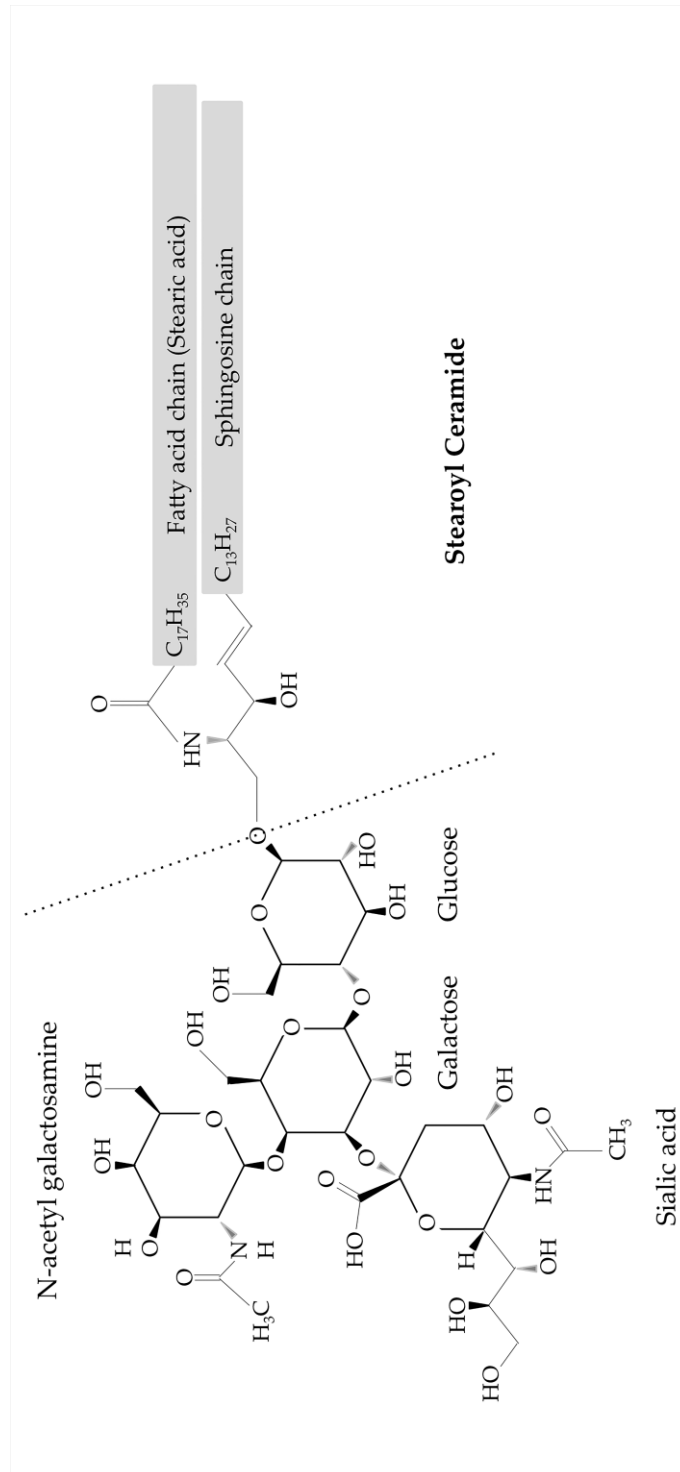


Figure 1- GM2 ganglioside

1.4 The β -hexosaminidase system

Human β -hexosaminidases (EC 3.2.1.52) are enzymes involved in the hydrolysis of both β -glycosidically linked N-acetylglucosamine, and N-acetylgalactosamine residues from a wide range of glycoconjugates. An N-acetylglucosaminidase was first observed in 1936⁷⁸, but later, it was recognized that this enzyme also cleaves terminal N-acetylgalactosamines⁷⁹, and therefore the name was revised and changed to “hexosaminidase”. The interest in studying these enzymes arose from their involvement in the lysosomal degradation pathway of GM2 ganglioside, a highly abundant sialic acid-containing glycosphingolipid in the central nervous system, as defects resulted in severe neurodegenerative diseases.

The β -hexosaminidases are built from two non-covalently linked polypeptides, α - and β -subunits, that assemble into dimers to construct three isozymes, Hex S ($\alpha\alpha$), Hex A ($\alpha\beta$), and Hex B ($\beta\beta$)⁸⁰ (**Table 1**). The α -subunit gene, *HEXA*, is 35 kb in length and located on the long arm of chromosome 15⁸¹⁻⁸³, whereas the β -subunit gene, *HEXB*, is 40 kb in length and located on chromosome 5^{84,85}.

1.4 The β -hexosaminidase system

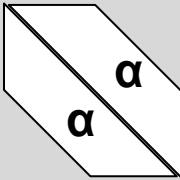

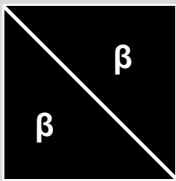
Gene Features	<i>HEXA</i>		<i>HEXB</i>	<i>GM2A</i>
Chromosome location	Band 15q23		Band 5q13	Band 5q31
Product	Alpha subunit		Beta subunit	GM2 activator protein
Structural subunits	HEX S; $\alpha\alpha$ 	HEX A; $\alpha\beta$  Complex Formation	HEX B; $\beta\beta$ 	Cofactor
Substrate	Glyco-conjugates	GM2 ganglioside Glyco-conjugates	GA2 ganglioside Glyco-conjugates	GM2 ganglioside
Disorder	Tay-Sachs (130 mutations)		Sandhoff (50 mutations)	AB Variant (5 mutations)
Brain accumulation	High GM2 level. Minor amount of GA2.		Highest GA2 levels. Lowest GM2 levels.	High GM2 levels. Significant GA2 levels.

Table 1- The GM2 ganglioside and the hexosaminidase system.

This table shows the relationship between the diseases, genes and the primary accumulated substrates.

1.4 The β -hexosaminidase system

Both genes have 13 introns and 14 exons that are arranged and spaced similarly^{82,83}. In addition to having similar gene size and organization, the peptide sequences of the α - and β -subunits are over 60% identical^{82,86,87}. This extensive homology indicates that both genes are derived from a common ancestral gene⁸⁸.

The synthesis of both subunits take place in the ER, where they dimerize to produce the pro-enzyme forms that are targeted to the lysosome by acquiring mannose-6-phosphate (M6P) in the cis Golgi⁸⁹⁻⁹². This dimerization is essential to stabilize the subunits and to avoid degradation by the endoplasmic reticulum-associated degradation (ERAD) systems. Normally, due to differences in the affinity between subunits of the same type and each other, β -subunits are readily associated, α - β association takes only a couple of hours, and α - α association is rare; this makes the α -subunits vulnerable for elimination by ERAD systems and prevents the production of Hex S in high concentration^{85,91,92}.

Normal human tissues contain mainly Hex A and Hex B at fairly comparable levels, whereas small amounts of Hex S are only detectable in patients with Sandhoff Disease, the O variant of GM2 gangliosidosis. Despite the structural similarity between the α - and β -subunits, Hex A, Hex B and Hex S, each of which has two active sites, show distinctive substrate specificity⁹³. Both active sites in the β -subunits of Hex B cleave uncharged

1.4 The β -hexosaminidase system

substrates, and only α -subunits in either Hex A or Hex S cleave negatively charged glycoconjugates.

The hydrolysis of GM2 ganglioside in humans can only proceed via the action of Hex A ($\alpha\beta$) in the presence of a non-catalytic glycoprotein called the GM2 activator protein (GM2AP). The GM2 activator is a small lysosomal lipid transfer protein encoded by a gene located on the long arm of chromosome 5⁹⁴; GM2AP follows the same synthesis, posttranslational modification and activation pathway as the hexosaminidase enzymes.⁹⁵ This protein acts as a substrate-specific cofactor that extracts the GM2 substrate within the intralysosomal membranes vesicles forming a soluble GM2AP-GM2 complex. With GM2 ganglioside held in its β -cup, GM2AP presents the substrate to Hex A⁹⁶ facilitating its degradation through a catalytic process involving a substrate-assisted nucleophilic attack that proceeds through a double-displacement mechanism⁹⁶⁻⁹⁹. Mutations in the genes encoding any of the α -subunit, β - subunit, or GM2 activator proteins can block or reduce GM2 hydrolysis causing GM2 gangliosidosis (**Fig. 2**).

1.4 The β -hexosaminidase system

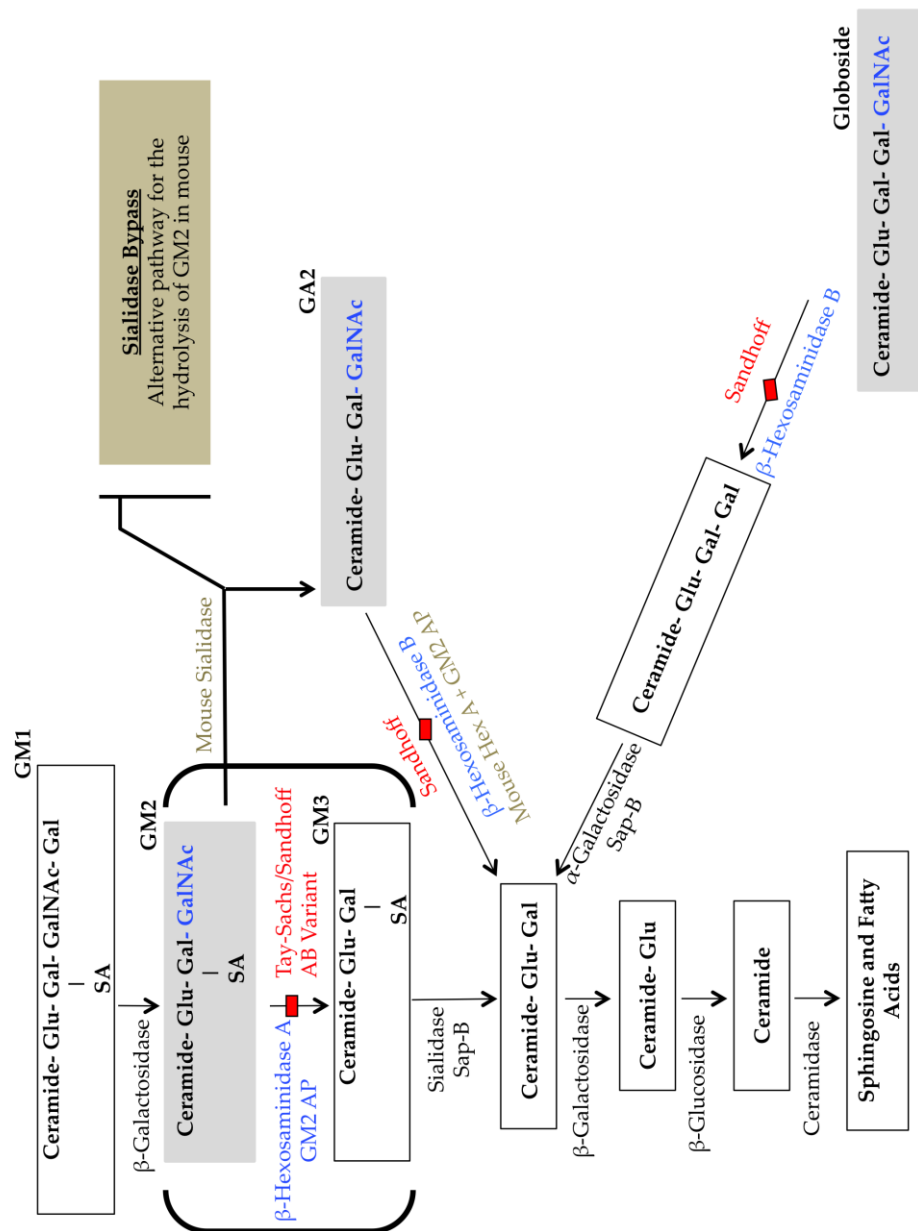


Figure 2- GM2 ganglioside degradation pathways and genetics disorders. Enzymes and their target sugar residue are indicated in blue and the disease(s) associated with defects in the indicated enzyme are shown in red. The alternative pathway for the hydrolysis of GM2 and GA2 in mouse is indicated. Abbreviations: Cer, ceramide; Gal, galactose; GalCer, galactosylceramide; GalNAc, N-acetylgalactosamine; Glc, glucose; GlcCer, glucosylceramide; SA, sialic acid

1.5 Classification of GM2 gangliosidoses

Deficiency in Hex A enzyme activity towards its natural substrate, GM2 ganglioside, is caused by allelic mutations in either enzyme subunit or cofactor genes, leading to accumulation of GM2 ganglioside, and its asialo- derivative GA2^{100,101}. The resulting GM2 gangliosidoses are rare, although the incidence is elevated in specific ethnic or geographically isolated groups.

Clinically, the GM2 gangliosidoses are classified based on the hexosaminidase isozyme activity present, measured using synthetic substrates that do not require the GM2 activator protein. These results are combined with the severity of symptoms and age of disease onset. Therefore, patients are classified as the B variant, Tay-Sachs disease (TSD), because they retain hexosaminidase B activity (deficiency in Hex A activity). Patients classified as O variants, Sandhoff disease (SD), lack both Hex A and Hex B activity, while those with the AB variant show no deficiency in either isozyme activity^{102,103}. Any of these disease variants can present clinically in a patient as infantile, juvenile, or adult forms^{104,105}.

GM2 ganglioside biosynthesis and turnover varies between organs, tissues and cell types, but as long as the capacity of the Hex A residual enzyme activity (Hex A in the presence of GM2 activator protein) exceeds the rate of GM2 ganglioside influx into the lysosome (threshold theory), no disease causing accumulation will occur. However,

1.5 Classification of GM2 gangliosidoses

when the enzyme activity in GM2 gangliosidoses falls below the critical threshold (<10%) for substrate turnover, accumulation results^{106,107}.

The symptoms and age of disease onset vary based on the severity of GM2 ganglioside accumulation, which would increase as the difference between threshold activity (10%) and residual enzyme activity increases¹⁰⁶⁻¹⁰⁸. Brain has the highest abundance of GM2 ganglioside, which also varies among neuron subsets. In the case of incomplete enzyme deficiency, the subset of cells with the highest ganglioside biosynthesis and turnover will accumulate GM2 ganglioside faster than others, accounting for the different clinical symptomatology particularly in patients with the adult chronic type of GM2 gangliosidoses^{104,109}.

Infantile/acute GM2 gangliosidoses are the most common disease form of the three variants: Tay-Sachs disease, Sandhoff disease, and activator protein deficiency. Patients with infantile/acute GM2 gangliosidoses have less than 2% residual enzyme activity¹¹⁰, resulting in a rapid and stereotypic course of disease. Affected infants appear normal at birth and the earliest sign of disease is hypotonia beginning at 3-5 months of age, along with hyperacusis (persistent startle reaction to loud noises and myoclonic jerks). They typically fail to achieve normal early gross motor skills, lose social contact and responsiveness, and exhibit seizures, macrocephaly and dysphagia before reaching 1 year of age. Ophthalmic examination reveals the presence of the macular

1.5 Classification of GM2 gangliosidoses

degeneration “cherry-red spot”, which is evident in all patients with this form of the disease. In the second year of life, patients lose their eyesight, hearing ability, and progress to a vegetative state. Death usually occurs by the age of 2 to 4 years. In addition to the severe neurodegenerative course, infants afflicted with the infantile O variant, Sandhoff disease, show evidence of non-neurological involvement. This includes peripheral organ enlargement, skeletal and cardiac abnormalities, oligosacchariduria, and storage cells in bone marrow, all caused by glycolipid accumulation^{111,112}, which exaggerates the disease course, leading to death before the age of 4 years.

In the case of juvenile/subacute GM2 gangliosidoses, patients have residual enzyme activity levels between 2 % and 7.5%¹¹⁰, and symptoms appear after the first year of age¹¹³. Patients show speech and fine motor coordination delay as the early prominent symptoms of this form. These rapidly progress to dysarthria, ataxia, incoordination, and increasing spasticity, with development of seizures before the end of the first decade of life. Unlike infantile forms, macular degeneration is rare, but optic atrophy and retinitis pigmentosa causing visual impairment may be seen. Patients enter a vegetative state by 10 to 15 years of age, and death follows within a few years. Delayed diagnosis is common among patients with juvenile/subacute GM2 gangliosidoses resulting in misclassification as adult/chronic GM2 gangliosidoses patients.

1.6 Molecular genetics and epidemiology of GM2 gangliosidoses

Adults with the chronic form of GM2 gangliosidoses have up to 10% residual enzyme activity and manifest very diverse symptoms, but all without developmental delay¹¹⁴⁻¹¹⁶. Patients show slowly progressive spinocerebellar ataxia¹¹⁷, with extrapyramidal signs such as; dystonia, choreoathetosis and bradykinesia dominating the clinical phenotype¹⁰⁹. Others present a combination of upper and lower motor neuron disease resembling amyotrophic lateral sclerosis^{118,119}. Also, 40% of adult/chronic GM2 gangliosidoses patients suffer from psychiatric abnormalities¹⁰⁴, including schizophrenia, paranoia, and recurrent psychotic depression¹¹⁵, as all respond poorly to antipsychotic drugs.

1.6 Molecular genetics and epidemiology of GM2 gangliosidoses

The hexosaminidase molecular era started with the characterization of the subunits and cofactor cDNAs and genes^{81,82,84-86,94,95,120}, which permitted the identification of the mutations causing GM2 gangliosidoses.

As these diseases are considerably rare in general^{88,121,122}, the search for mutations was focussed on populations with a high incidence; French Canadians in Eastern Québec, the Ashkenazi Jewish populations, and later the Louisiana Cajun, were characterized before studies extended to include other groups and isolated cases. Since

1.6 Molecular genetics and epidemiology of GM2 gangliosidoses

then, nearly 190 mutations (about 130 in *HEXA*, 50 in *HEXB*, 5 in *GM2A*) resulting from single base substitutions (most commonly), deletions, duplications, insertions, or gene rearrangements, have been reported to cause different variants and severities of GM2 gangliosidoses. Most of these were identified as private mutations that presented in a single case or family. Only a few mutations account for the high carrier frequency and/or incidences in particular ethnic or geographically isolated groups.

1.6.1 Mutations in the α -subunit gene

Among the 130 Tay-Sachs (*HEXA*) mutations, the most common null mutations are found in the French Canadian and Ashkenazi Jewish populations. A 7.6 kb deletion including exon 1 precluding the production of the α subunit was found as the major mutation in the French Canadian population^{123,124}. In Ashkenazi Jews, a c.1277insTATC duplication in exon 11 was identified¹²⁵ that accounts for over 80% of the cases¹²⁶, and a c.1421+1G>C mutation at the 5' end of intron 12 was identified that accounted for 15% of cases^{125,127,128}. In the Cajun population, a c.1073+1G>A single base substitution in intron 9 and the c.1277insTATC duplication are the two main mutations^{105,129,130}. In these three groups, Ashkenazi Jews, French Canadians, and Louisiana Cajun, the carrier rate is approximately 1 in 27, placing these groups at risk for Tay-Sachs disease.

In general, the c.1073+1G>A mutation in intron 9, and c.1277insTATC mutation in exon 11 account for 17% and 32% respectively, of the Tay-Sachs alleles in non-Jewish

1.6 Molecular genetics and epidemiology of GM2 gangliosidoses

Tay-Sachs disease cases^{105,126,130-133}. Other frequent mutations include a c.571-1G>T substitution in intron 5 found in 80% of Tay-Sachs cases in Japanese¹³⁴, and a c.910delTTC in exon 8, a c.IVS-2A>G in intron 5, and a c.509G>A in exon 5, causing over 80% of TSD in Moroccan Jews¹³⁵.

Some other common mutations are associated with limited enzyme activity. The most frequent is a c.805G>A mutation at the 3-prime end of exon 7 found in Ashkenazi Jewish (3%) and non- Ashkenazi Jewish (5%) patients affected with adult/chronic Tay-Sachs disease¹³⁶⁻¹³⁸. A second mutation, c.533G>A in exon 5 causes a defect in Hex A's activity toward GM2 ganglioside. It is found in patients from various ethnic backgrounds, but has the highest incidence in northern Portugal. The homozygous state of c.533G>A results in a juvenile/subacute form of Tay-Sachs disease^{128,139,140}.

These mutations may be found in a homozygous state, but are often found in a compound heterozygous state with a private mutation, or other common mutation, thus resulting in biochemical and clinical heterogeneity among Tay-Sachs patients^{126,131-133,141}.

1.6.2 Mutations in the β -subunit gene

Mutations in the *HEXB* gene have been less extensively identified and studied. Among the nearly 50 mutations identified, a 16 kb deletion at the 5'- end of *HEXB*, which encompasses exons 1-5, is considered the most common mutation (27%-30%) in all areas of the world¹⁴²⁻¹⁴⁷. The highest carrier frequency for Sandhoff disease was found among the Maronite community in Cyprus, 1 in 7, and is caused by a c.76delA in exon 1^{148,149}. Based on in silico analysis, two single base substitution, a c.1601G>T in exon 13 and a c.165G>A in exon 14¹⁵⁰, and a single base deletion, c.115delG, in exon 1 found in patients¹⁵¹ account for the 1 in 15 carrier frequency and high Sandhoff disease incidence in the Metis community of north Saskatchewan¹⁵⁰. In the Creoles of northern Argentina, the most common mutation is a c.445+1G>A substitution in intron 2¹⁵².

As in Tay-Sachs disease, these *HEXB* mutations can be found in a homozygous, or in a compound heterozygous state with a private mutation, or other common mutation, and result in biochemical and clinical heterogeneity among patients with Sandhoff disease^{147,153-156}.

1.6.3 Mutations in the GM2A activator gene

The occurrence of GM2 gangliosidosis as a result of mutations in *GM2A* is extremely rare. Only five mutations have been reported, all found in homozygous state, and cause an infantile variant of the disease¹⁵⁷⁻¹⁶⁰.

1.7 Mouse models of GM2 gangliosidoses

To better understand GM2 ganglioside metabolism and the defects in its degradation, mouse models have been generated through targeted gene disruption of *Hexa*, *Hexb*, and *Gm2a* in mouse embryonic stem cells. Biochemically, these mouse models have the same isozyme patterns found in their corresponding variant of the human disease and show accumulation of GM2 ganglioside. However, the resulting phenotypes are distinctive compared to the human diseases.

The Tay-Sachs mouse model (*Hexa*^{-/-}) has about 50% of normal hexosaminidase (Hex) activity, owing to the presence of the Hex B isozyme. It accumulates only GM2 ganglioside, and not GA2, in restricted brain regions. Moreover, the storage of GM2 ganglioside was very minimal and caused no neuronal pathology, in contrast to the stereotypical phenotype of the GM2 gangliosidoses found in humans^{161,162}. It was suggested that late in their natural life span, mice might show mild neurological symptoms, but only repeatedly bred female mice developed late onset Tay-Sachs disease¹⁶³.

The Sandhoff mouse model (*Hexb*^{-/-}), with ≤ 2% of normal Hex activity due to the Hex S isozyme, showed extensive neuronal accumulation of GM2 ganglioside (and its asialo-derivative GA2) throughout the central nervous system. Progressive deterioration in motor function started at 12 weeks of age; *Hexb*^{-/-} mice manifested gait

1.7 Mouse models of GM2 gangliosidoses

abnormalities and spastic movements that advanced to paralysis and an inability to eat or drink before 20 weeks of age. Unlike the Tay-Sachs mouse model, the clinical features of disease progression and neuronal deterioration in the Sandhoff mouse model resembled that observed in infantile/acute Sandhoff patients (and other GM2 gangliosidoses variants)¹⁶⁴.

Lastly, the AB-variant mouse model (*Gm2a*^{-/-}), with GM2 activator deficiency, showed normal Hex A activity and accumulated GM2 and a low level of GA2. Although the neuronal storage was restricted in specific brain regions, as in the Tay-Sachs mouse model (*Hexa*^{-/-}), the build-up was more pronounced in the *Gm2a*^{-/-} mouse. The level of accumulation compromised their motor activity, especially balance and coordination, but not their life span¹⁶⁵.

The phenotypic differences between the Tay-Sachs and Sandhoff mouse models are explained by the presence of mouse sialidase, an enzyme responsible for removing the sialic acid sugar residue from a wide range of sialylated glycoconjugates. Unlike human sialidase, mouse sialidase 4 (Neuraminidase 4) is highly active toward GM2 gangliosides. It converts GM2 ganglioside to its neutral counterpart, GA2, allowing the Hex B enzyme present in the Tay-Sachs mouse model to continue the sequential hydrolysis of the terminal sugars. Therefore, the sialidase in the Tay-Sachs mouse model bypasses the need for Hex A and GM2 activator to hydrolyze GM2. However, the

1.8 Treatment approaches

intermediate phenotype of the AB-variant mouse indicates that the GM2 activator is required for optimal degradation of GA2. Further studies confirmed that in the mouse, GA2 is degraded by the Hex B enzyme and, to a less extent, by the Hex A and the GM2 activator¹⁶⁶.

These mouse models are valuable tools in understanding the metabolism of glycoconjugates, and the molecular pathology associated with the GM2 diseases, as well as evaluating different therapeutic strategies for GM2 gangliosidoses^{163,167-169}.

1.8 Treatment approaches

With the biochemical and molecular defects causing GM2 gangliosidoses well understood, the need for an effective therapy has become the focus of research. Most therapies are based on the enzyme activity threshold (presented by Conzelmann and Sandhoff 1983 and Leinekugel et al. 1991)^{107,108} (see section 1.5), as the target to prevent GM2 diseases manifestations. The treatments must aim to restore or increase the degradation capacity (hexosaminidase activity) above the critical threshold, and/or decrease the influx of GM2 substrate within the lysosome below the degradation capacity of the available enzyme activity. Given that a small percentage of enzyme activity can have a profound effect on the clinical presentation of the GM2 gangliosidoses, which when taken in consideration with the cellular cross correction

phenomena, noticed by Neufeld E.F. group in 1968 and 1970 (reviewed in “From serendipity to therapy” by Neufeld E.)¹⁷⁰, makes enzyme replacement therapies a logical and genuine approach for treatment.

1.8.1 Cross correction phenomena of lysosomal enzymes

Lysosomes contain more than 60 acidic hydrolases and their cofactor proteins, which are responsible for degrading and subsequent recycling of both extracellular and intracellular macromolecules. After synthesis in the ER, the pro-enzymes are transported to the Golgi where specific terminal mannose residues become phosphorylated on the sixth position (M6P) resulting in targeting to the lysosome¹⁷¹. However, a small percentage of these enzymes fail to be phosphorylated, or to bind to the mannose phosphate receptor (MPR), and are instead secreted from the cell where they are available for recapture by the same, or neighboring cells, via cell membrane glycan receptors. These include the cation-independent M6P receptor (CI-M6PR) or mannose receptor (MR), which allows their endocytosis and delivery to the lysosome¹⁷².

1.8.2 Therapeutic strategies

To provide clinical benefit to patients with GM2 gangliosidosis, adequate enzyme or cofactor must reach and be utilized by cells in the CNS, where the main pathology of these diseases are manifested. Strategies to provide the deficient protein in LSDs and many other metabolic disorders include direct infusion of a recombinant version of the

1.8 Treatment approaches

missing protein into circulation, and/or bone marrow/hematopoietic stem cell transplantations. The donor hematopoietic stem cells indirectly supply the body with the missing protein by proliferating and populating different organs. Other approaches are more specific to LSDs and include enzyme enhancement and substrate reduction therapies¹⁷³.

Enzyme replacement therapy (ERT)

Bone marrow and hematopoietic stem cell transplantations (HSCT) are a standard therapy for many metabolic and hematological disorders, and was the first approach introduced to treat LSDs. Their use as indirect enzyme replacement therapy to treat some LSDs like type III Gaucher disease, MPS types I, VI and VII, alpha-mannosidosis, fucosidosis, and Krabbe disease, showed some promising results. If a suitable donor is available, HSCT is also considered the preferred treatment for patients with severe MPS I diagnosed before the age of 2.5 years, and might be considered in older MPS I^{174,175}, Krabbe and metachromatic leukodystrophy patients with mild and intermediate phenotypes only if the progression of disease is limited at the time of treatment^{176,177}. However, the efficacy of HSCT in treating LSDs is inconclusive as the numbers of patients in clinical trials have been small, and the outcomes were extremely variable¹⁷⁸.

Direct enzyme replacement therapies have the advantage that there is no need for donors or major surgeries. Nevertheless, the manufactured enzymes must be

1.8 Treatment approaches

administered on an ongoing basis to meet disease management needs. Success in many LSDs has made ERT a standard treatment for type I Gaucher disease^{179,180}, as well as MPS I, II and VI¹⁷⁵, Fabry¹⁸¹⁻¹⁸³ and Pompe diseases^{184,185} (reviewed in ¹⁷³).

The level of success for treating any of the LSDs with direct enzyme replacement therapy is determined by several factors. Most importantly is the organ systems involved in the disease. Infused enzyme can easily correct the pathology in blood cells, circulatory organs such as liver and spleen, whereas the skeletal system, cardiovascular and renal system are more challenging targets. More crucially, neurological pathology found in most LSDs is refractory to ERTs as the blood brain barrier (BBB) keeps the central nervous system inaccessible¹⁸⁶.

With regard to the GM2 gangliosidoses, the initial attempt to restore the enzymatic activity was by intravenously delivering normal donor plasma enriched in β -hexosaminidase intravenously to a 13 month old Sandhoff patient. This was followed by many other attempts including, multiple intravenous, intraventricular, and intracisternal injections with purified Hex A, or purified native placental Hex A and Hex A-conjugated with poly-vinyl-pyrrolidone¹⁸⁷. Others tried indirect enzyme replacement therapy, where hematopoietic stem cell is transplants into patients were performed to compensate for the deficiency in circulating enzyme¹⁸⁷. However, the failure of the enzyme to crossing the BBB rendered these treatments ineffective.

Substrate reduction therapy (SRT)

Besides recombinant enzyme replacement therapy, only substrate reduction therapy is considered a routine practice in “managing” LSDs. In this approach, the cellular accumulation of glycosphingolipid (GSL) is decreased, by inhibiting the catalytic enzyme in the initial step of their biosynthesis, glucosylceramide synthase. The decrease in GSL synthesis is intended to allow a better match between the residual enzyme activity present and the influx of substrates. Miglustat (N-butyldeoxynojirimycin), a small imino-sugar with the ability to cross the BBB, was the first glucosylceramide synthase inhibitor to prove efficacy *in vitro*^{188,189} and subsequently in mouse models of GM1 gangliosidoses, GM2 gangliosidoses, Fabry, and Niemann Pick disease¹⁹⁰. Miglustat is considered the first specific treatment for LSDs, but side effects limited its licensing as an enzyme inhibitor (see enhancement therapy) to include only patients with Niemann Pick-C and mild to moderate type 1 Gaucher disease where ERT is not an option¹⁹¹. Other inhibitors are being developed but none are designed to treat GM2 gangliosidoses¹⁸⁶.

Enhancement therapy

The mutations causing subacute and chronic forms of LSDs typically result in an abnormal protein that is improperly folded, and cleared by the quality control ERAD system. The low levels of protein that escape clearing by ERAD retain some if not all the catalytic activity of that enzyme/cofactor¹⁹². Using “chaperone” molecules,

1.8 Treatment approaches

enhancement approaches takes advantage of the presence of these misfolded proteins and aim to enhance their correct folding and/or assembly. Proteins that are successfully folded can be processed and transported to their cellular destination¹⁹². In the case of lysosomal enzymes, the low pH forces chaperone molecules to dissociate from the proenzymes, leaving the functional enzyme behind¹⁹³.

Until recently, pharmacological chaperones (PCs) were all substrate-like chemical structures that were used as a competitive inhibitor for a specific hydrolase. When taken at a sub-inhibitory concentration, these inhibitors acted as chaperones, partially rescuing the misfolding and increasing the enzyme activity. Since the proof of principle demonstration in cell culture for the enzyme deficient in Fabry disease¹⁹⁴, different enzyme inhibitors have reached clinical trials. Currently, other non-inhibitory chemical molecules and different heat shock proteins¹⁹⁵ are being investigated for their possible ability to rescue the level of mutant proteins (reviewed in¹⁹⁶).

Progress in this area led to the phase III clinical trial of Migalastat as the first enhancer chaperone for treating Fabry disease, whereas Duvoglustat is being tested to treat Pompe disease (phase II). Other clinical trials are also ongoing to test each of these chaperones in combination with enzyme replacement therapy¹⁸⁶. Less advanced is the testing of two FDA approved drugs, pyrimethamine and ambroxol, as chaperone candidates to treat late-onset GM2 gangliosidoses and Gaucher disease. In a small

1.9 Gene therapy

phase II Sandhoff disease trial; participants treated with 75 mg daily doses of pyrimethamine exhibited neurological side effects, whereas those treated with 50 mg daily doses had a variable enhancement effect¹⁸⁶.

The ability of chaperones to cross the BBB gives them an advantage in treating LSDs with neurological involvement. However, the inhibitory nature of these compounds makes dosing critical to favour beneficial effects. Their use is limited to patients with residual enzyme activity and without severe neurological involvement. Therefore, even when combined with an enzyme replacement approach, enzyme enhancement or substrate reduction therapy can only delay disease progression in GM2 gangliosidosis patients with near 10% residual enzyme activity suffering with the chronic form of the disease.

Still to date, the fact remains that as a disease of the brain, the GM2 gangliosidosis are among the most severe neurological disorders, which, despite the knowledge of the underlying causes and consequences, linger without a cure.

1.9 Gene therapy

Treating neurodegenerative diseases centers on eliminating the cause of the damage. In the case of the GM2 gangliosidosis and other lysosomal storage disorders, the

1.9 Gene therapy

production of substrates cannot be stopped, and recombinant enzymes cannot reach the brain. Thus, the possibility of replacing the mutated gene became the direction of interest.

1.9.1 Definition

A gene therapy approach is defined as the packing of a recombinant nucleic acid material as an active substance inside a vector particle to mediate its delivery into the cell where it is meant to replace, regulate, repair, add or delete a genetic sequence (Fig. 2)¹⁹⁷.

Each LSD is caused by a single gene mutation, mostly affecting a lysosomal hydrolase. Introducing a functional wild-type gene to cells is predicted to compensate for the dysfunctional gene and resolve the metabolic block. However, reaching the CNS requires a safe and efficient delivery route, which confers long-term expression.

The knowledge gained after two decades since the initial gene therapy trial approved by the FDA in September 14th 1990,¹⁹⁸ followed by more than 1700 clinical trials worldwide, is that the success of gene therapy depends on the effectiveness of gene delivery to the target organ or organs. Vectors such as liposomes and

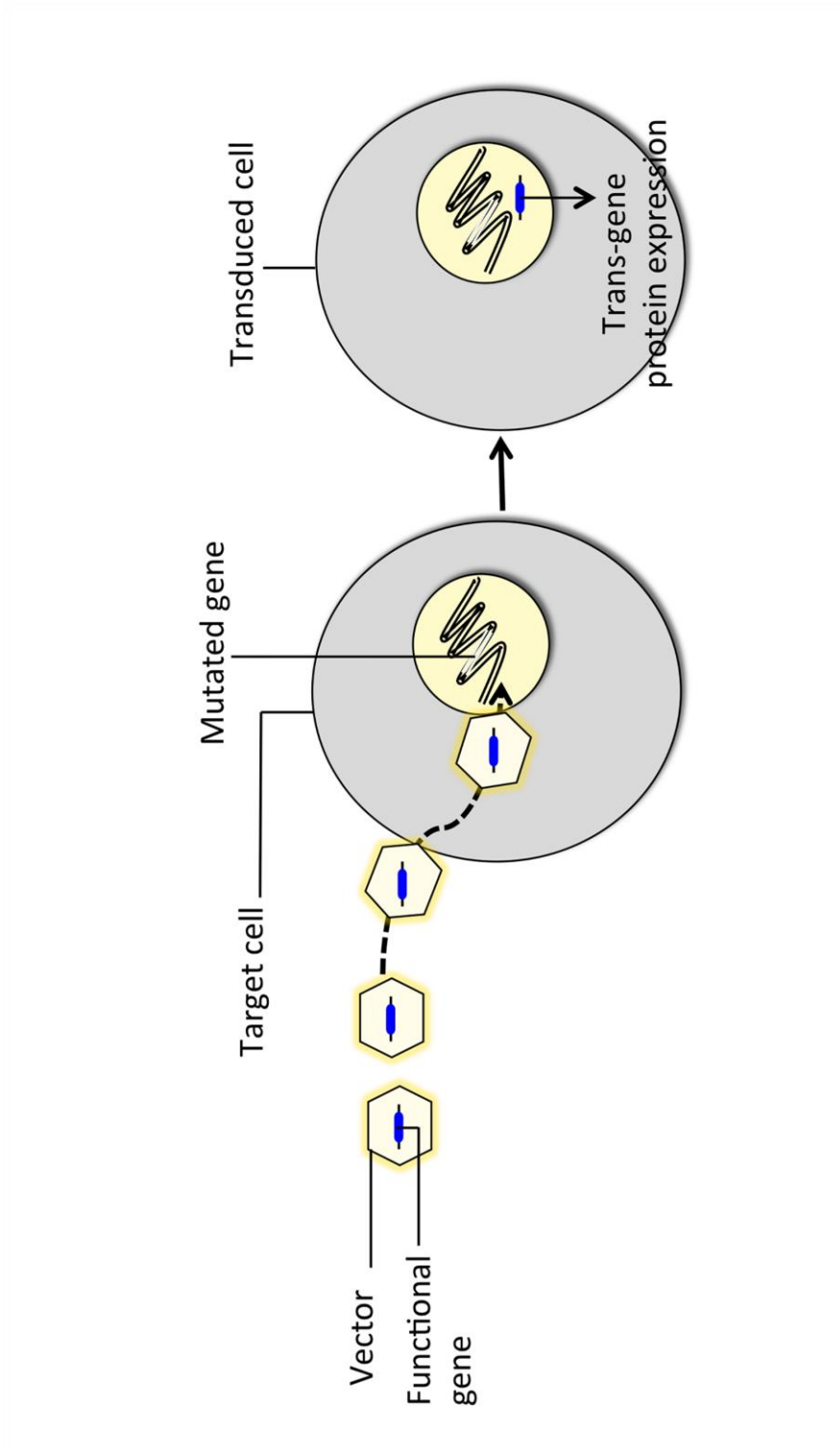


Figure 3- Gene therapy

1.9 Gene therapy

nanoparticles can carry larger sequence but fail to mediate high or sustained gene expression when compared to viral-vectors. The utilization of recombinant retro-, adeno-, herpes-, and adeno-associated virus derived vectors is currently considered the most effective means for gene transfer¹⁹⁷.

Retroviruses are RNA viruses with glycoprotein envelopes that transcribe their single-stranded RNA genome into a double-stranded DNA copy utilizing its own reverse transcriptase. The DNA double-stranded copy of their genome can then integrate into host chromosomes using another enzyme produced by the virus, integrase. This grants continuous replication of the genomic materials in daughter cells. Some retroviral vectors can only transduce dividing cells, whereas others, such as the lentiviral subfamily of retroviruses, also transduce non-dividing cells. Vectors derived from retroviruses were the first to be used in gene therapy, and the trial to treat severe combined immune deficiency (X-linked SCID) represents one of the most successful applications of gene therapy¹⁹⁹.

Adenoviruses are non-enveloped, capsid enclosed double-stranded DNA viruses. The genetic material of adenoviruses is not incorporated into the host genome but remains free in the nucleus where it is transcribed as any other gene. As the viruses themselves, vectors driven from this family are highly immunogenic. They can transduce a broader range of both quiescent and dividing cell types compare to

1.9 Gene therapy

retroviral vectors, mediating robust, but transient, gene expression. This system gained support in treating cancer and the p53-based adenoviral product, Gendicine, was the first to be licensed to treat head and neck squamous cell carcinoma in China²⁰⁰.

Herpes viruses are double-stranded linear DNA viruses with a glycoprotein envelope, and persist as nonreplicating episomal elements inside the nucleus of host cells. HSV vectors can transduce both dividing and non-dividing cells, and ensure long-term expression of transgenes in different cell types. As they are naturally neurotropic viruses, Herpes derived vectors can efficiently transduce neurons of the CNS which they access through sensory ganglia. The large size capacity of HSV derived vectors make them attractive for packing more than one gene. The main limiting factor is the highly cytotoxic effect of any co-production helper virus, confining the test/use of this type of vectors to cancer therapy trails^{201,202}.

Adenoviral, herpes simplex, and lentiviral (retroviral) derived vectors can transduce dividing and non-dividing cells, but they are also associated with pathological effects or host response; adenoviral vectors are known to provoke a strong host immune responses; herpes virus derived vectors induce cytotoxicity; and lentiviral vectors have a high risk for integration and insertional mutagenesis, limiting their use largely to cancer gene therapy trials. These complications have led the adeno-associated

1.9 Gene therapy

viral (AAV) vectors (see 1.9.2) to be the choice to treat neurological disorders and monogenic diseases^{197,201,202}.

1.9.2 Adeno-associated viruses AAVs

Adeno-associated viruses are nonpathogenic²⁰³, small parvoviruses²⁰⁴, with either a 4.7 kbp positive or negative polarity single-stranded DNA genome. The genome is enclosed in a 18–25 nm diameter capsid²⁰⁵ and no envelop²⁰⁶. AAVs lack the ability to replicate in the absence of a helper virus such as adenovirus, thus the name, that provides elements necessary for reproduction. The genome contains two inverted terminal repeats (ITRs) of two 145 nucleotides in length²⁰⁷. The two sequences flanking two open reading frame genes; the rep gene coding proteins necessary for viral replication²⁰⁸, and the cap gene coding 60 proteins that form the viral capsid. Each inverted terminal repeat (ITR) forms a T-shaped hairpin structure by complementary base pairing with a sequence within its first 125 nucleotides that functions as a replication origin^{209,210}. Upon infecting human cells, and in the absence of a helper virus, the AAV genome exists episomally in circular and linear forms^{211,212}, or specifically integrates into the chromosome 19q13.4 site, at a rate of about 0.5%²¹³⁻²¹⁵. **Fig. 4**

Twelve AAV serotypes have currently been identified in humans (AAV1 to AAV12)²¹⁶, all similar in size, structure, and genome organization. These serotypes differ in their amino acid capsule composition, although not affecting their icosahedral

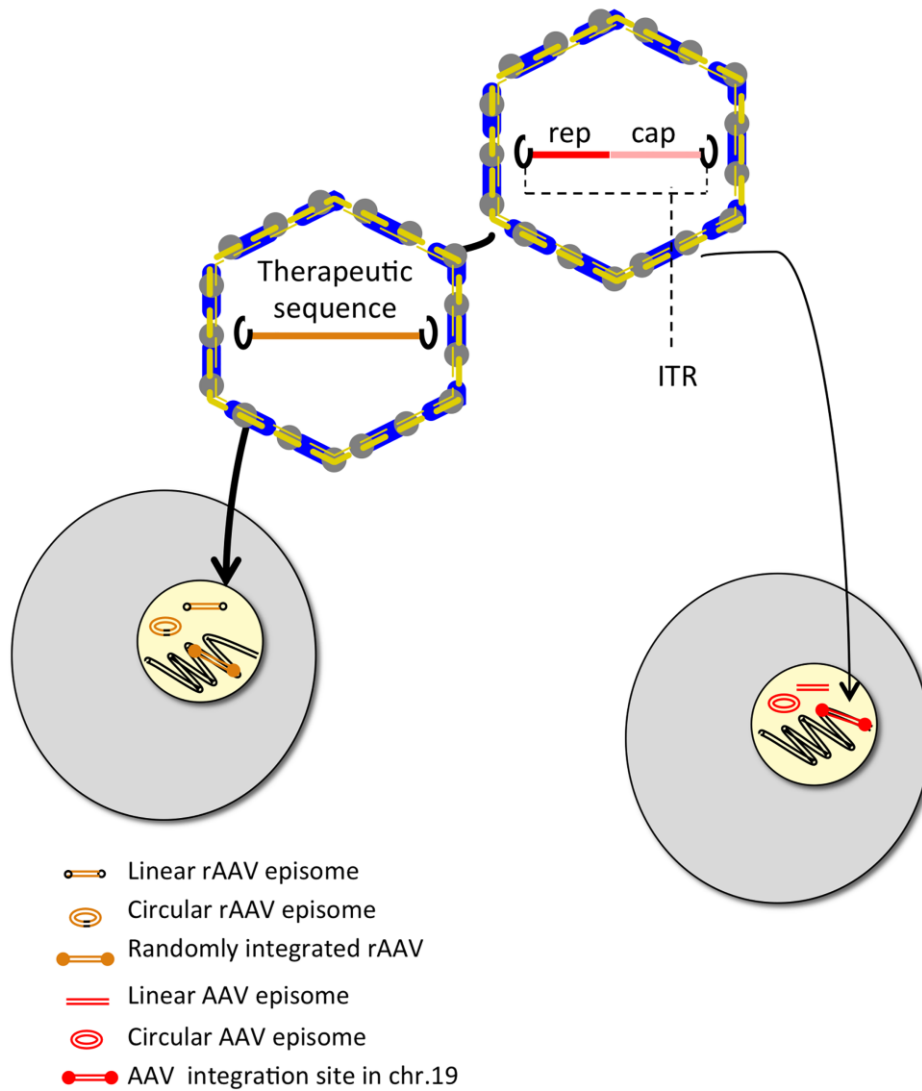


Figure 4- Adeno-associated virus

symmetry shape of the capsid, it causes local variation in capsid structure, does alter receptor specificity and accounts for the particular tissue-specific tropism of AAVs²¹⁷.

1.9.2.1 Neutralizing antibodies

The humoral immune response resulting from previous exposure to one or more AAV serotypes is well documented²¹⁸. Anti-AAV Ig-G antibodies (Abs) are prevalent; 67% of the general population carries Abs against AAV1; 72% against AAV2, 40% against AAV5, 46% against AAV6, and 38% carrying Abs against AAV8, and 47% against AAV9²¹⁹⁻²²¹. This mild immune response was not correlated with any disease, which again supports the non-pathological nature of AAVs.

Despite AAVs limited packaging capacity of 4.6 kbp and preexisting neutralizing antibodies, many factors make AAVs an attractive vehicle for gene delivery. Most importantly, the ability to infect non-dividing cells²²², the absence of association with human disease, its persistent nature, the over 100 serotypes that can be used to target specific tissues and cell types, and the available molecular technology to engineer capsids, modify tropism, and alter the antigenic epitope when antibodies are present²²³.

Over 20 years followed the initial description of the AAV vector in 1984 to the first AAV-based human gene therapy trial in cystic fibrosis patients²²⁴. Promising results have been obtained from many AAV-based studies to treat a range of diseases in animal

1.9 Gene therapy

models and humans, including Pompe disease²²⁵, Parkinson's disease²²⁶, Leber's congenital amaurosis²²⁷⁻²²⁹, Batten Disease²¹⁶, hemophilia B²³⁰, Alzheimer's disease²³¹, Duchenne muscular dystrophy²³², and Canavan disease²³³. Collectively, data from pre-clinical studies and clinical trials show a minimal immune response with lack of toxicity and inflammation, and prove the safety and tolerability of rAAVs in different tissues²³⁴. These encouraging outcomes led to the first approval of the rAAV1-based drug, uniQure's Glybera, to treat lipoprotein lipase deficiency by the European Commission in 2012²³⁵.

Highlighting the importance of serotype choice and the route of administration for optimal tissue and specific cell type targeting, these studies showed that when administered systemically, the recommended capsid is/are; AAV8 for liver targeting; AAV1, AAV6 or AAV9 for targeting heart and skeletal muscles; AAV5 for targeting lung; AAV4, AAV8, and AAV9 for targeting eye; and AAV9 for targeting CNS^{218,236-238}. Importantly, AAV9 showed the best viral genome distribution and highest protein levels in different tissues following intravenous systemic administration in mice and rats^{237,239}.

When particularly targeting the CNS or a region in the CNS, AAV1, AAV5, and AAV9 induced the highest reported spread and transduction efficiency following direct inoculation into the brain parenchyma. AAV1 and AAV9 transduced neurons, whereas AAV5 transduced both neurons and glia, and AAV4 targeted astrocytes^{237,240-242}. AAV9

1.9 Gene therapy

and less efficiently AAV8, were reported to cross the BBB and transduce both neurons and glia in the brain and spinal cord following intravenous administration^{237,243-245}.

Diseases such as amyotrophic lateral sclerosis (ALS), leukodystrophies, Huntington's disease, and lysosomal storage diseases all have pathology involving the nervous system, and therefore require global delivery of a trans-gene to the brain. AAV9 is a serotype of human origin that shares 82% capsid identity to AAV2, the first AAV to be identified and used in most early studies. The two serotypes differ in the receptors that mediate their endocytosis. AAV9 uses N-linked galactose as a primary receptor and the 37/67-kilodalton laminin as a secondary receptor, whereas AAV2 primarily relies on the heparin sulphate proteoglycan receptor, and has multiple secondary receptors. Going forward from *Foust and colleague's* report "Intravascular AAV9 preferentially targets neonatal neurons and adult astrocytes", many labs reported their finding confirming the ability of AAV9 to cross the BBB in mice^{243,245-247}, rat²⁴⁸, rhesus macaque²⁴⁹, and cynomolgus macaque²⁵⁰ and differentially transduced neuronal cells in an age dependent manner, regardless of the route of administration. Establishing AAV9 as the first choice in neurodegenerative disease gene therapy trials, promising therapeutic effect has been reported in different animal models SMA²⁵¹⁻²⁵³, ALS²⁵⁴, Parkinson's disease²⁵⁵, MPS I²⁵⁶, and MPS IIIB²⁵⁷ (reviewed in^{258,259}).

Hypothesis

2.1 Hypothesis

Systemic gene therapy with a rAAV9 vector expressing the mouse *HexB* gene will ameliorate the neurological and biochemical phenotype in a Sandhoff disease mouse model.

2.2 Rationale

Monogenic diseases lacking treatment, such as GM2 gangliosidoses, are candidates for gene therapy trials. The choice of adeno-associated virus is grounded on its human safety profile. Gaining access to the CNS required the use of AAV serotype 9 that showed the highest reported tropism toward neuronal cells.

SD mice were treated either as neonates or adults to determine the therapeutic value of AAV9, if any, in both age groups since factors such as the maturity of the BBB, and the extent of GM2 ganglioside neuronal accumulation and damage, can govern the outcome of therapy.

2.3 Experimental design

To test this hypothesis, the therapeutic AAV9 vector containing the HexB-encoded cDNA (AAV9-HexB), or the control vector containing β -galactosidase- encoded cDNA (AAV9-

2.3 Experimental design

LacZ) was intravenously administrated to normal control and Sandhoff mice either as neonates or adults (n=40). Postnatal day 1 or 2 control and Sandhoff neonatal mice received a 100 µl volume single injection containing 3×10^{11} vector genomes (vg) (2.5×10^{14} vg/kg) via the superficial temporal vein (n=20), and 6 weeks (wks) old adult control and Sandhoff mice received a single injection of 7×10^{11} vg (3.5×10^{13} vg/kg) in a 100 µl volume through the tail vein (n=20) (Table 2). Mice were followed until they reached the experiment end point of 43 wks of age, or an earlier humane end point. We evaluated the therapeutic value of AAV9-HexB by monitoring the motor function, survival of mice, and measuring β -hexosaminidase serum enzyme activity during the experimental time period. GM2 ganglioside accumulation, inflammation, as well as β -hexosaminidase activity in the brain were evaluated after sacrificing the mice as they reached a humane or the experimental end point.

2.3 Experimental design

	Injection	Phenotype	Group
Neonatal (n=20)	AAV9-HexB (n=10)	Sandhoff disease	Neonatal treated SD; n SD-HexB (n=5)
		Normal control	Control; n Control-HexB (n=5)
	AVV-LacZ (n=10)	Sandhoff disease	Untreated SD; SD-LacZ (n=5)
		Normal control	Control; Control-LacZ (n=5)
Adult (n=20)	AAV9-HexB (n=10)	Sandhoff disease	Adult treated SD; a SD-HexB (n=5)
		Normal control	Control; a Control-HexB (n=5)
	AVV-LacZ (n=10)	Sandhoff disease	Untreated SD; SD-LacZ (n=5)
		Normal control	Control; Control-LacZ (n=5)

Table 2- Experimental design

Materials and Methods

3.1 Experimental animals

The Sandhoff mouse model strain *C57BL/6:C129* was a generous gift of Dr. Roy Gravel (University of Calgary, Alberta).¹⁶² The model was derived by disruption of the murine *Hexb* gene and transferring into the mouse genome through embryonic stem cell technology as described in Yamanaka et al. 1994 and Sango et al., 1995. Experimental mice were obtained from heterozygous intercrosses and held under conventional non-sterile conditions where they had free access to food and water. Access to food and water was moved closer, or placed on the bottom of the cage, for mice that had limited mobility. A humane end-point was defined as when mice were unable to obtain adequate food and water, even with accommodation for reduced mobility.

The *Hexb* genotype was determined by PCR of DNA isolated from ear clippings at 12 days using the primers and experimental conditions described previously.¹⁶² SD mice (*Hexb*^{-/-}) do not make β -hexosaminidase A or B because a neomycin resistance expression cassette is inserted into exon 2 of *Hexb*.

All procedures and care of the animals were in compliance with the Canadian Council on Animal Care and approved by the Animal Care Committee at the University of Manitoba.

3.2 Analysis of motor function.

To assess motor function, mice were analyzed in an open field test. Mice were videotaped for 15 minutes at different time points. Data collected were used to assess motor function as distance travelled, maximum speed, and number of head rotations by analysis of the videos using ANY-maze software.

3.3 Construction of rAAV2/9 viral vectors

The plasmid AAV2.1 expressing CMV promoter and the murine *Hexb* cDNA under the control of the CMV (AAV2.1 CMV-HexB), was constructed by PCR. Amplification of the 1.0 Kb HEXB from pre-existing vector, p β Hex54²⁶⁰, using two primers, sense 5'-gccggccgggagcagtcgcccgcag-3' incorporating an *EagI* restriction enzyme site, and antisense 5'-cgggatcccagaatcaacatgatcatagctgg-3' incorporating a *BamHI* restriction enzyme site, This fragment was subcloned into the AAV2.1 expressing CMV and *LacZ* cDNA (pAAV2.1 CMV-LacZ)²⁶¹ by removing the *LacZ* sequence with *EagI*/*BamHI*, and replacing it with the *Hexb* cDNA, creating pAAV2.1 CMV-HexB. The vector sequence was confirmed by dideoxy sequencing at the Toronto Centre for Applied Genomics.

The therapeutic vector containing the ITR of AAV2 and expressing *HexB* were packed inside the AAV9 capsid by triple co-transfection of human embryonic kidney (HEK) 293 cells together with pAAV2.1 CMV-HEXB, pAd Δ F6 which provides the three

3.5 Tissue and serum processing

adenoviral helper genes, and pre-viral plasmid pAAV/SP70 containing the sequence for ITR2 and AAV9 capsid gene, followed by purification as described previously.²⁶¹

The titers were determined by PCR amplification following previously described procedures²⁶¹. AAV2/9.CMV.LacZ.bGH was purchased from the University of Pennsylvania Vector Core Facility (Philadelphia, PA, USA).

3.4 Intravenous injection of rAAV9

The vector dose was administrated in a 100 µl volume under a dissecting microscope for better visualization of veins, especially the temporal vein in the neonatally injected group. The neonatal SD (n=10) and normal control (n=10) mice received 2.5×10^{14} vg/kg of rAAV9 vector expressing either HexB (n=5) or the control vector, LacZ (n=5) at postnatal day 1 or 2 in through the superficial temporal vein. The adult group of SD (n=10) or normal control (n=10) mice received 3.5×10^{13} vg/kg of rAAV9 vector expressing either HexB (n=5), or the control LacZ (n=5) at 6 wks of age through the tail vein. Normal control mice were age-matched littermates that were either wild type (*Hexb*^{+/+}) or heterozygous (*Hexb*^{+/-}) for the targeted *Hexb* gene.

3.5 Tissue and serum processing

Blood samples were collected from the saphenous vein at 10, 16, 28, and by cardiac

3.7 β -Hexosaminidase assay

puncture at 43 wks, or at the humane end point if it preceded 43 wks. Serum was collected from clotted blood samples and stored at -20°C for future assays. Organs harvested from euthanized mice were divided in two parts-one portion was snap-frozen and stored at -20°C, while the second was fixed overnight with 10% buffered formalin and processed for embedding. Before use, the frozen brain tissue was homogenized in phosphate buffered saline (PBS) at 10% weight per volume and stored at -20°C to allow it to be used for multiple assays.

3.6 Determination of vg number

The vg copy number was determined by quantitative PCR of genomic DNA extracted from brain or liver tissue that was collected at death. Primers were designed to target the bGH poly(A): BGH FW and BGH REV (5'-tctagttgccagccatctgttgt-3' and 5'tgggagtggcaccttcca-3', respectively). The probe was 5'-[6-FAM]tccccgtgccttccttgacc-[BHQ1a-Q]-3'. Samples were run on a LightCycler® 480 Instrument II (Roche, Mississauga, Canada).

3.7 β -Hexosaminidase assay

Total β -hexosaminidase activity was determined in serum or brain lysates using 4-methylumbelliferyl-2-acetamido-2-deoxy- β -D-glucopyranoside (4-MUG) or the sulfated

3.8 Protein Assay

form of 4-MUG as a substrates.²⁶² Serum sample, homogenized brain lysate, and substrate were diluted with 0.01 M phosphate citrate buffer, pH 4.4, containing 0.6% bovine serum albumin. The enzymatic reaction was carried out using 10 μ l of each sample or standard (in duplicate) mixed with 20 μ l of 3 mM substrate and incubated at 37°C for 30 minutes. The reaction was stopped by adding 970 μ l of glycine carbonate buffer, pH 9.8. Fluorescence was read at 360 nm excitation wavelength and 415 nm emission wavelength using a plate reader (SpectraMax M2e, Molecular Devicees). Total β -hexosaminidase activity was calculated using a standard curve with 20 to 800 nmole of methylumbelliferone, and lysate buffer as negative control (blank). For serum, the activity was determined per μ l, while brain activities were calculated per μ g of protein.

3.8 Protein Assay

Protein concentration in brain lysates were determined using the microplate Bradford assay with a kit supplied by ThermoFisher Scientific (Ottawa, ON) and following the manufacturer's instructions. Aliquots of diluted brain lysate and albumin standards were mixed with 200 μ l of working solution and incubated at 37°C for 30 minutes. Plates were cooled at room temperature and absorbance was read at 562 nm using a plate reader (SpectraMax M2e, Molecular Devices). The final concentration was calculated based on the standard curve.

3.9 Ganglioside analysis

Gangliosides were extracted from brain homogenates (300 mg of protein) with a chloroform-methanol (1:2) mixture and G_{M2} was phase partitioned using chloroform: methanol:ddH₂O (1:2:1.4). The upper phase containing G_{M2} ganglioside was collected, dried, suspended in ddH₂O and dialyzed against water using an 8000 kDa cut-off membrane. After drying, the sample was dissolved in 100 µl of chloroform: methanol: ddH₂O (60:30:4.4), and half was spotted alongside monosialoganglioside standards (Matreya LLC, Pleasant Gap, PA) on a high performance thin layer chromatography (HPTLC) silica gel 60 plate with a concentrating zone (Millipore Canada Ltd, Etobicoke, ON), and separated using 55:45:10 chloroform: methanol: 0.2% CaCl₂ as the mobile phase. The bands were visualized with resorcinol reagent and the plates were dried at 100°C for 30 minutes. Densitometry to quantify the bands was performed with a BioRad ChemiDoc MP instrument and using Image Lab™4.1 Software.

3.10 Histology and microscopy

For evaluation of cytoplasmic vacuolation, 1.5 micron paraffin-embedded brain sections were stained with toluidine blue (TB). Paraffin-embedded tumour, tissues were sectioned at 3 microns and stained with hematoxylin and eosin to evaluate overall morphology of tumor tissues. Immunohistochemical detection of microglia was performed on 5 micron brain sections with a 1/50 dilution of the mouse monoclonal

3.12 Analysis of AAV9 insertion sites

anti-F4/80 (AbD Serotec, Cederlane Laboratories, Burlington, ON). The primary antibody was detected with biotinylated goat anti-rat IgG (Invitrogen, ThermoFisher Scientific), followed by an avidin-linked horse-radish peroxidase and the 3, 3'-diaminobenzidine substrate (Vector Laboratories [Canada] Inc., Burlington, ON). Slides were viewed with a Zeiss AxioCam A1 compound microscope equipped with a colour AxioCam MRc camera, and photomicrographs were processed using AxioVision software.

3.11 Semi-quantitative histology scoring

Toluidine blue stained brain sections were scored according to the severity of cytoplasmic vacuolization observed with Zeiss AxioCam A1 compound microscope equipped with a colour AxioCam MRc camera using 20x power. 10 to 30 fields in each region of the brain were scored between 0, indicating no vacuoles, and 5 indicating severely vacuolated.

3.12 Analysis of AAV9 insertion sites

The sequencing library was prepared as previously described, isolating AAV-containing fragments via linker-mediated PCR²⁶³. The first round of PCR used the AAV ITR primer, 5'-GGAGTTGGCCACTCCCTCTCTG-3' and the linker primer, 5'-GTAATACGACTCACTATAGGGCACGCGTG-3' using cycle conditions of 95°C for 2 minutes followed by 25 cycles of 95°C for 15 seconds, 55°C for 30 seconds and 72°C for 1 minute.

3.12 Analysis of AAV9 insertion sites

The resulting amplicons were diluted 1:50 and a second PCR was performed with AAV ITR nested primer, 5'-TCTCTGCGCGCTCGCTCG-3' and nested linker primer, 5'-GCGTGGTCGACTGCGCAT-3'. Cycle conditions were 95°C for 2 minutes followed by 20 cycles of 95°C for 15 seconds, 58°C for 30 seconds, and 72°C for 1 minute. The sequence barcodes on the linkers were used here to both differentiate the AAV samples, and to multiplex the samples with unrelated samples. Each sample received two barcodes. Integration sites were identified by using AAV_GelST, a modification of the GelST program used for murine leukemia virus (MLV) detection²⁶⁴. The steps that had trimmed the MLV long terminal repeat were each replaced with a step that trimmed the portion of the AAV ITR matching the ITR primer used in the second round of linker-mediated PCR, and a step that trimmed the remainder of the variable-length ITR. All versions of GelST are designed to identify the junction at which viral DNA meets cellular genomic DNA. As such, the program requires that each amplicon contain both viral DNA and genomic DNA, thereby filtering out potential episomal contamination. AAV_GelST used BamTools version 2.3.0, Cutadapt version 0.9.3, and Bowtie version 0.12.7, and aligned reads to assembly GRCm38²⁶⁵⁻²⁶⁷. A minimum cut off of 30 fragments per integration per barcode was employed as a means of filtering out spurious alignments. The 415 putative integrations that mapped within *Hexb* (chr13:97,176,332-97,198,357) were discarded, as these reads were more likely to represent amplification of the vector than actual integration event.²⁶⁸ The integrations were annotated using Ensembl genes 75, downloaded from BioMart^{269,270}. The DNA sequences used for these analyses have been

deposited in GenBank as BioProject PRJNA257830.

3.13 Statistical analyses

All statistical analyses were performed using GraphPad V6 software. The log-rank (Mantel-Cox) test was used for the analysis of survival and a one way ANOVA was used to analyze the increase in mice life span, motor activity and the severity of vacuolization in different regions of the brain. For all other analyses unpaired one or two-tailed Student's t-tests were used to test significance. Significance was taken as $P < 0.05$.

Results

4.1 Impact of AAV9-HexB on survival

To evaluate the efficacy of a single intravenous injection of rAAV9 expressing the mouse *Hexb* cDNA (AAV9-HexB) in ameliorating the biochemical and neurological phenotype in SD, AAV9-HexB or AAV9-LacZ (β -galactosidase expressing control vector) was administered to postnatal day 1 or 2 neonates (2.5×10^{14} vector genomes [vg]/kg via superficial temporal vein), and 6-week (wk) old adults (3.5×10^{13} vg/kg via tail vein). Mice were followed until they reached 43 wks of age, or a humane end point (see Materials and Methods).

4.1 Impact of AAV9-HexB on survival

Progressive neuronal damage in untreated SD mice (*Hexb*^{-/-}) results in their death before five month of age²⁷¹. In our study, untreated SD mice (SD-LacZ injected) showed severe paralysis and/or frequent tonic seizures that impaired their ability to obtain food and water, and were all humanely sacrificed by the 17th wk of age. This pattern of disease progression was closely monitored in the two SD groups treated with AAV9 vector expressing the HexB gene, adult- and neonatally-treated SD mice, and normal control (*Hexb*^{+/-} or *Hexb*^{+/+}) mice until 43 wks.

A significant extension of the life span of SD mice was observed in AAV9-HexB treated groups (**Fig.5**). Compared to AAV9-LacZ injected SD mice (SD-LacZ), with a median survival of 17 wks (mean=16 wks), a single intravenous injection of AAV9-HexB

4.1 Impact of AAV9-HexB on survival

into neonatal SD mice (n SD-HexB) was sufficient to ensure their long-term survival with P value of < 0.0001 (mean= 43 wks, **Fig.5**); the n SD-HexB mice were sacrificed at the experimental end point of 43 wks with no evidence of paralysis or seizures although two exhibited a slight tremor and three had a minor tendency to clasp their limbs on a tail suspension test.

The prolonged life span within the five adult SD-treated mice (a SD-HexB) that received the rAAV9-HexB intravenous treatment at 6 wks was highly variable (**Fig.5**). Each mouse of the adult SD-HexB (n=5) treated group reached a humane end point at a different age (17, 18, 19, 23, and 35 wks), with a median of 19 wks and P value < 0.01 (mean = 22.4 wks, **Fig.5**), demonstrating a possible beneficial outcome even when rAAV9 intravenous treatment is delayed.

4.1 Impact of AAV9-HexB on survival

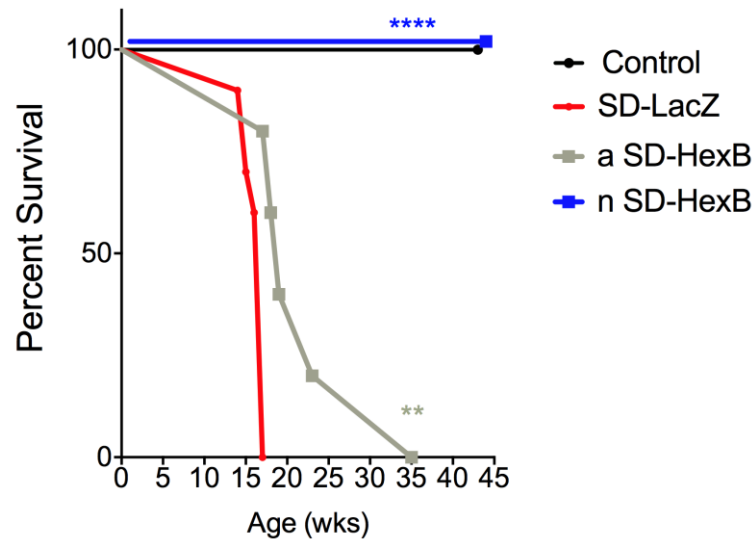


Figure 5- Survival of rAAV9-injected mice.

SD or control mice were injected as neonates or adults with AAV9-LacZ or AAV9-HexB and monitored for up to 43 wks. Each point represents the percentage of the mice surviving at that time. Note that AAV9-HexB injected neonates (n=5) were the only control animals held to 43 wks because other controls were sacrificed at the same time as their LacZ-injected or adult-treated SD counterparts. Control (n=5); SD-LacZ (n=10); a SD-HexB (n=5); n SD-HexB (n=5). ** $P < 0.01$; **** $P < 0.0001$.

4.2 Impact on motor activity of SD mice

The impaired motor activity typically observed in the SD mouse model became evident at 12 wks of age as a gait abnormality and tremors, which advanced to spasticity, seizures, and severe muscle atrophy observed as total paralysis by the 16th wk. To determine if administration of AAV9-HexB improved motor activity in the adult- and neonatally-treated SD mice, we used an open-field test to analyze distance travelled as a general indicator of the motor cortex function²⁷², and maximum speed as an indicator of muscle strength. We also analyzed number of head rotations as an indicator of the function of the cerebellum in motor coordination^{273,274} (Ito et al. 1974, Ito 1993) starting at 14 wks when motor deterioration in SD mice is predictably severe, and continued to 30 wks.

During the testing period, neonatal SD mice injected with AAV9-HexB showed no sign of impaired locomotion, travelled at a comparable rate to the normal control, and were significantly more active than the untreated SD AAV9-LacZ injected mice (**Fig. 6**). In contrast, the SD mice injected with AAV9-HexB as adults had a similar activity level to that of the untreated SD AAV9-LacZ injected mice ($P > 0.05$; **Fig. 6**), but the decline in motor activity in the adult treated SD-HexB group extended over a longer time period compared to the SD-LacZ mice, indicating a delay in disease progression, which we believe to be worth noting albeit not statistically significant (**Fig. 6**).

4.2 Impact on motor activity of SD mice

When comparing head rotations, neonatal SD mice treated with AAV9-HexB as neonates had a significantly higher number than that observed in SD mice injected with AAV9-LacZ at all time points leading up to the end point (**Fig. 7**, $P < 0.01$). Similar to the survival curve, adult AAV9-HexB treated SD mice showed no statistically significant improvement in head rotations (**Fig. 7**).

The parameter maximum speed gave similar results to those observed for distance travelled and head rotations. SD mice that received the AAV9-HexB treatment as neonates moved at a similar speed to the normal controls at all time points (**Fig. 8**, $P < 0.01$), whereas SD mice that received the treatment at 6 wks showed a reduced speed indicating weakening comparable to LacZ-injected mice (**Fig. 8**).

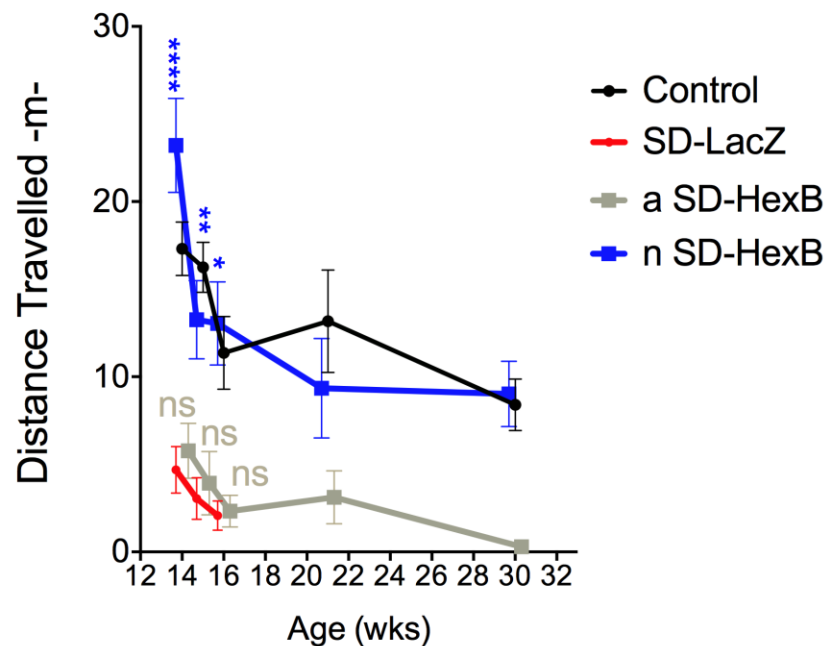


Figure 6- Evaluation of motor cortex function.

Mice were videotaped in an open field for 15 minutes duration at 3-5 time points after administration of the rAAV9, and the distance travelled was analyzed using ANY-maze software. Values at each time point represent the mean \pm SEM. The control group includes mice injected as neonates or adults with either LacZ or HexB, as no significant difference was found among these groups (Table 4). No statistical comparison of the HexB and LacZ-injected SD mice was possible after 16 wks because all members of the comparison groups had died; however, there was no statistically significant difference between the n HexB-treated SD group and the control group group. * $P < 0.05$; ** $P < 0.01$; *** $P < 0.001$; **** $P < 0.0001$; ns-not significant.

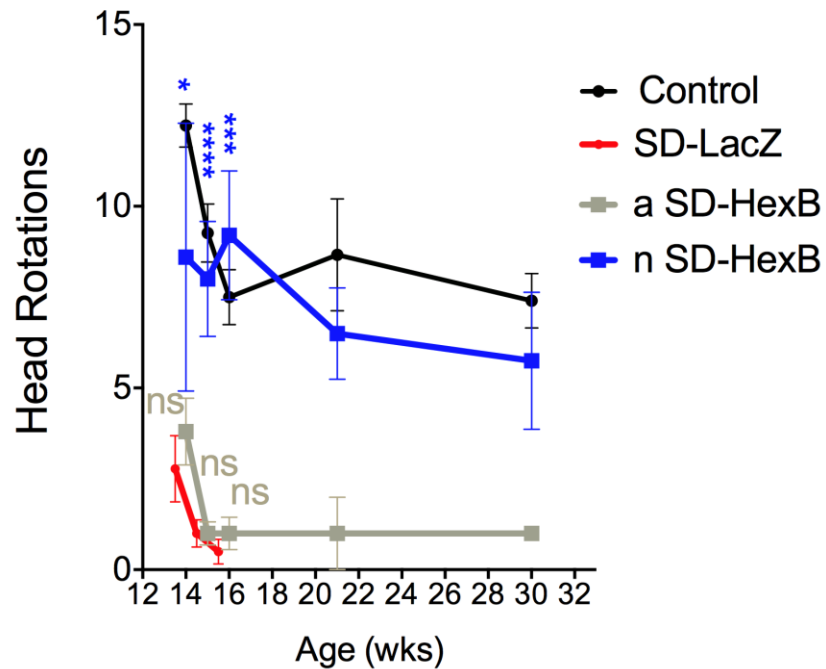


Figure 7- Evaluation of motor coordination.

Mice were videotaped in an open field for 15 minutes duration 3-5 time points after administration of the rAAV9, and head rotations was analyzed using ANY-maze software. Values at each time point represent the mean \pm SEM. The control group includes mice injected as neonates or adults with either LacZ or HexB, as no significant difference was found among these groups (Table 4). No statistical comparison of the HexB and LacZ-injected SD mice was possible after 16 wks because all members of the comparison groups had died; however, there was no statistically significant difference between the n HexB-treated SD group and the control group. * $P < 0.05$; ** $P < 0.01$; *** $P < 0.001$; **** $P < 0.0001$; ns-not significant.

4.2 Impact on motor activity of SD mice

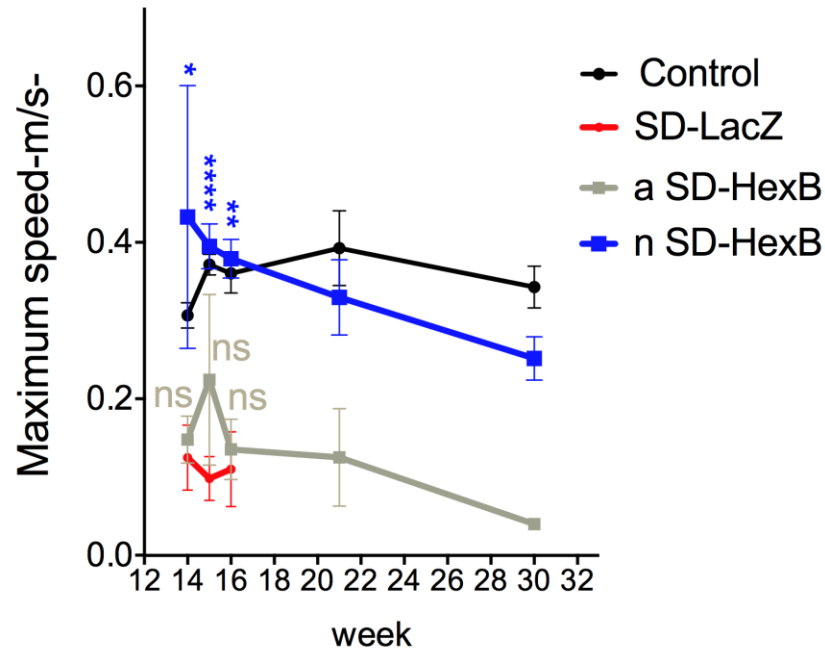


Figure 8- Evaluation of muscle strength.

Mice were videotaped in an open field for 15 minutes duration 3-5 time points after administration of the rAAV9, and speed was analyzed using ANY-maze software. Values at each time point represent the mean \pm SEM. The control group includes mice injected as neonates or adults with either LacZ or HexB, as no significant difference was found among these groups. No statistical comparison of the HexB and LacZ-injected SD mice was possible after 16 wks because all members of the comparison groups had died; however, there was no statistically significant difference between the n HexB-treated SD group and the control group. * $P < 0.05$; ** $P < 0.01$; *** $P < 0.001$; **** $P < 0.0001$; ns-not significant.

4.3 Effect of AAV9-HexB treatment on GM2 ganglioside storage

The increased survival and motor activity in SD mice treated neonatally with AAV9-HexB suggested that the intravenously administered viral vector had crossed the BBB and reduced the level of GM2 ganglioside storage preventing or, at least slowing down, the neuronal death. To assess GM2 ganglioside in the brain, we used TB staining to visualize the extent of lysosomal vacuolization (**Figs. 9,10**), and HPTLC, after chloroform/methanol isolation of the brain ganglioside fraction, to examine the ganglioside levels after chloroform/methanol isolation (**Figs. 11,12**).

Histologically, extensive accumulations of GM2 ganglioside caused pathological alterations in the shapes of neuronal cells, which appeared as cytoplasmic swelling and vacuolization, and was evident in the brains of untreated SD AAV9-LacZ mice (**Fig. 9**). In the adult AAV9-HexB treated SD group, the extent of vacuolization was similar to that was observed in SD-LacZ mice, whereas as all SD mice treated as neonates with AAV9-HexB showed a substantial reduction in vacuolization all over the brain (**Fig. 9**). A semi-quantitative analysis of the severity of vacuolization observed in TB stained brain sections in each mouse was performed, showing significant reduction in vacuolization in all regions of the neonatally AAV9-HexB treated SD mice ($P<0.0001$). Adult AAV9-HexB treated SD mice showed a minor reduction of vacuolization that was significant only in

4.3 Effect of AAV9-HexB treatment on GM2 ganglioside storage

three brain regions; the cerebral cortex/hippocampus, the thalamus/hypothalamus/septum, and olfactory bulb (**Fig. 10**). When compared to the normal control group (n=20), neonatally AAV9-HexB treated SD mice still had a significant increase in vacuolization although not as that severe as that in adult AAV9-HexB treated SD mice (**Fig. 10**).

Biochemical analysis using HPTLC supported these findings as GM2 ganglioside was not detectable in normal mice, and at reduced levels in SD mice injected with AAV9-HexB as neonates (**Figs. 11,12**). In contrast, GM2 ganglioside levels were significantly higher in SD mice injected with AAV9-LacZ or AAV9-HexB (as adults), than normal or SD mice treated with AAV9-HexB as neonates (**Figs. 11,12**).

4.3 Effect of AAV9-HexB treatment on GM2 ganglioside storage

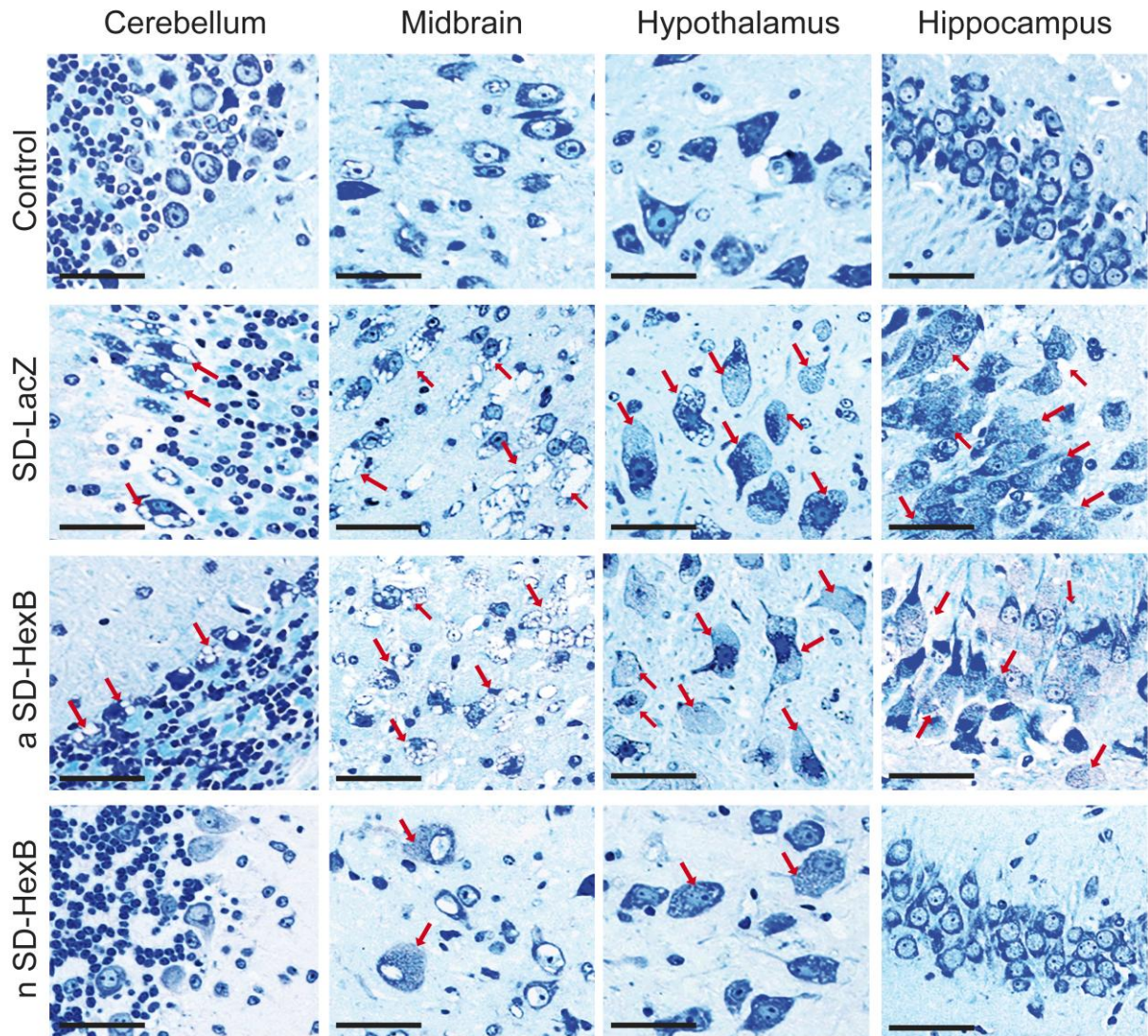


Figure 9- Histological assessment of GM2 ganglioside accumulation.

Brains from SD and age-matched normal control mice were collected at either the humane end point (17-19 weeks) or the end of the study at 43 wks. TB stained paraffin sections (1.5 microns) were examined for vacuolization using a compound microscope. Representative images are shown for three different brain regions. Original photos were taken at 20X; scale bars represent 50 μ m.

4.3 Effect of AAV9-HexB treatment on GM2 ganglioside storage

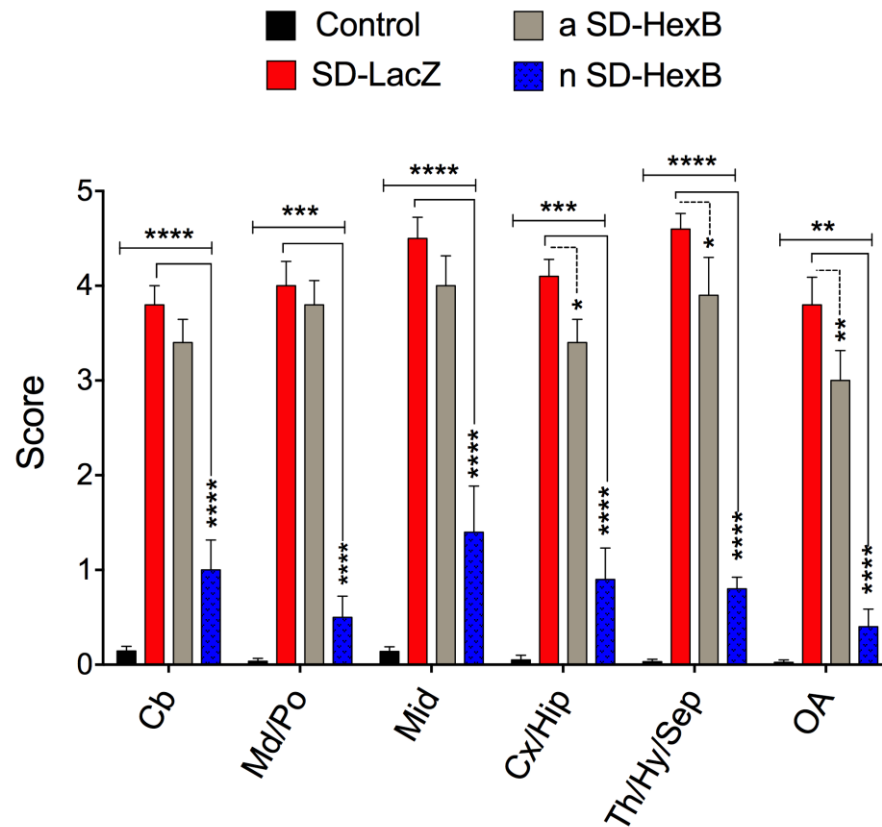


Figure 10- Semi-quantitative analysis of cellular vacuolization.

Multiple fields (10 to 30) in each region of the brain were scored based on severity of vacuolization with 0 indicating no vacuoles and 5 indicating severely vacuolated. Columns represent the mean \pm SEM. The control group includes mice treated as neonates or adults with either LacZ or HexB (n=20), as no significant difference was found among these groups (Table 4); SD-LacZ (n=10); a SD-HexB (n=5); n SD-HexB (n=5). Cb- cerebellum; Md- medulla; Po- Pons; Mid- midbrain; Cx- cerebral cortex; Hip- hippocampus; Th-thalamus; Hy- hypothalamus; Sep-septum; OA- olfactory bulb. *P<0.5; **P<0.01; ***P<0.001 ****P<0.0001.

4.3 Effect of AAV9-HexB treatment on GM2 ganglioside storage

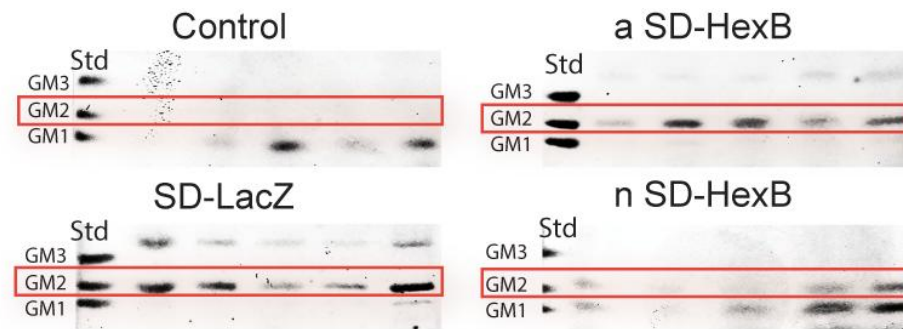


Figure 11- HPTLC analysis of ganglioside content.

Gangliosides isolated from flash-frozen brains as well as ganglioside standards were separated by HPTLC and detected with resorcinol. Samples from the brains of all 5 mice in the adult (a) SD-HexB group, and neonatal (n) SD-HexB group are shown as well as 5 representative samples from the normal control and SD-LacZ injected groups. The position of GM2 ganglioside is indicated by a red box. Although no standard was included on the plates for GA2, the upper band that is more abundant in SD mice injected with AAV9-LacZ is likely to be GA2.

4.3 Effect of AAV9-HexB treatment on GM2 ganglioside storage

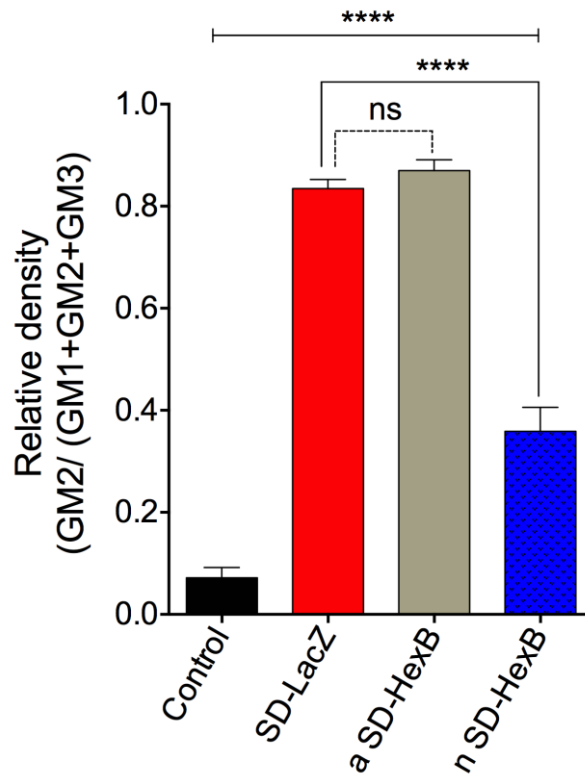


Figure 12- Densitometry-based quantification of GM2 ganglioside in the brain.

HPTLC plates of brain gangliosides were analyzed by densitometry and GM2 ganglioside levels are represented as a proportion of the combined total of GM1, GM2, and GM3 ganglioside levels. Control (n=20); SD-LacZ (n=10); a SD-HexB (n=5); n SD-HexB (n=5). *P<0.05, **P<0.01, ***P<0.001, ****P<0.0001, ns-not significant.

4.4 β -Hexosaminidase analyses

Enzymatic activities in serum and brain were determined fluorometrically using the synthetic substrate 4-MUG that can be cleaved with both Hex A and Hex B, and 4-MUGS that can be cleaved more efficiently by Hex A.

Total serum β -hexosaminidase activity was significantly higher at all tested time points in all AAV9-HexB treated mice including the normal control (**Figs. 13,14**). Although there was a notable decrease in β -hexosaminidase over time in the neonatally treated group, both AAV9-HexB-treated adult and neonatal groups had significantly higher levels of activity than the LacZ-treated controls at the end of the study (Fig. 11). The increased serum β -hexosaminidase activity indicated successful and sustained transduction of non-central nervous system tissues, especially the liver, but may not reflect the rAAV9 transduction levels in the brain.

Total brain β -hexosaminidase activity levels were also measured in lysates prepared from brains collected at the endpoint when mice were sacrificed (**Fig. 15**). Consistent with the level of brain GM2 ganglioside, brain β -hexosaminidase activity in neonatal mice injected with AAV9-HexB was between 82 and 594 nm/ μ g/h of protein, significantly higher than the levels in AAV9-LacZ-injected SD mice (between 11 and 39 nm/ μ g/h, $P < 0.01$; **Fig. 15**). The levels of β -hexosaminidase activity in adult SD mice injected with AAV9-HexB did not differ significantly from those injected with AAV9-LacZ,

4.4 β -Hexosaminidase analyses

indicating that the level of transduction in the brain was low and/or not sustained until the humane end point.

Brain β -hexosaminidase activity measured using 4-MUGS as the substrate, showed no increased in activity in SD mice treated as neonates. The level of activity was similar to SD-LacZ group, indicating that the increase in the total brain β -hexosaminidase activity was due to the formation of the $\beta\beta$ dimer Hex B enzyme (**Fig. 16**).

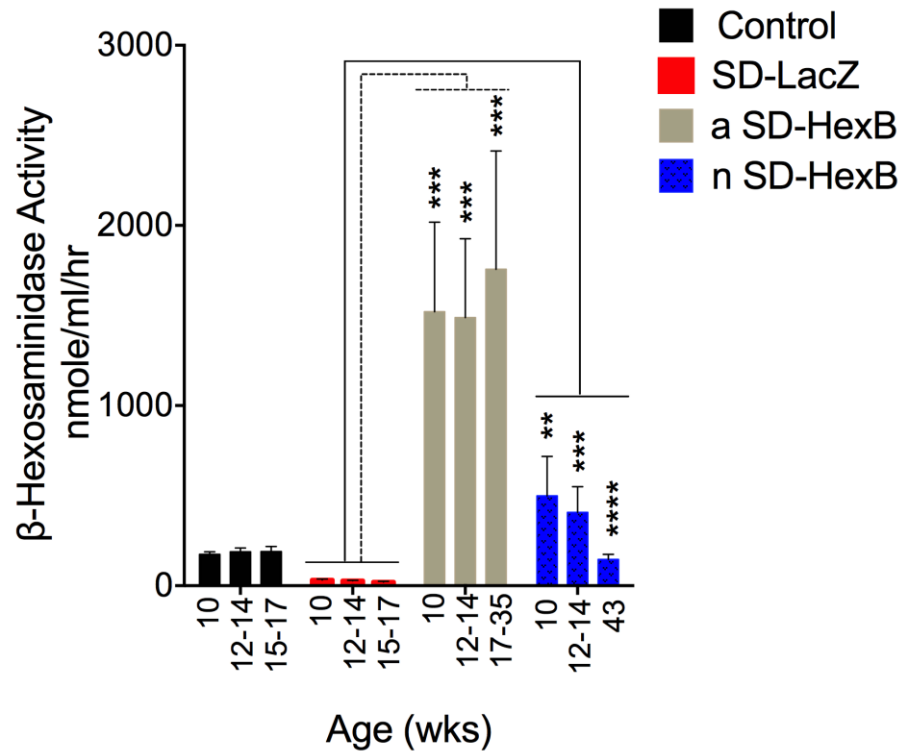


Figure 13- Serum β -hexosaminidase enzyme activity.

Effect of AAV9-HexB injection on serum β -hexosaminidase activity using the substrate, 4-MUG. Columns represent the mean β -hexosaminidase activity per ml of serum \pm SEM and include the values collected at each time point. For both representation and statistical analyses of the enzyme activity only the 10 normal animals injected as adults or neonates with AAV9-LacZ (n=10) are shown in the control group to allow for comparison to normal enzyme levels. As expected, the β -hexosaminidase activity levels in normal adults and neonates injected with AAV9-HexB (n=10) are significantly higher than normal (Table 4), and therefore were excluded from the control group in this Figure. Control (n=10); SD-LacZ (n=10); a SD-HexB (n=5); n SD-HexB (n=5). **p<0.01; ***p<0.0001; ****p<0.00001.

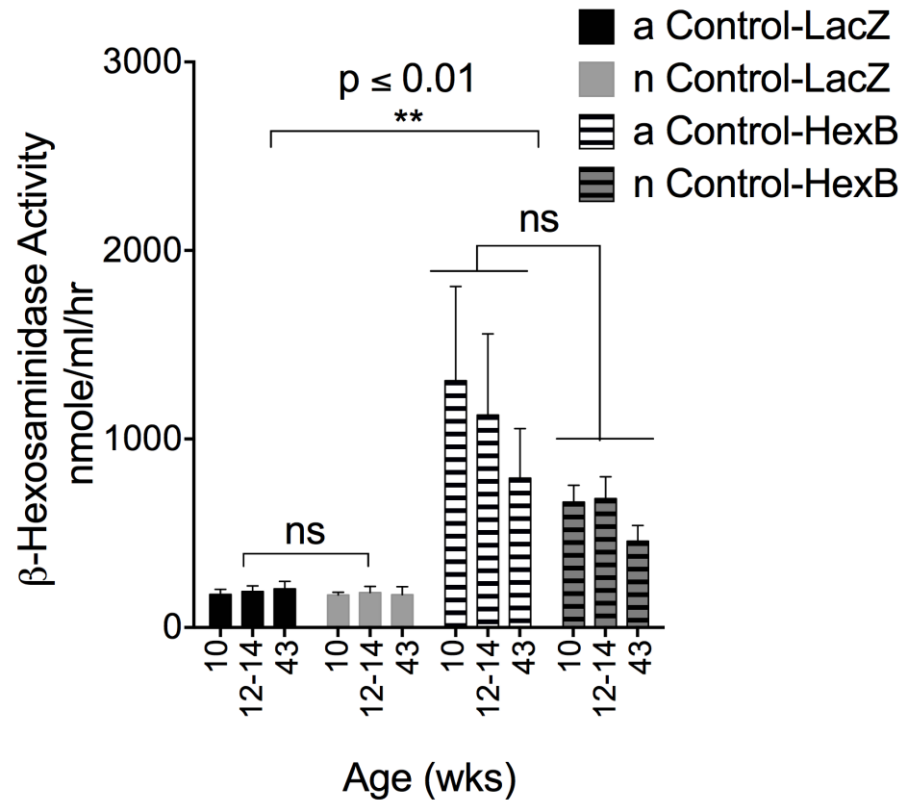


Figure 14- β -hexosaminidase activity levels in control groups.

Total β -hexosaminidase activity was determined using 4-MUG as a substrate. Bars represent the average activity + SEM. Sera were collected at 10, 12-14, and 15-43 wks (just before death). Control animals injected with HexB had significantly more activity than normal LacZ-injected mice. Therefore only LacZ-injected mice were included in Fig.11 of this thesis as controls. a Control-LacZ (n=5); a Control-HexB (n=5); n Control-LacZ (n=5); n Control-HexB (n=5). **p<0.01; ns-not significant.

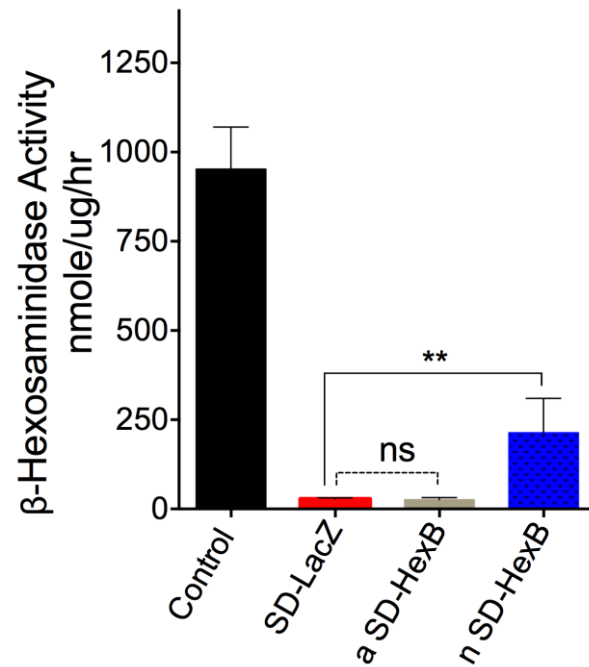


Figure 15- 4-MUG Brain β -hexosaminidase enzyme activity.

Effect of AAV9-HexB injection on brain β -hexosaminidase activity. Lysates prepared from a portion of the brain frozen immediately after sacrifice, was used for determination of β -hexosaminidase activity using the substrate, 4-MUG. The columns represent mean brain β -hexosaminidase activity normalized to protein \pm SEM. For both representation and statistical analyses of the enzyme activity only the 10 normal animals injected as adults or neonates with AAV9-LacZ (n=10) are shown in the control group to allow for comparison to normal enzyme levels. Control (n=10); SD-LacZ (n=10); a SD-HexB (n=5); n SD-HexB (n=5). **p<0.01; ns-not significant.

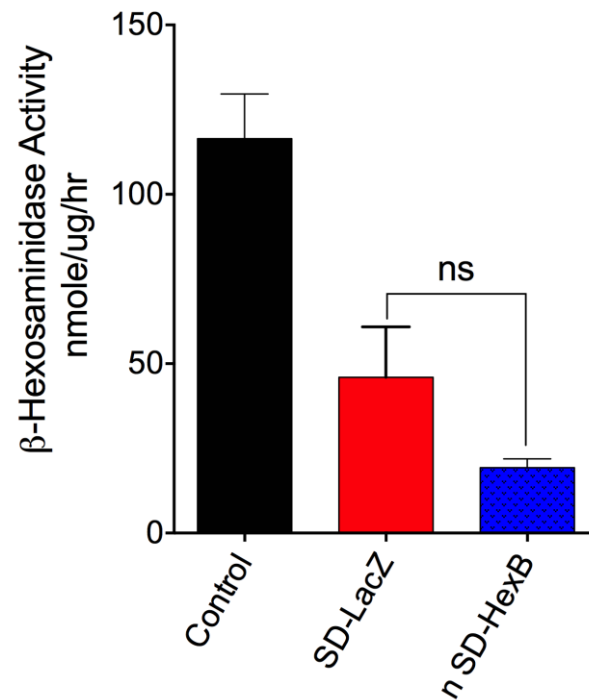


Figure 16- 4-MUGS Brain β -hexosaminidase enzyme activity.

Effect of AAV9-HexB injection on brain β -hexosaminidase activity using the substrate, 4-MUGS. Columns represent the mean β -hexosaminidase activity per ml of serum \pm SEM. Control (n=7); SD-LacZ (n=3); n SD-HexB (n=5). ns-not significant.

4.5 Inflammation in the brains of AAV9-HexB treated mice

Inflammation has been demonstrated to be an important mediator of neurodegeneration in SD mice, and as microglia and brain macrophages^{275,276} are the major phagocytic cells of the brain, activation of these cells is associated with neural cell dysfunction and death. We qualitatively evaluated the level and/or activation of the mononuclear phagocytic cells in the CNS expressing the F4/80 surface marker in the brains²⁷⁷ of AAV9-HexB or -LacZ injected SD and normal control mice.

During inflammation, activated microglia cells, brain macrophage as well as infiltrated monocytes, if present, show an increase expression of F4/80 antigen²⁷⁶, which indicated by strong orange/brown staining in **Fig. 17**. Abundant F4/80 expression was observed in AAV9-LacZ injected SD mice compared to AAV-LacZ or -HexB injected control and AAV9-HexB injected neonatal SD mice (**Fig. 17**). However, in AAV9-HexB injected adult SD mice, the level of F4/80 expression was similar to that in the AAV9-LacZ injected SD mice (**Fig. 17**), whereas in AAV9-HexB injected neonatal SD mice showed lower level of expression. Although neuroinflammation, indicated by the F4/80 expression, was still clearly evident in neonatally treated SD mice, in general, decreased neuroinflammation was associated with decreased GM2 ganglioside storage.

4.5 Inflammation in the brains of AAV9-HexB treated mice

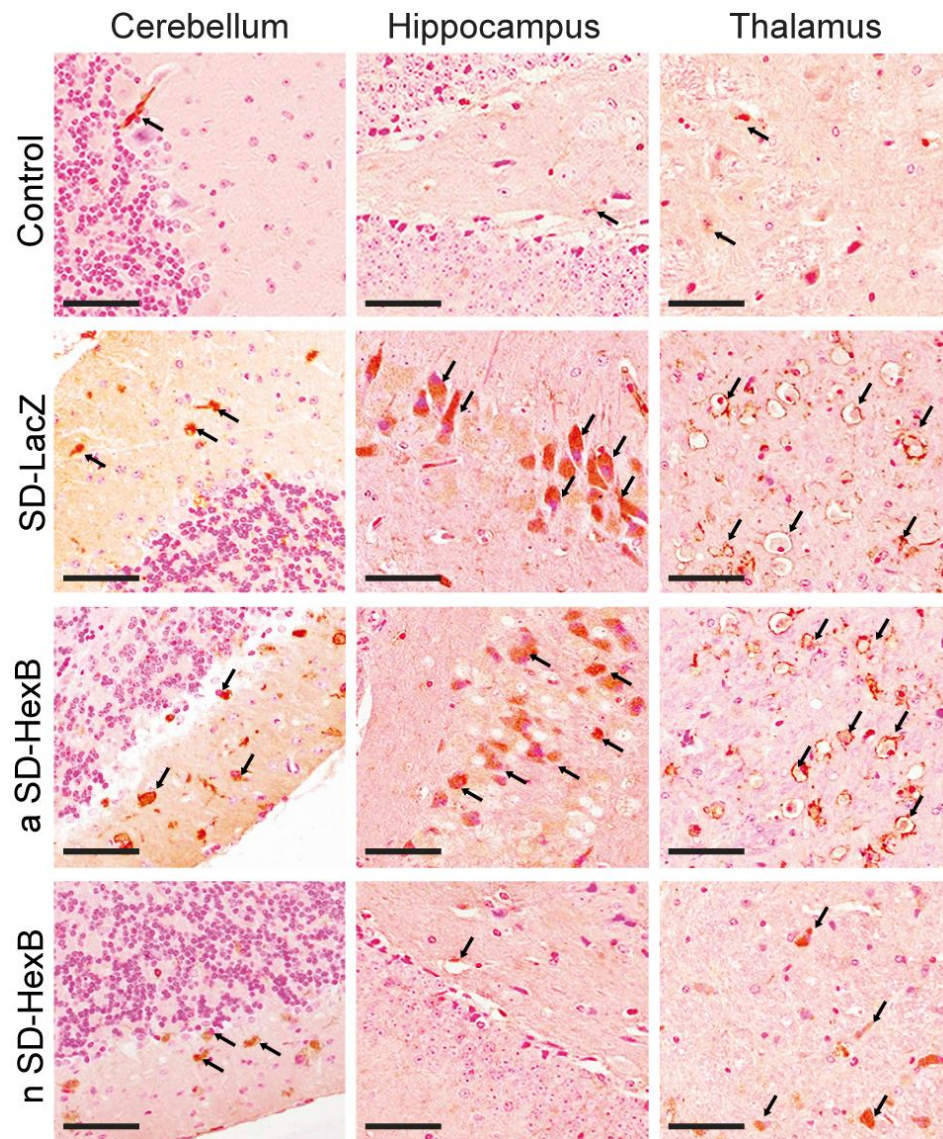


Figure 17- Brain inflammation.

Immunohistochemistry with the F4/80 antibody that detects mononuclear phagocytic cells was used to examine brain sections from mice after they reached a humane end point; 15-17 wks (SD-LacZ), 17-35 wks (a SD-HexB), or the experimental end point of 43 wks for n SD-HexB group and control group. Each panel represents a different section of the brain and the brown staining indicates activated glial cells (arrows). Original photos taken at 20X; scale bars represent 50 μ m.

4.6 Copy number in the brain and liver of rAAV9 treated mice

The vg copies per diploid genome (dg) in mice treated as neonates or adults were determined in both the brain and liver by quantitative PCR. Given that the dose per kg was approximately 7 fold lower in adult-treated mice, we expected fewer cells to be transduced in adult brains.

As shown in Fig. 18, the number of vg in the brain of adult-injected mice was variable, with a mean of 0.63 vg/dg, more than 9-fold lower than the mean of 6 vg/dg in neonates. However, the opposite was found in the liver (**Fig. 18**), with a mean of 272 vg/dg in adult injected mice, approximately 10 fold higher than the mean of 22 vg/dg in neonatally injected mice. Although different doses of virus were introduced into adults and neonates, it appears that the brain is less readily transduced in adults.

4.6 Copy number in the brain and liver of rAAV9 treated mice

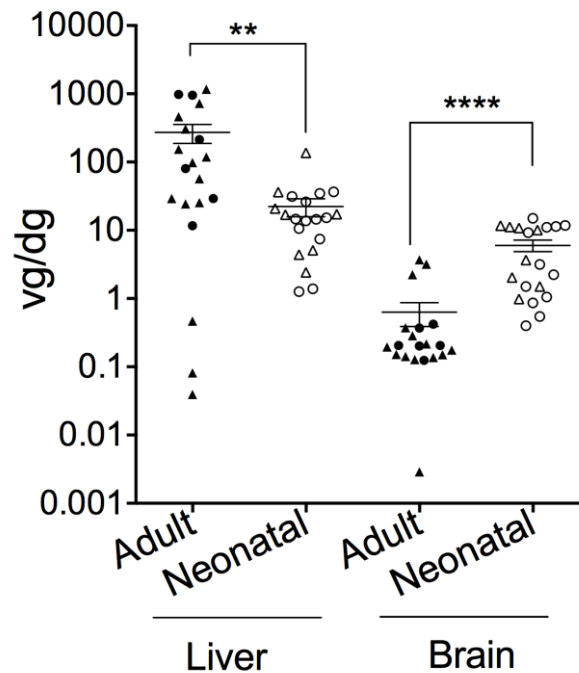


Figure 18- AAV9 vg copy number

AAV9 vg copy number in the brains and livers of rAAV9-treated mice. PCR quantification of the AAV9 vg copy numbers were performed on DNA isolated from frozen liver or brain tissue lysates and calculated per diploid genome (dg). Scatter plot of the vg copy number in liver and brain. Male (triangle) and female (circle) mice injected as adults (closed fill) and neonates (open fill) showed no significant difference in transduction efficiencies (Table 5). All points are plotted (n=20 for each group) and the horizontal line represents the mean, and the vertical line represents the SEM. **indicates $p < 0.01$ and **** indicates $p < 0.0001$.

4.7 Tumour pathology in rAAV9 treated mice

At the 43 wks experimental end point, we performed a gross examination of organs as part of necropsy, which revealed the presence of tumours in eight of ten neonatally AAV9-HexB injected SD and control mice; seven animals had liver tumours and one had multiple lung tumours.

Tumours were not observed in the mice that reached a humane end point at 24 wks or earlier, or in the single pair of adult mice that survived for 35 wks, suggesting that these tumours had developed only in the neonatally injected mice as they aged. The pathology report based on hematoxylin and eosin stained paraffin sections from the liver tumours indicated benign hyperplasia, but did not rule out hepatocellular adenoma (**Fig. 19**).

Tissue from the tumours, which contained numerous nodules as well as normal tissue, was also used for the analysis of insertion sites using inverse PCR and linker-ligation mediated PCR to amplify junctions between the AAV vectors and mouse cellular DNA using two unique barcodes per sample. Among the 579 unique integration sites we mapped, we found chromosome 2 to have the highest absolute number of integrations, while the Mir341 gene on chromosome 12 had the highest rate of insertion per kb of DNA (**Fig. 20**). Insertions in the previously identified hepatocellular carcinoma site in *Rian*²⁷⁸ were present in 2 mice injected neonatally with AAV9-HexB, one SD and one

4.7 Tumour pathology in rAAV9 treated mice

control. A unique insertion site in the growth factor receptor gene- *FGFR2*, a known cause of lung cancer²⁷⁹, was found in the sample that exhibited lung tumours.

Every tumour sample was run in two replicas, and when an insertion site was identified in both replicates with more than 30 fraction numbers, it was assigned with the highest confidence (**Table 3**).

b

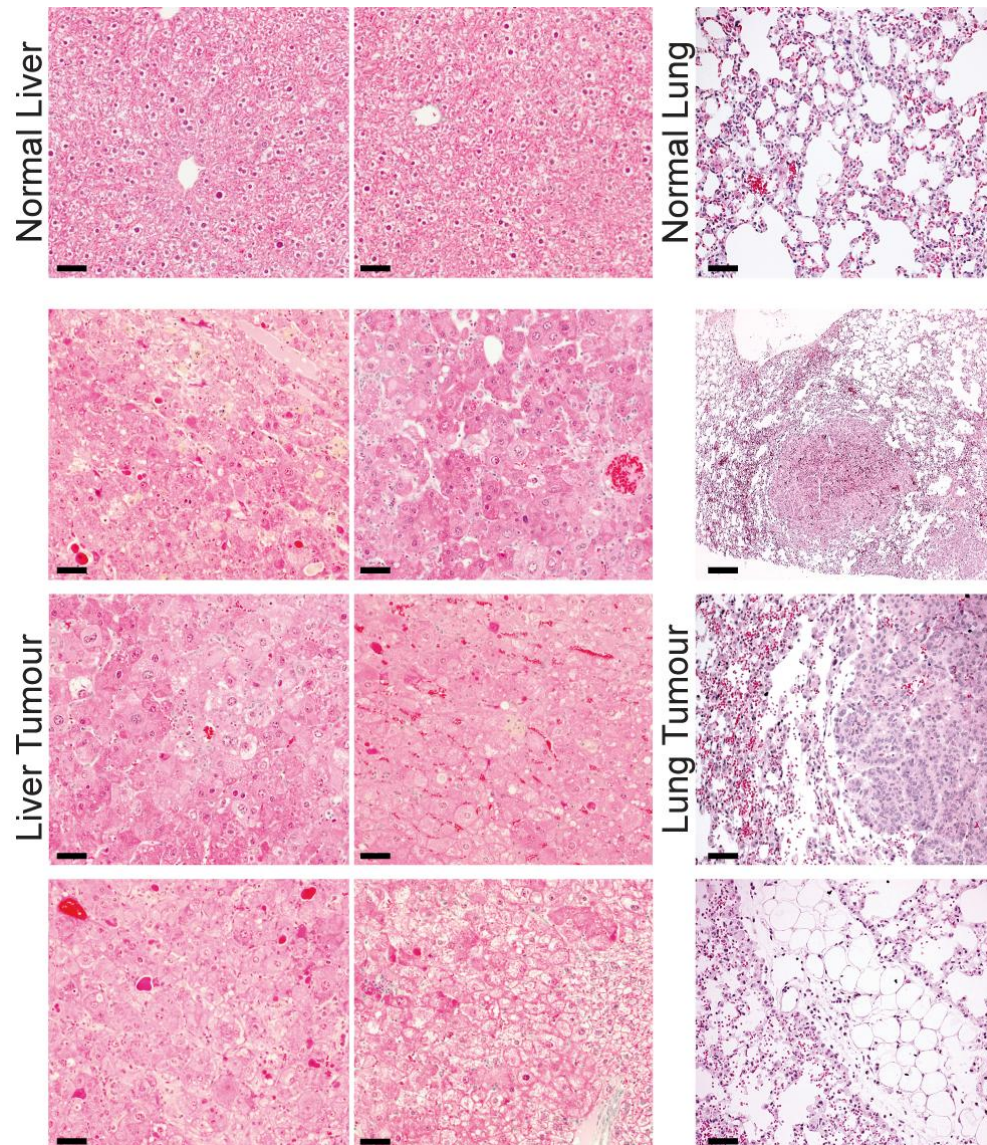


Figure 19- Histological analysis of tumor tissues.

Paraffin sections (5 microns) prepared from tumors collected at 43 wks as the animals were sacrificed, and stained with hematoxylin and eosin. The top panel is from normal liver and lung tissue and the bottom three panels are from tumor tissue. a) Images of normal liver and liver tumors from independent mice. b) Images of normal lung and lung tumor. Images taken at 20X magnification. Scale bars represent 50 μ m.

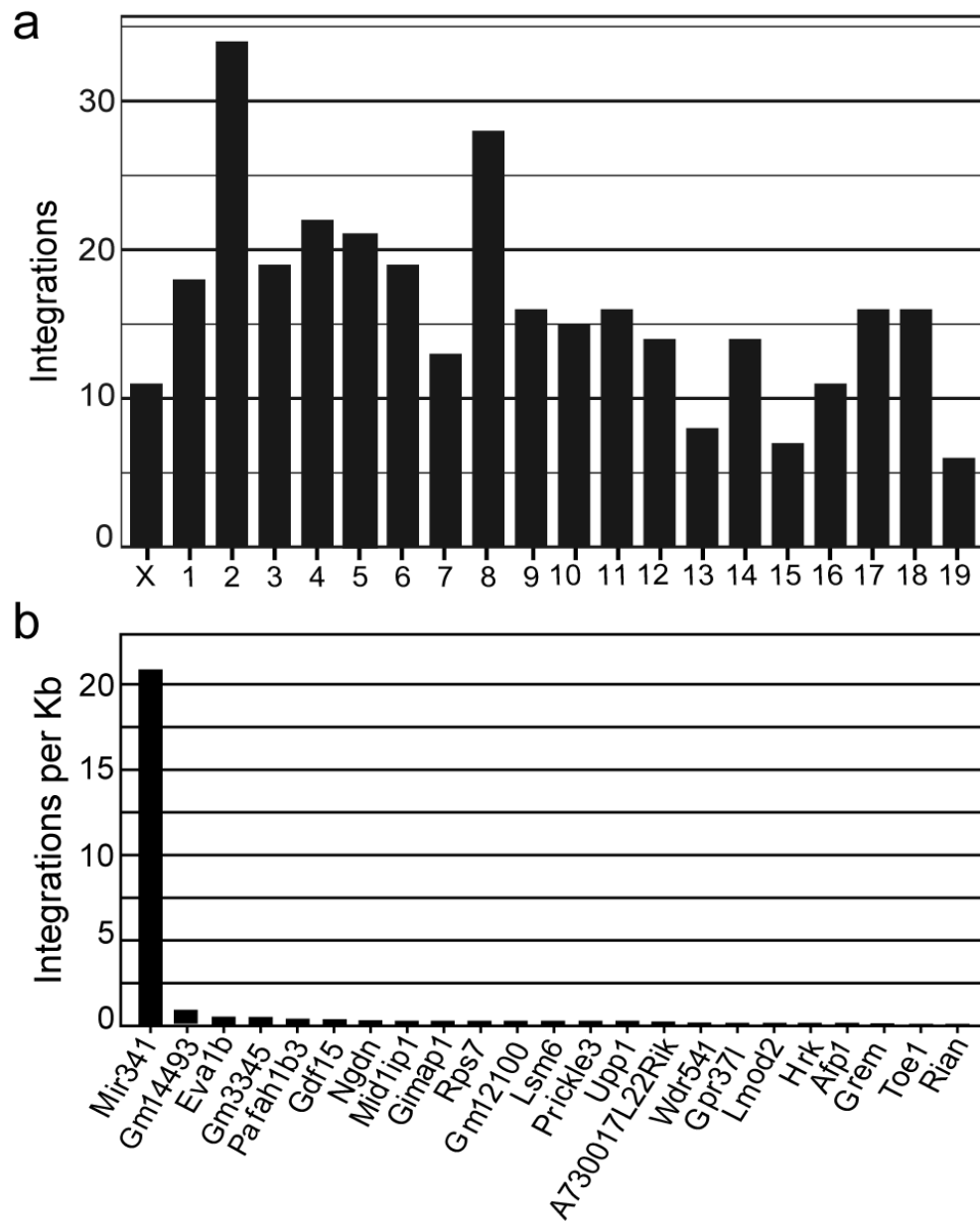


Figure 20- AAV9 Integration Sites.

(a) Integrations per chromosome. (b) Genes with largest number of integrations per kb of DNA.

4.7 Tumour pathology in rAAV9 treated mice

Table 3- Insertion sites with highest confidant.

<i>Chr.</i>	<i>Site</i>	<i>Type</i>	<i>Gene name</i>	<i>Sample</i>	<i>Tissue</i>
2	143355224	Intergenic	(x)	12 control-HexB 40 n SD-HexB	Healthy Liver-N/V tumours Liver nodule/tumour
2	134890091	Intron	Plcb1	12 control-HexB	Healthy Liver-N/V tumours
2	130876940	Intron	A730017 L22Rik	38 control-HexB	Liver nodule/tumour
2	35572583	Intron	Dab2ip	39 control-HexB	Liver nodule/tumour
2	7272551	Intron	Celf2	38 control-HexB 40 n SD-HexB	Liver nodule/tumour Liver nodule/tumour
3	135585125	Exon	Nfkb1	37 n SD-HexB 39 control-HexB	Liver nodule/tumour Liver nodule/tumour
3	127408496	Intron	Ank2	8 n SD-HexB 37 n SD-HexB 10 n SD-HexB 39 control-HexB	Liver nodule/tumour Liver nodule/tumour Healthy Liver-N/V tumours Liver nodule/tumour
4	137999211	Intron	Eif4g3	8 n SD-HexB 37 n SD-HexB 10 n SD-HexB 39 control-HexB	Liver nodule/tumour Liver nodule/tumour Healthy Liver-N/V tumours Liver nodule/tumour
7	130164094	Exon	Fgfr2	41 n SD-HexB	Lung nodule/tumour
8	126790577	Intergenic	(x)	39 control-HexB	Liver nodule/tumour
8	115019795	Intron	Wwox	37 n SD-HexB 39 control-HexB	Liver nodule/tumour Liver nodule/tumour
8	45236465	Intergenic	(x)	10 n SD-HexB 37 n SD-HexB	Healthy Liver-N/V tumours Liver nodule/tumour

4.7 Tumour pathology in rAAV9 treated mice

10	11244971	Exon	4930432 B10Rik	12 control-HexB	Healthy Liver-N/V tumours
11	86275172	Intron	46324191 22Rik	38 control-HexB	Liver nodule/tumour
11	9123927	Intron	Upp1	12 control-HexB	Healthy Liver-N/V tumours
12	109611524	Exon	Mir341	37 n SD-HexB	Liver nodule/tumour
12	109607781	Intron	Rian	9 control-HexB 42 control-HexB	Liver nodule/tumour Liver nodule/tumour
13	94702901	Intergenic	(x)	37 n SD-HexB 39 control-HexB	Liver nodule/tumour Liver nodule/tumour
13	27292608	Intergenic	(x)	40 n SD-HexB	Liver nodule/tumour
16	76306564	Intron	Nrip1	37 n SD-HexB 39 control-HexB	Liver nodule/tumour Liver nodule/tumour
17	65512865	Intron	Tmem23 2	39 control-HexB	Liver nodule/tumour
18	28691337	Intergenic	(x)	40 n SD-HexB	Liver nodule/tumour
X	10718223	Intron	Gm1449 3	39 control-HexB	Liver nodule/tumour

Supplementary

5.1 Statistical analysis

Table 4- Statistical comparisons of control groups that are merged within figures.

Data/Related Figure	Comparison	P value	Test
Total distance travelled/ Figure 4	at wk 14 a Control-LacZ (n=5) a Control-HexB (n=5) n Control-LacZ (n=4) n Control-HexB (n=5)	P = 0.729	One way ANOVA
	At wk 15 a Control-LacZ (n=5) a Control-HexB (n=5) n Control-LacZ (n=4) n Control-HexB (n=5)	P = 0.718	One way ANOVA
	At Wk 16 a Control-HexB (n=5) n Control-LacZ (n=5) n Control-HexB (n=4)	P = 0.25	One way ANOVA
	At Wk 21 a Control-HexB (n=2) vs n Control-HexB (n=5)	P = 0.872	Two tailed T-test

5.1 Statistical analysis

	At wk 30 n Control-HexB (n=5)	1 group no intragroup comparison	None
Vacuolization / Figure 7	a Control-LacZ (n=5) a Control-HexB (n=5) n Control-LacZ (n=5) n Control-HexB (n=5) In CB Md/Po Mid CX/Hp Thy/HY/Sep OA	p = 0.925 p = 0.418 p = 0.890 p = 0.585 p = 0.933 p = 0.547	One way ANOVA
GM2 ganglioside proportions/ Figure 10	a Control-LacZ (n=5) a Control-HexB (n=5) n Control-LacZ (n=5) n Control-HexB (n=5)	p = 0.091	One way ANOVA
Serum hex activity/ Figure 11	At wk: 10, 12-14, final a Control-LacZ vs n Control-LacZ a Control-HexB vs n Control-HexB a Control-LacZ and n Control-LacZ vs a Control-HexB a Control-LacZ and n Control-LacZ vs n Control-HexB	p > 0.05 at all times points p > 0.05 at all time points *p value ≤ 0.05 at all time points (see Fig. a) *p value ≤ 0.05 at all time points (see Fig. S2a)	Two tailed t-tests
Brain hex activity/ Figure 13	a Control-LacZ vs n Control-LacZ a Control-HexB vs n Control-HexB	p > 0.05 *p value = 0.0117	Two tailed t-test

5.1 Statistical analysis

Table 5- Statistical comparisons of vector genome copy number in male vs. female.

Data/Related Figure	Comparison	P value	Test
Vector copy number in brain/ Figure 16	Male vs female	a Control = 0.3192 M (n=14), F (n=6) n Control = 0.7340 M (n=8), F (n=12) a Control-HexB =0.787 M (n=6), F (n=4) a Control-LacZ = 0.103 M (n=8), F (n=2) n Control-HexB = 0.420 M (n=3), F (n=7) n Control-LacZ = 0.3241 M (n=5), F (n=5)	Two tailed t-test
Vector copy number in liver/ Figure 16	Male vs female	a Control = 0.4215 M (n=14), F (n=6) n Control = 0.3524 M (n=8), F (n=12) a Control-HexB =0.5390 M (n=6), F (n=4) a Control-LacZ = 0.4323 M (n=8), F (n=2) n Control-HexB = 0.2740 M (n=3), F (n=7) n Control-LacZ = 0.4650 M (n=5), F (n=5)	Two tailed t-test

Discussion, future directions and conclusion

6.1 Discussion

The GM2 gangliosidoses are prototypic neurodegenerative lysosomal storage disorders where accumulation of storage material results in severe neuronal damage and death in the early years of life. Mice deficient in both major hexosaminidase isozymes, Hex A and Hex B, mimic the disease severity in the human condition including the motor deterioration, the histopathological findings, and the premature death. This study aims to evaluate the utility of intravenously delivered AAV9 based gene therapy in treating GM2 gangliosidoses using the SD (*Hexb*^{-/-}) mouse model.

Our results demonstrated that a single intravenous dose of rAAV9-HexB to neonatal SD mice could provide enough β -hexosaminidase to the brain to reduce/prevent GM2 ganglioside storage and inflammation, correct motor function, and prolong survival. However, the single injection we administered to adult SD mice was not nearly as effective, leaving ganglioside storage similar to that of mice treated with the control vector, AAV9-LacZ, and only minimal improvement in motor function or survival.

The efficiency of rAAV9 transduction in adults and neonates cannot be directly compared because the dose of vg/kg was lower in the adult mice. However, it is clear that AAV9 crossed the BBB and transduced cells in the brain, both in adults and neonates, as seen in previous studies^{244,245}. The increased number of vg in the brain of

6.1 Discussion

neonates compared to adult mice, and vice versa in the liver, suggests that the liver of adult mice is transduced much more effectively than that of neonates. There are several factors that need to be considered in the interpretation of these findings. First, the neonatal livers would have undergone substantial growth after AAV9 treatment, leading to a decrease in the vg/dg compared to adult-treated mice. In addition, the low levels of transduced brain cells in the adult mouse may be due to the high level of damage already existing at the time of intervention, so that new enzyme activity could not rescue cell death; the recovery of neuronal function can only occur when the neuronal impairment is not beyond repair²⁸⁰. There is also the possibility that the extended sialic acid containing ganglioside deposition in adult mice at the time of injection is blocking the AAV9 transduction, which was previously observed in other LSDs²⁸¹. The impact of the less mature BBB on rAAV9 transduction efficiency in neonatal mice is debatable. Many attributed the high neuronal to astrocyte transduction in neonatal mice²⁴⁴ to the low number of astrocytes in early life²⁸², and that at the time of birth, few astrocytic endfeet are associated with cerebral blood vessels compared to that of the adult brain²⁸³. The possibility of distribution of the BBB with the large volume injection in neonates seems unlikely and the other group reported the same pattern of transduction in both neonates and adults with a smaller volume injection²⁸⁰. However, because we used more rAAV9 in the treatment of neonates, it is impossible to be certain of the basis of the increased transduction.

6.1 Discussion

The prenatal accumulation of GM2 ganglioside does not compromise early brain development, but disease manifestations advance rapidly after birth when no intervention is introduced²⁸⁴. Results presented here show that treatment with AAV9-HexB cannot be delayed after birth in order to correct the pathological features of SD disease. Administering AAV9-HexB expressing vector to 1-2 days old mice provided enough brain β -hexosaminidase to reverse the prenatal storage of GM2 gangliosides, prevent further accumulation as well as the subsequent impact on neuron and neurological function. The detectable level of GM2 storage at the 10 months (43 wks) experiment end point in neonatal treated SD mice were remarkably lowered compared to that found in the *LacZ*-injected SD mice which reach a humane end point in 17 weeks. The brain β -hexosaminidase activity provided when the vector was injected at the early time-point cleared and prevented most of the glycosphingolipid accumulation, preserving the overall histological appearance of brain tissue.

The loss of motor coordination observed early in the course of disease is attributed to reduce neuronal function. This is due to inflammation and/or neuronal death in hippocampus and cerebellum together with the thalamus as the center to relay sensory signals²⁸⁵⁻²⁸⁷. We established that the lost motor function is prevented when treatment is received early in life; most essential is the long-term preservation of the motor activity as was found in the neonatal treated group. Despite the apparent tremor, the animals remained very active throughout the study.

6.1 Discussion

There is overwhelming evidence supporting the role of inflammation in neurodegenerative diseases. The activation of microglia (and astrocytes) maintains the inflammatory process and negativity contributes to the disease progression. The mechanism underlying this role is still unknown, although specific nervous system modulation to the inflammation process is believed to exist. We compared the expression of monocytic marker F4/80²⁸⁸ between untreated SD mice and the two treated groups. The AAV9-HexB treatment clearly decreased inflammation, presumably by decreasing the levels of GM2 ganglioside storage in cells early enough in the neonatally treated group to prevent the cascading immune response.

In the neonatally treated group, the activity of brain beta-hexosaminidase enzyme cleared most of the stored glycosphingolipid, but at the 43 wks experimental end point, a significant level of accumulation and inflammation was detected. The inflammation observed was more pronounced in the thalamus area, accounting for the noticed tremor in this group. This indicates that a higher level of enzyme is necessary to keep the pathology at bay for the normal mice life span.

Our data shows that the use of only the β -subunit for the gene therapy was very effective when administrated early in life, and resulted in an increase in total β -hexosaminidase activity. It is likely that the therapeutic effect in our study is largely the result of Hex B which is able to degrade GA2 generated from GM2 by the sialidase

6.1 Discussion

bypass. Indeed, very little activity is detected in AAV9-Hexb injected mice using the sulfated form of 4-MUG which is specific for α -subunit containing dimers.

Despite the proven ability of rAAV9 to transduce cells in the adult brain, there was no increase in brain β -hexosaminidase activity in SD mice treated at the asymptomatic 6 weeks of age. This could be because viral particles and enzyme activities were lost due to the advanced pathological process leading to apoptosis of neurons. When we treated mice as young adults and sacrificed them as they reached a humane end point, we observed minimum clearance of glycosphingolipid accumulation and no difference in the F4/80 labeling compared to untreated SD mice. This suggests that the moderate increase in life span among this group resulted from delayed neuronal degeneration rather than by reversing the pathological features of the disease. This raises the possibility of combining gene therapy with agents targeting inflammation to enhance the therapeutic benefits for patients with GM2 gangliosidosis. The importance of early treatment to preserve brain function in LSDs has also been supported by recent studies showing therapeutic benefit can only be achieved with early treatment even with intracranial injection of rAAV2/1 expressing both subunit genes²⁸⁹. This group reported similar pattern of viral transduction, transgene expression and distribution at all ages of treatment, but mice that received the earliest intervention at 4 wks of age benefited most. The abundant and wide distribution of enzyme achieved by intracranial vector injection did not translate into improved function or survival in mice that received the

6.1 Discussion

intracranial injection at 12 wks of age. Such findings stress the fact that the cell death is inevitable when intervention is delayed^{280,290,291}, at least when therapy is limited to enzyme replacement.

The detection of tumours in the neonatally treated mice was disappointing, but not surprising as our neonatal dose of rAAV9 was high. Similar findings have been reported in mice treated neonatally for β -glucuronidase²⁹² and as 9-11 wk old adults for ornithine transcarbamylase deficiencies²⁹³⁻²⁹⁵. In both cases, there was an increased occurrence of hepatocellular carcinoma in mice that survived for more than 13 months. This was attributed to insertional mutagenesis by the AAV vectors which integrated, in some of the tumours, within a 6-kb window on chromosome 12, near the Rian and Mirg (located within the Rian) genes²⁷⁸. Studies have shown that in mice, integration of the provirus in this region leads to increased expression of surrounding genes, resulting in hepatocellular carcinoma. Three of our mice did show integrations in this same region. Our results are difficult to interpret however, as multiple nodules surrounded by normal tissue were used in the analysis of the insertion sites. The H & E stained nodules/tumours sections were reported as nodular hyperplasia, however, the endpoint of our study was only 10 months, so it is possible that these benign nodules might have turned malignant in the future had we continued our study to a later time point. These findings emphasize the importance of continued awareness in ongoing gene therapy studies using AAV, as had been suggested previously.

6.2 Future directions

Our positive outcome with just a single intravenous dose of AAV9-HexB provides hope for less invasive therapies for the GM2 gangliosidoses and benefit the peripheral tissues affected by lysosomal storage of GM2 ganglioside.

6.2 Future directions

Currently, GM2 gangliosidoses patients are often born to families with no history of the disease and in communities without screening programs. In these cases, the neuronal pathology at the time of diagnosis is evident, which necessitates very effective intervention approaches.

6.2.1 Eliminating obstacles

One of the most common factors that limits the therapeutic effect of systemic gene delivery using rAAV vectors is the host immune response to the virus particle, in most cases to the capsid of AAV vectors. Adeno-associated virus is usually found in samples with adenovirus, and the latter is a very common cause of a range of infections in children as well as adults, and thus pre-existing humoral immune responses to both viruses is expected. These produced antibodies will neutralize the administered therapeutic vector in circulation and prevent an effective transduction even at a low titer level. Such effects of antibodies can be prevented or overcome by various vector and immune related strategies^{218,296}.

6.2 Future directions

Patients with pre-existing antibodies, either due to previous exposure to the wild-type virus or its recombinant vector, can benefit from plasmapheresis, an available technique to isolate different blood components. With this strategy, pre-existing antibodies are transiently removed before treatment, which would allow the viral vector to reach the cell²⁹⁷. Another approach is the B-cell depletion meant to prevent the humoral response to the vector capsid, as well as the transgene, in patients with no pre-existing antibodies. This approach would also allow repeated administration of the therapy vector if needed. Agents such rituximab can be use alone or in combination with B-cell inhibitory agents, e.g cyclosporine A and bortezomib, to decrease the titer of already existing antibodies and prevent further recognition of the therapeutic vector antigens²⁹⁸⁻³⁰². The plasmapheresis^{297,303} and the B-cells depletion and inhibition agents³⁰⁴, are already proven to enhance patient's chances of a beneficial rAAV gene therapy treatment.

Other possibilities to overcome the pre-existing antibodies against AAV capsids are the use of a capsid decoy, such as an empty wild type or vector capsid and peptides or domains corresponding to the antibodies, for neutralizing the antibodies and limiting the clearance of the therapeutic vector^{305,306}, or the use of an engineered capsid lacking the B-cell epitopes which can be generated using site-specific mutagenesis^{307,308}. For instance, Mingozzi and colleges developed an empty mutant capsid that can interact with neutralizing antibodies but not enter the cell (Mingozzi et al., 2013).

6.2.2 Timing of intervention

Because of the limited CNS plasticity, timing of treatment is anticipated to significantly control the outcome of the therapy; determining delay versus arrest of the disease progression is likely. Unlike the slower-onset, juvenile and adult forms, the infantile GM2 gangliosidoses are rapidly progressing diseases requiring an early and thorough intervention.

The advantage of early treatment is attributed to the progressive nature of the GM2 gangliosidosis disorders. During the disease course, in addition to the GM2 ganglioside accumulation, a cascade of neuronal inflammation leads to the activation and the expansion of the phagocytic cells in the brain, both microglia and macrophage, in an effort to clear the dysfunction of neurons and maintain CNS hemostasis³⁰⁹. Because these phagocytic cells also lack the β -hexosaminidases, they fail to degrade neurons and the accumulated substrates inside leading to further CNS aggravations through expansion of the phagocytic cell population and, with their mobile ability, spreading inflammation. The role of inflammation in the progression of GM2 gangliosidoses diseases, although secondary to GM2 ganglioside neuronal accumulation, is fundamental to the pathogenicity. Unlike the GM2 accumulation that can be reversed if the enzyme reaches the cells, subsiding immune response is much more complicated. Such effect of inflammation can be minimized by early treatment in the course of the disease. A proof of the role of inflammation in these diseases has been shown in a

6.2 Future directions

mouse model where the decrease of the inflammatory responses improved activity and prolonged life span in mice even without replacing the missing enzyme. Recently the deletion of tumour necrosis factor- α in SD mice showed that decreasing inflammation greatly slowed the progression of the disease³¹⁰. Thus, the outcome of any GM2 gangliosidoses treatment, and other neurodegenerative disease, is controlled by the extent of inflammation at the time of intervention.

When deciding the best timing for viral mediated gene therapy, it is important to consider the maturity of the immune system at different ages. Although AAV itself is not known to stimulate the innate immune response³¹¹, adaptive immune responses, in the form of anti-AAV capsid antibodies, are very common. Infants are born with a less mature immune system and they usually develop anti-AAVs antibodies, mostly AAV2, around 2 years of age³¹². The absence of an antibody and lower immune system reactivity to gene therapy viral vectors as well as the therapeutic protein, give advantages to neonatal gene therapy. In a murine model of haemophilia A and following neonatal treatment with rh10 AAV, prolonged wild transgene expression was achieved due to these factors³¹³.

Another element that contributes to the importance of timing of therapy is that the systemic administration AAV9 into neonatal animals results in robust transduction of neurons throughout the brain, whereas in adult mice, it mainly leads to transduction of astrocytes³¹⁴. This pattern, and extent of transduction, can be attributed to

6.2 Future directions

differences between neonates and adults in the extracellular matrix composition, neuron to astrocyte ratio, or BBB maturity, although none are currently established. Also there is the fact that human brain contains higher astrocytes to neurones ratio (3:2) than other species³¹⁵. Thus the impact of rAAV9 transduction patterns in human gene therapy is still to be determined.

6.2.3 Transduction and expression efficiency

Targeting the CNS started with choosing the vector with the best reported spread and highest efficiency of transduction of non-dividing cells, AAV9³¹⁶. However, there is an ongoing effort to develop and identify vector elements that would enhance the rAAV transduction and transgene expression, in addition to circumvent the immune response.

Considering the transgene, the single-stranded rAAV genome is not functional before the conversion to a double-stranded genome, a process that takes place gradually in the nucleus over a period of 6 wks²⁸⁰. Using self-complementary (sc) AAV is reported to induce an immediate therapeutic effect³¹⁷, and a 10 to 50 fold increase in the transduction as well as enhanced neuronal transduction in adult^{243,318}.

There is also the impact of using different promoters. Several studies have shown that the use of neuron-specific promoters would enhance the expression of the

6.2 Future directions

transgene in neuronal tissue^{258,317,319}. But with LSDs, the goal of a systemic gene therapy is to ensure transgene expression in different cell types, thus the two mostly used promoters are cytomegalovirus (CMV) promoter or the truncated chicken beta actin (CBA). In an effort to enhance gene expression for a systemic therapy, Gray et al. (2011a) constructed a hybrid CBA (CBh) promoter that allowed more stable and stronger expression of the transgene than what was observed with CMV or CBA promoters.

Another approach is to replace the promoter with a tissue-specific microRNA (miRNAs)-binding site in the AAV genome which has the advantage of increasing the packaging capacity of rAAVs³²⁰. Xie and colleges reported decreased liver and heart transduction when incorporating three copies of the miRNA122-binding site or miRNA1-binding site in the rAAV genome, a strategy that reduced the transduction in liver and heart and might avoid liver toxicity (see 6.2.4).

Capsid engineering strategies can be used to design new AAV variants by mutagenesis of VP proteins, incorporation of specific peptide ligands at the virus surface, or directed evolution³²¹. Reports by Zhong et. al. and others showed that replacing one of the exposed tyrosine residues on the surface of a systemically administrated rAAV2, rAAV8 and rAAV9 capsids by phenylalanine enabled further retinal transduction³²²⁻³²⁴. Other groups identified two mutated rAAV9 capsids with a 10-fold decrease in liver transduction without reduction in the transduction of other organs

6.2 Future directions

following tail vein injection³²⁵. The use of peptide motifs inserted into the rAAV capsid was utilized to increase rAAV2 affinity for coronary or cerebral endothelium using a specific brain vascular endothelia epitope^{221,326}.

In addition, disease-specific modulation might be necessary. For GM2 gangliosidoses Chen and colleges reported that cellular deposition of sialic acid limits the transduction ability of AAV9 in an MPS VII mouse model. To overcome the blocking effect of sialic acid, this group inserted the same peptide modification reported to enhance the transduction of rAAV2 to cerebral endothelium to rAAV9²⁸¹. As sialic acid brain content is elevated in GM2 gangliosidoses, a similar effect can be expected.

Another consideration when attempting to treat GM2 gangliosidoses patients is the difference in ganglioside metabolism between rodents and human. The GM2 ganglioside can only degraded by Hex A in the present of the GM2 activator protein, whereas in rodents, GM2 ganglioside is degraded to GM3 by Hex A, or to GA2 by sialidase, an ineffective pathway in human. Also in rodents, the GM2 activator protein efficiently stimulates GA2 hydrolysis by mouse Hex A and to a lower extent by Hex B¹⁶⁶. Such differences explain the variations in Tay-sachs and AB variants disease phenotypes between human and mouse models, and also highlight the important of Hex A production to treat GM2 gangliosidoses in human. The use of both α - and β -subunits of β -hexosaminidase together for gene therapy is likely to result in higher levels of Hex A

6.2 Future directions

by avoiding the short supply of the endogenous subunits that may be limiting when only one of the gene subunit is transduced³²⁷. Thus, the intravenous administration of a vector expressing both α - and β -subunits, or vectors expressing the two subunits independently, are likely to ensure the production of the Hex A enzyme as the only enzyme capable of degrading GM2 ganglioside in human. Recent development of a novel hybrid protein that can be packed into a single vector, overcoming the limited packing capacity of rAAV vectors, and combining the activities of the α - and β -subunits of β -hexosaminidase, opens the stage for the construction of a single rAAV vector expressing an enzyme capable of GM2 ganglioside degradation³²⁸. Another approach to overcome the need of more than one gene is the use of dual-AAV Vector-Based Systems, to double the packaging capacity of rAAV vectors. A proof of the functionality of such vectors was demonstrated by Dongsheng Duan's group in 2011³²⁹.

6.2.4 Potential risk

Despite the proven efficacy of rAAV vector gene therapy for different diseases in animal models and the recent approval of clinical trials³³⁰, safety concerns are still controversial. Experience with the use of rAAV vectors showed that the immune response to vector capsids is the biggest challenge for effective and long-term gene therapy. Nevertheless, insertion mutagenesis is becoming a concern as rAAV loose the

6.2 Future directions

site-specific integration into the safe location of human chromosome 19 by the removal of the *rep* gene.

6.2.4.1 Tumorigenesis

The safety of rAAV gene therapy was first examined by Donsante et al in 2007 following the report of HCC carcinoma induction in mouse model of MPS VII (Observed incidence of tumorigenesis in long-term rodent studies of rAAV vectors. *Gene Ther.* 2001;8(17):1343–1346). In their study, the tumour formation was attributed to the integration of rAAV into the *Dlk1–Dio3* locus containing the *Rian* and *Mirg* genes on chromosome 12 when vector is administered neonatally. Although many studies followed arguing the causative effect of AAV^{294,331-336}, no tumour has been reported in human and other large mammals. The implications of the *Dlk1–Dio3* locus in human HCC raise concern. Recently, Charles P. Venditti's group suggested that many aspects of rAAV gene therapy, at least in mice, including vector dose, promoter selection and therapeutic timing, influence genotoxicity³³⁷.

Measures to avoid random integration of rAAV vectors have been proposed to decrease the chance of insertion mutagenesis. One of which is altering AAV9 tropism toward liver tissue by peptide modification³³⁸ which will decrease the chances of liver tumorigenesis by decreasing overall liver transduction. Others suggested engineering rAAV vectors with site-directed integration to allow the transgene to integrate into a

6.2 Future directions

safe site in the genome^{339,340}. The later proposal, site directed integration, carries higher potential to ensure the long-term therapeutic goal of gene therapy as it will ensure safe and continuous present of the transgene in different cell types.

6.2.5 Conclusion

The available strategies that allow further enhancement of neuronal tropism, decrease the inflammatory reaction and humoral immune response, minimize the risk of tumorigenesis, and the potential for easily deliver for the human GM2 gangliosidosis make gene therapy a very promising approach. Combining gene therapy with immune system modulators is expected to enhance the benefit of treatment, especially when inflammation reaches a pathological level as the disease progresses. Taken together, rAAV vectors carry great potential to treat the GM2 gangliosidosis as well as other neurodegenerative diseases.

REFERENCES

- (1) Appelqvist, H.; Waster, P.; Kagedal, K.; Ollinger, K. The lysosome: from waste bag to potential therapeutic target. *Journal of molecular cell biology* **2013**, *5*, 214-226.
- (2) Settembre, C.; Fraldi, A.; Medina, D. L.; Ballabio, A. Signals from the lysosome: a control centre for cellular clearance and energy metabolism. *Nature reviews. Molecular cell biology* **2013**, *14*, 283-296.
- (3) Lüllmann-Rauch, R.: History and Morphology of the Lysosome. In *Lysosomes*; Medical Intelligence Unit; Springer US, 2005; pp 1-16.
- (4) Saftig, P.; Klumperman, J. Lysosome biogenesis and lysosomal membrane proteins: trafficking meets function. *Nature reviews. Molecular cell biology* **2009**, *10*, 623-635.
- (5) Bucci, C.; Thomsen, P.; Nicoziani, P.; McCarthy, J.; van Deurs, B. Rab7: A Key to Lysosome Biogenesis. *Molecular Biology of the Cell* **2000**, *11*, 467-480.
- (6) Bainton, D. F. The discovery of lysosomes. *The Journal of Cell Biology* **1981**, *91*, 66-76.
- (7) Conner, S. D.; Schmid, S. L. Regulated portals of entry into the cell. *Nature* **2003**, *422*, 37-44.
- (8) Doherty, G. J.; McMahon, H. T. Mechanisms of endocytosis. *Annual review of biochemistry* **2009**, *78*, 857-902.
- (9) Kaushik, S.; Cuervo, A. M. Chaperone-mediated autophagy: a unique way to enter the lysosome world. *Trends in Cell Biology* **2012**, *22*, 407-417.
- (10) Cuervo, A. M.; Dice, J. F. When lysosomes get old☆. *Experimental Gerontology* **2000**, *35*, 119-131.
- (11) Egil Hansen, T.; Johansen, T. Following autophagy step by step. *BMC Biol* **2011**, *9*, 1-4.
- (12) Ohkuma, S.; Poole, B. Fluorescence probe measurement of the intralysosomal pH in living cells and the perturbation of pH by various agents. *Proceedings of the National Academy of Sciences of the United States of America* **1978**, *75*, 3327-3331.
- (13) Eskelinen, E.-L.; Tanaka, Y.; Saftig, P. At the acidic edge: emerging functions for lysosomal membrane proteins. *Trends in Cell Biology* **2003**, *13*, 137-145.
- (14) Braulke, T.; Bonifacino, J. S. Sorting of lysosomal proteins. *Biochimica et Biophysica Acta (BBA) - Molecular Cell Research* **2009**, *1793*, 605-614.

- (15) Ghosh, P.; Dahms, N. M.; Kornfeld, S. Mannose 6-phosphate receptors: new twists in the tale. *Nature reviews. Molecular cell biology* **2003**, *4*, 202-213.
- (16) Bonifacino, J. S.; Traub, L. M. SIGNALS FOR SORTING OF TRANSMEMBRANE PROTEINS TO ENDOSOMES AND LYSOSOMES *. *Annual Review of Biochemistry* **2003**, *72*, 395-447.
- (17) Roberg, K.; Ollinger, K. Oxidative stress causes relocation of the lysosomal enzyme cathepsin D with ensuing apoptosis in neonatal rat cardiomyocytes. *The American Journal of Pathology* **1998**, *152*, 1151-1156.
- (18) Mizushima, N.; Komatsu, M. Autophagy: Renovation of Cells and Tissues. *Cell* **2011**, *147*, 728-741.
- (19) Rodríguez, A.; Webster, P.; Ortego, J.; Andrews, N. W. Lysosomes Behave as Ca(2+)-regulated Exocytic Vesicles in Fibroblasts and Epithelial Cells. *The Journal of Cell Biology* **1997**, *137*, 93-104.
- (20) Gerasimenko, J. V.; Gerasimenko, O. V.; Petersen, O. H. Membrane repair: Ca²⁺-elicited lysosomal exocytosis. *Current Biology*, *11*, R971-R974.
- (21) Reddy, A.; Caler, E. V.; Andrews, N. W. Plasma Membrane Repair Is Mediated by Ca²⁺-Regulated Exocytosis of Lysosomes. *Cell* **2001**, *106*, 157-169.
- (22) Roy, D.; Liston, D. R.; Idone, V. J.; Di, A.; Nelson, D. J.; Pujol, C.; Bliska, J. B.; Chakrabarti, S.; Andrews, N. W. A Process for Controlling Intracellular Bacterial Infections Induced by Membrane Injury. *Science* **2004**, *304*, 1515-1518.
- (23) Han, R.; Campbell, K. P. Dysferlin and muscle membrane repair. *Current Opinion in Cell Biology* **2007**, *19*, 409-416.
- (24) Blott, E. J.; Griffiths, G. M. Secretory lysosomes. *Nature reviews. Molecular cell biology* **2002**, *3*, 122-131.
- (25) Stinchcombe, J. C.; Griffiths, G. M. Secretory Mechanisms in Cell-Mediated Cytotoxicity. *Annual Review of Cell and Developmental Biology* **2007**, *23*, 495-517.
- (26) Logan, M. R.; Lacy, P.; Odemuyiwa, S. O.; Steward, M.; Davoine, F.; Kita, H.; Moqbel, R. A critical role for vesicle-associated membrane protein-7 in exocytosis from human eosinophils and neutrophils. *Allergy* **2006**, *61*, 777-784.
- (27) Wesolowski, J.; Paumet, F. The impact of bacterial infection on mast cell degranulation. *Immunol Res* **2011**, *51*, 215-226.
- (28) Ren, Q.; Ye, S.; Whiteheart, S. W. The Platelet Release Reaction: Just when you thought platelet secretion was simple. *Current opinion in hematology* **2008**, *15*, 537-541.
- (29) Stinchcombe, J.; Bossi, G.; Griffiths, G. M. Linking Albinism and Immunity: The Secrets of Secretory Lysosomes. *Science* **2004**, *305*, 55-59.

- (30) Tulsiani, D. R.; Yoshida-Komiya, H.; Araki, Y. Mammalian fertilization: a carbohydrate-mediated event. *Biology of Reproduction* **1997**, *57*, 487-494.
- (31) Andrews, N. W. Regulated secretion of conventional lysosomes. *Trends in Cell Biology* **2000**, *10*, 316-321.
- (32) Andrews, N. W. Membrane repair and immunological danger. *EMBO Reports* **2005**, *6*, 826-830.
- (33) Aits, S.; Jäättelä, M. Lysosomal cell death at a glance. *Journal of Cell Science* **2013**, *126*, 1905-1912.
- (34) Palmieri, M.; Impey, S.; Kang, H.; di Ronza, A.; Pelz, C.; Sardiello, M.; Ballabio, A. Characterization of the CLEAR network reveals an integrated control of cellular clearance pathways. *Human Molecular Genetics* **2011**, *20*, 3852-3866.
- (35) Sardiello, M.; Palmieri, M.; di Ronza, A.; Medina, D. L.; Valenza, M.; Gennarino, V. A.; Di Malta, C.; Donaudy, F.; Embrione, V.; Polishchuk, R. S.; Banfi, S.; Parenti, G.; Cattaneo, E.; Ballabio, A. A Gene Network Regulating Lysosomal Biogenesis and Function. *Science* **2009**, *325*, 473-477.
- (36) Laplante, M.; Sabatini, D. M. mTOR signaling in growth control and disease. *Cell* **2012**, *149*, 274-293.
- (37) Ward, P. S.; Thompson, C. B. Signaling in Control of Cell Growth and Metabolism. *Cold Spring Harbor Perspectives in Biology* **2012**, *4*, a006783.
- (38) Zoncu, R.; Sabatini, D. M.; Efeyan, A. mTOR: from growth signal integration to cancer, diabetes and ageing. *Nature reviews. Molecular cell biology* **2011**, *12*, 21-35.
- (39) Rocznik-Ferguson, A.; Petit, C. S.; Froehlich, F.; Qian, S.; Ky, J.; Angarola, B.; Walther, T. C.; Ferguson, S. M. The Transcription Factor TFEB Links mTORC1 Signaling to Transcriptional Control of Lysosome Homeostasis. *Science signaling* **2012**, *5*, ra42-ra42.
- (40) Sancak, Y.; Bar-Peled, L.; Zoncu, R.; Markhard, A. L.; Nada, S.; Sabatini, D. M. Ragulator-Rag complex targets mTORC1 to the lysosomal surface and is necessary for its activation by amino acids. *Cell* **2010**, *141*, 290-303.
- (41) Efeyan, A.; Zoncu, R.; Sabatini, D. M. Amino acids and mTORC1: from lysosomes to disease. *Trends in molecular medicine* **2012**, *18*, 524-533.
- (42) Bellettato, C.; Scarpa, M. Pathophysiology of neuropathic lysosomal storage disorders. *J Inherit Metab Dis* **2010**, *33*, 347-362.
- (43) Lutgens, S. P. M.; Cleutjens, K. B. J. M.; Daemen, M. J. A. P.; Heeneman, S. Cathepsin cysteine proteases in cardiovascular disease. *The FASEB Journal* **2007**, *21*, 3029-3041.

- (44) Yang, D.-Q.; Feng, S.; Chen, W.; Zhao, H.; Paulson, C.; Li, Y.-P. V-ATPase subunit ATP6AP1 (Ac45) regulates osteoclast differentiation, extracellular acidification, lysosomal trafficking, and protease exocytosis in osteoclast-mediated bone resorption. *Journal of bone and mineral research : the official journal of the American Society for Bone and Mineral Research* **2012**, 27, 1695-1707.
- (45) Zhao, H.; Ito, Y.; Chappel, J.; Andrews, N. W.; Teitelbaum, S. L.; Ross, F. P. Synaptotagmin VII Regulates Bone Remodeling by Modulating Osteoclast and Osteoblast Secretion. *Developmental cell* **2008**, 14, 914-925.
- (46) Watts, C. The endosome-lysosome pathway and information generation in the immune system(). *Biochimica et Biophysica Acta* **2012**, 1824, 14-21.
- (47) Kirkegaard, T.; Jäättelä, M. Lysosomal involvement in cell death and cancer. *Biochimica et Biophysica Acta (BBA) - Molecular Cell Research* **2009**, 1793, 746-754.
- (48) Boustany, R.-M. N. Lysosomal storage diseases[mdash]the horizon expands. *Nat Rev Neurol* **2013**, 9, 583-598.
- (49) Schulze, H.; Sandhoff, K. Lysosomal Lipid Storage Diseases. *Cold Spring Harbor Perspectives in Biology* **2011**, 3, a004804.
- (50) Cox, T. M.; Cachón-González, M. B. The cellular pathology of lysosomal diseases. *The Journal of Pathology* **2012**, 226, 241-254.
- (51) Alroy, J.; Lyons, J. A. Lysosomal Storage Diseases. *Journal of Inborn Errors of Metabolism & Screening* **2014**, 2.
- (52) Platt, F. M.; Boland, B.; van der Spoel, A. C. Lysosomal storage disorders: The cellular impact of lysosomal dysfunction. *The Journal of Cell Biology* **2012**, 199, 723-734.
- (53) Ballabio, A.; Gieselmann, V. Lysosomal disorders: From storage to cellular damage. *Biochimica et Biophysica Acta (BBA) - Molecular Cell Research* **2009**, 1793, 684-696.
- (54) Tay, W. A third instance in the same family of symmetrical changes in the region of the yellow spot in each eye of an infant, closely resembling those of embolism. *Trans Ophthalmol Soc UK* **1884**, 4, 158-159.
- (55) Tay, W. SYmmetrical changes in the region of the yellow spot in each eye op an infant. *Archives of Neurology* **1969**, 20, 104-106.
- (56) Tay, W. A fourth instance of symmetrical changes in the yellow spot region of an infant closely resembling those of embolism. *Trans. Ophthalmol. Soc. UK* **1892**, 12, 125.
- (57) B, S. ON ARRESTED CEREBRAL DEVELOPMENT, WITH SPECIAL REFERENCE TO ITS CORTICAL PATHOLOGY.1. *The Journal of Nervous and Mental Disease* **1887**, 14, 541-541.

- (58) EC, K. A rare fatal disease of infancy, with symmetrical changes at the macula lutea. *Trans Ophthalmol Society* **1892**, 12: 126–137.
- (59) A FAMILY FORM OF IDIOCY, GENERALLY FATAL, ASSOCIATED WITH EARLY BLINDNESS. (AMAUROTIC FAMILY IDIOCY). *The Journal of Nervous and Mental Disease* **1896**, 21, 475–475.
- (60) Baran, B.; Bitter, I.; Fink, M.; Gazdag, G.; Shorter, E. Károly Schaffer and his school: The birth of biological psychiatry in Hungary, 1890–1940. *European psychiatry : the journal of the Association of European Psychiatrists* **2008**, 23, 449–456.
- (61) NErvous and mental disorders from birth through adolescence. *American Journal of Diseases of Children* **1926**, 32, 481–481.
- (62) Sachs, B. B. AMAurotic family idiocy and general lipoid degeneration. *Archives of Neurology & Psychiatry* **1929**, 21, 247–253.
- (63) Slome, D. The genetic basis of amaurotic family idiocy. *Journ. of Genetics* **1933**, 27, 363–376.
- (64) Aronson, S. M.; Valsamis, M. P.; Volk, B. W. INFANTILE AMAUROTIC FAMILY IDIOCY: Occurrence, Genetic Considerations and Pathophysiology in the Non-Jewish Infant. *Pediatrics* **1960**, 26, 229–240.
- (65) Myrianthopoulos. Some epidemiologic and genetic aspects of Tay-Sachs disease. In “Cerebral Sphingolipidoses” *Academic Press, New York*. **1962**, pp. 359–374.
- (66) Aronson, S. M., and Volk, . Genetic and demographic considerations concerning Tay-Sachs disease. In “Cerebral Sphingolipidoses” *Academic Press, New York*. **1962**, pp. 375–394.
- (67) Myrianthopoulos, N. C., and Aronson. Reproductive fitness and selection in Tay-Sachs disease. In “Inborn Disorders of Sphingolipid. **1967**.
- (68) Klenk, E. Über die Natur der Phosphatide und anderer Lipide des Gehirns und der Leber bei der Niemann-Pick’schen Krankheit. *Z. Physiol. Chem* **1935**, vol. 235, pp. 24–25.
- (69) Klenk, E. Beiträge zur Chemie der Lipoidosen. Niemann-Picksche Krankheit und amaurotische Idiotie. *Hoppe-Seyler’s Z. Physiol. Chem* **1939**, 262, 128–143.
- (70) Klenk, E. Neuraminsäure, das Spaltprodukt eines neuen Gehirnlipoids. *Hoppe-Seyler’s. Z. Physiol. Chem* **1941**, 268, 50–58.
- (71) Klenk, E., and Langerbeins. U“ber die Verteilung der Neuraminsäure in Gehirn. *Hoppe-Seyler’s Z. Physiol. Chem* **1941**, vol. 273, pp. 76–86.

(72) Klenk, E. Über die Ganglioside, eine neue Gruppe von zuckerhaltigen Gehirnlipoiden. *Hoppe-Seyler's Z. Physiol. Chem* **1942**, vol. 273, pp. 76–86.

(73) Blix, G., Svennerholm, L., and Werner, I. The isolation of chondrosamine from Gangliosides and from submaxillary mucin. **1952**.

(74) G. B. "Über die Kohlenhydratgruppen des Submaxillärismusins." **1936**.

(75) Svennerholm, L. The chemical structure of normal human brain and Tay-Sachs gangliosides. *Biochemical and Biophysical Research Communications* **1962**, 9, 436–441.

(76) H, K. R. a. W. Die Konstitution der Ganglio-N-tetraose und des Gangliosides GI. *Chemische Berichte*, vol. 96, pp. 866–880. **1963**.

(77) Ledeen R, S. K. Structure of the Tay-Sachs' ganglioside. *Biochemistry*. *Biochemistry* 4: 2225–2233. doi: 10.1021/bi00886a040 **1965**.

(78) WATANABE, K. BIOCHEMICAL STUDIES ON CARBOHYDRATES: XXIV. On Animal β -N-Monoacetylglycosaminidase. III. Report: Kinetics of the enzyme action. *Journal of Biochemistry* **1936**, 24, 315–326.

(79) Sandhoff, K., and Wasse, W. Anreicherung und Charakterisierung zweier Formen der menschlichen N-Acetyl-D-hexosaminidase. *Hoppe-Seyler's Z. Physiol. Chem.* 352, 1119–1133. **1971**.

(80) Beutler E, S. S. Studies in Tay-Sachs and Sandhoff's diseases. Immunologic and structural properties of hexosaminidase A and hexosaminidase B. **1973**.

(81) Lalley, P. A., Rattazzi, M. C., Shows, T. B. . Human beta-D-N-acetylhexosaminidases A and B: expression and linkage relationships in somatic cell hybrids. *Proc. Nat. Acad. Sci.* 71: 1569–1573 **1975**.

(82) Myerowitz, R.; Piekarz, R.; Neufeld, E. F.; Shows, T. B.; Suzuki, K. Human beta-hexosaminidase alpha chain: coding sequence and homology with the beta chain. *Proceedings of the National Academy of Sciences of the United States of America* **1985**, 82, 7830–7834.

(83) Myerowitz, R.; Proia, R. L. cDNA clone for the alpha-chain of human beta-hexosaminidase: deficiency of alpha-chain mRNA in Ashkenazi Tay-Sachs fibroblasts. *Proceedings of the National Academy of Sciences of the United States of America* **1984**, 81, 5394–5398.

(84) Gilbert, F.; Kucherlapati, R.; Creagan, R. P.; Murnane, M. J.; Darlington, G. J.; Ruddle, F. H. Tay-Sachs' and Sandhoff's diseases: the

assignment of genes for hexosaminidase A and B to individual human chromosomes. *Proceedings of the National Academy of Sciences of the United States of America* **1975**, 72, 263-267.

(85) O'Dowd, B. F.; Quan, F.; Willard, H. F.; Lamhonwah, A. M.; Korneluk, R. G.; Lowden, J. A.; Gravel, R. A.; Mahuran, D. J. Isolation of cDNA clones coding for the beta subunit of human beta-hexosaminidase. *Proceedings of the National Academy of Sciences of the United States of America* **1985**, 82, 1184-1188.

(86) Korneluk, R. G.; Mahuran, D. J.; Neote, K.; Klavins, M. H.; O'Dowd, B. F.; Tropak, M.; Willard, H. F.; Anderson, M. J.; Lowden, J. A.; Gravel, R. A. Isolation of cDNA clones coding for the alpha-subunit of human beta-hexosaminidase. Extensive homology between the alpha- and beta-subunits and studies on Tay-Sachs disease. *Journal of Biological Chemistry* **1986**, 261, 8407-8413.

(87) Proia, R. L.; Soravia, E. Organization of the gene encoding the human beta-hexosaminidase alpha-chain. *Journal of Biological Chemistry* **1987**, 262, 5677-5681.

(88) Triggs-Raine, B. L.; Akerman, B. R.; Clarke, J. T.; Gravel, R. A. Sequence of DNA flanking the exons of the HEXA gene, and identification of mutations in Tay-Sachs disease. *American Journal of Human Genetics* **1991**, 49, 1041-1054.

(89) Hasilik, A.; Neufeld, E. F. Biosynthesis of lysosomal enzymes in fibroblasts. Synthesis as precursors of higher molecular weight. *Journal of Biological Chemistry* **1980**, 255, 4937-4945.

(90) Hasilik, A.; Neufeld, E. F. Biosynthesis of lysosomal enzymes in fibroblasts. Phosphorylation of mannose residues. *Journal of Biological Chemistry* **1980**, 255, 4946-4950.

(91) d'Azzo, A.; Proia, R. L.; Kolodny, E. H.; Kaback, M. M.; Neufeld, E. F. Faulty association of alpha- and beta-subunits in some forms of beta-hexosaminidase A deficiency. *Journal of Biological Chemistry* **1984**, 259, 11070-11074.

(92) Proia, R. L.; d'Azzo, A.; Neufeld, E. F. Association of alpha- and beta-subunits during the biosynthesis of beta-hexosaminidase in cultured human fibroblasts. *Journal of Biological Chemistry* **1984**, 259, 3350-3354.

(93) Kytzia, H. J.; Sandhoff, K. Evidence for two different active sites on human beta-hexosaminidase A. Interaction of GM2 activator protein with beta-hexosaminidase A. *Journal of Biological Chemistry* **1985**, 260, 7568-7572.

(94) Burg J, C. E., Sandhoff K, Solomon E, Swallow DM. Mapping of the gene coding for the human GM2 activator protein to chromosome 5. **1985b**.

(95) Burg J, B. A., Sandhoff K. Molecular forms of GM2-activator protein. A study on its biosynthesis in human skin fibroblasts. **1985a**.

- (96) Mark, B. L.; Mahuran, D. J.; Cherney, M. M.; Zhao, D.; Knapp, S.; James, M. N. G. Crystal Structure of Human β -Hexosaminidase B: Understanding the Molecular Basis of Sandhoff and Tay-Sachs Disease. *Journal of Molecular Biology* **2003**, 327, 1093-1109.
- (97) Lemieux, M. J.; Mark, B. L.; Cherney, M. M.; Withers, S. G.; Mahuran, D. J.; James, M. N. G. Crystallographic Structure of Human β -Hexosaminidase A: Interpretation of Tay-Sachs Mutations and Loss of GM2 Ganglioside Hydrolysis. *Journal of Molecular Biology* **2006**, 359, 913-929.
- (98) Maier, T.; Strater, N.; Schuette, C.; Klingenstein, R.; Sandhoff, K.; Saenger, W. The X-ray Crystal Structure of Human β -Hexosaminidase B Provides New Insights into Sandhoff Disease. *Journal of Molecular Biology* **2003**, 328, 669-681.
- (99) Mark, B. L.; James, M. N. G. Anchimeric assistance in hexosaminidases. *Canadian Journal of Chemistry* **2002**, 80, 1064-1074.
- (100) Sandhoff K, C. E., Neufeld EF, Kaback MM, Suzuki K. in The metabolic basis of inherited disease, The GM2 gangliosidosis,. **1989**.
- (101) Gravel RA1, T.-R. B., Mahuran DJ. Biochemistry and genetics of Tay-Sachs disease. **1991**.
- (102) Sandhoff K, H. K., Wässle W, Jatzkewitz H. Enzyme alterations and lipid storage in three variants of Tay-Sachs disease. **1971**.
- (103) Conzelmann, E.; Sandhoff, K. AB variant of infantile GM2 gangliosidosis: deficiency of a factor necessary for stimulation of hexosaminidase A-catalyzed degradation of ganglioside GM2 and glycolipid GA2. *Proceedings of the National Academy of Sciences of the United States of America* **1978**, 75, 3979-3983.
- (104) Neudorfer O1, P. G., Zeng BJ, Gianutsos J, Zaroff CM, Kolodny EH. Late-onset Tay-Sachs disease: phenotypic characterization and genotypic correlations in 21 affected patients. **2005**.
- (105) Zlotogora, J. Is the presence of two different Tay-Sachs disease mutations in a Cajun population an unexpected observation? *American Journal of Human Genetics* **1993**, 52, 1014-1016.
- (106) Conzelmann E1, S. K. Biochemical basis of late-onset neuropilipidoses. **1991**.
- (107) Conzelmann E, S. K. Partial enzyme deficiencies: residual activities and the development of neurological disorders. **1983**.
- (108) Leinekugel P1, M. S., Conzelmann E, Sandhoff K. Quantitative correlation between the residual activity of beta-hexosaminidase A and arylsulfatase A and the severity of the resulting lysosomal storage disease. **1992**.
- (109) Kolodny, O. N. a. E. H. Late-Onset Tay-Sachs Disease. **2004**.

(110) Kytzia HJ, H. U., Sandhoff K. Diagnosis of infantile and juvenile forms of GM2 gangliosidosis variant 0. Residual activities toward natural and different synthetic substrates. **1984**.

(111) Sandhoff K, A. U., Jatzkewitz H. Deficient hexosaminidase activity in an exceptional case of Tay-Sachs disease with additional storage of kidney globoside in visceral organs. **1968**.

(112) Venugopalan, P.; Joshi, S. N. Cardiac involvement in infantile Sandhoff disease. *Journal of Paediatrics and Child Health* **2002**, *38*, 98-100.

(113) Maegawa, G. H. B.; Stockley, T.; Tropak, M.; Banwell, B.; Blaser, S.; Kok, F.; Giugliani, R.; Mahuran, D.; Clarke, J. T. R. The Natural History of Juvenile or Subacute GM2 Gangliosidosis: 21 New Cases and Literature Review of 134 Previously Reported. *Pediatrics* **2006**, *118*, e1550-e1562.

(114) Argov Z, N. R. Clinical and genetic variations in the syndrome of adult GM2 gangliosidosis resulting from hexosaminidase A deficiency. **1984**.

(115) Navon, R.; Proia, R. L. Tay-Sachs disease in Moroccan Jews: deletion of a phenylalanine in the alpha-subunit of beta-hexosaminidase. *American Journal of Human Genetics* **1991**, *48*, 412-419.

(116) Navon, R.; Nutman, J.; Kopel, R.; Gaber, L.; Gadoth, N.; Goldman, B.; Nitzan, M. Hereditary heat-labile hexosaminidase B: its implication for recognizing Tay-Sachs genotypes. *American Journal of Human Genetics* **1981**, *33*, 907-915.

(117) Oonk JG, v. d. H. H., Martin JJ. Spinocerebellar degeneration: hexosaminidase A and B deficiency in two adult sisters. **1979**.

(118) Cashman NR, A. J., Hancock LW, Dawson G, Horwitz AL, Johnson WG, Huttenlocher PR, Wollmann RL. N-acetyl-beta-hexosaminidase beta locus defect and juvenile motor neuron disease: a case study. **1986**.

(119) Mitsumoto H, S. R., Schafer IA, Sternick CS, Kaufman B, Wilbourn A, Horwitz SJ. Motor neuron disease and adult hexosaminidase A deficiency in two families: evidence for multisystem degeneration. **1985**.

(120) Nagarajan, S.; Chen, H. C.; Li, S. C.; Li, Y. T.; Lockyer, J. M. Evidence for two cDNA clones encoding human GM2-activator protein. *Biochemical Journal* **1992**, *282*, 807-813.

(121) Cantor, R. M., Kaback, M. M. . Sandhoff disease (SHD) heterozygote frequencies (HF) in North American (NA) Jewish (J) and non-Jewish (NJ) populations:. **1985**.

(122) MM., K. Population-based genetic screening for reproductive counseling: the Tay-Sachs disease model. **2000**.

(123) Myerowitz, R.; Hogikyan, N. D. Different Mutations in Ashkenazi Jewish and Non-Jewish French Canadians with Tay-Sachs Disease. *Science* **1986**, 232, 1646-1648.

(124) De Braekeleer, M.; Hechtman, P.; Andermann, E.; Kaplan, F. The French Canadian Tay-Sachs disease deletion mutation: identification of probable founders. *Hum Genet* **1992**, 89, 83-87.

(125) Myerowitz, R.; Costigan, F. C. The major defect in Ashkenazi Jews with Tay-Sachs disease is an insertion in the gene for the alpha-chain of beta-hexosaminidase. *Journal of Biological Chemistry* **1988**, 263, 18587-18589.

(126) Triggs-Raine, B. L.; Feigenbaum, A. S. J.; Natowicz, M.; Skomorowski, M.-A.; Schuster, S. M.; Clarke, J. T. R.; Mahuran, D. J.; Kolodny, E. H.; Gravel, R. A. Screening for Carriers of Tay-Sachs Disease among Ashkenazi Jews. *New England Journal of Medicine* **1990**, 323, 6-12.

(127) Arpaia, E.; Dumbrille-Ross, A.; Maler, T.; Neote, K.; Tropak, M.; Troxel, C.; Stirling, J. L.; Pitts, J. S.; Bapat, B.; Lamhonwah, A. M.; Mahuran, D. J.; Schuster, S. M.; Clarke, J. T. R.; Lowden, J. A.; Gravel, R. A. Identification of an altered splice site in Ashkenazi Tay-Sachs disease. *Nature* **1988**, 333, 85-86.

(128) Ohno, K.; Suzuki, K. A splicing defect due to an exon-intron junctional mutation results in abnormal β -hexosaminidase α chain mRNAs in Ashkenazi Jewish patients with Tay-Sachs disease. *Biochemical and Biophysical Research Communications* **1988**, 153, 463-469.

(129) Mules, E. H.; Hayflick, S.; Miller, C. S.; Reynolds, L. W.; Thomas, G. H. Six novel deleterious and three neutral mutations in the gene encoding the alpha-subunit of hexosaminidase A in non-Jewish individuals. *American Journal of Human Genetics* **1992**, 50, 834-841.

(130) Thurmon, T. F. Tay-Sachs genes in Acadians. *American Journal of Human Genetics* **1993**, 53, 781-783.

(131) Paw, B. H.; Moskowitz, S. M.; Uhrhammer, N.; Wright, N.; Kaback, M. M.; Neufeld, E. F. Juvenile GM2 gangliosidosis caused by substitution of histidine for arginine at position 499 or 504 of the alpha-subunit of beta-hexosaminidase. *Journal of Biological Chemistry* **1990**, 265, 9452-9457.

(132) Grebner, E. E.; Tomczak, J. Distribution of three alpha-chain beta-hexosaminidase A mutations among Tay-Sachs carriers. *American Journal of Human Genetics* **1991**, 48, 604-607.

(133) Akli S1, C. J., Kahn A, Poenaru L. A null allele frequent in non-Jewish Tay-Sachs patients. **1993**.

(134) Tanaka, A.; Fujimaru, M.; Choeh, K.; Isshiki, G. Novel mutations, including the second most common in Japan, in the [beta]-hexosaminidase

[alpha] subunit gene, and a simple screening of Japanese patients with Tay-Sachs disease. *J Hum Genet* **1999**, 44, 91-95.

(135) Kaufman M1, G.-C. J., Karpati M, Peleg L, Goldman B, Akstein E, Adam A, Navon R. Tay-Sachs disease and HEXA mutations among Moroccan Jews. **1997**.

(136) Navon, R.; Proia, R. L. The Mutations in Ashkenazi Jews with Adult G_{M2} Gangliosidosis, the Adult Form of Tay-Sachs Disease. *Science* **1989**, 243, 1471-1474.

(137) Paw, B. H.; Kaback, M. M.; Neufeld, E. F. Molecular basis of adult-onset and chronic GM2 gangliosidoses in patients of Ashkenazi Jewish origin: substitution of serine for glycine at position 269 of the alpha-subunit of beta-hexosaminidase. *Proceedings of the National Academy of Sciences of the United States of America* **1989**, 86, 2413-2417.

(138) Navon, R.; Kolodny, E. H.; Mitsumoto, H.; Thomas, G. H.; Proia, R. L. Ashkenazi-Jewish and non-Jewish adult GM2 gangliosidosis patients share a common genetic defect. *American Journal of Human Genetics* **1990**, 46, 817-821.

(139) dos Santos, M. R.; Tanaka, A.; Sá Miranda, M. C.; Ribeiro, M. G.; Maia, M.; Suzuki, K. GM2-gangliosidosis B1 variant: analysis of beta-hexosaminidase alpha gene mutations in 11 patients from a defined region in Portugal. *American Journal of Human Genetics* **1991**, 49, 886-890.

(140) Tanaka, A.; Ohno, K.; Suzuki, K. GM2-gangliosidosis B1 variant: A wide geographic and ethnic distribution of the specific β -hexosaminidase α chain mutation originally identified in a puerto rican patient. *Biochemical and Biophysical Research Communications* **1988**, 156, 1015-1019.

(141) Kaback MM1, D. R. Tay-Sachs disease: from clinical description to molecular defect. **2001**.

(142) Bikker H1, v. d. B. F., Wolterman RA, de Vijlder JJ, Bolhuis PA. Demonstration of a Sandhoff disease-associated autosomal 50-kb deletion by field inversion gel electrophoresis. **1989**.

(143) Bikker H1, v. d. B. F., Wolterman RA, Kleijer WJ, de Vijlder JJ, Bolhuis PA. Distribution and characterization of a Sandhoff disease-associated 50-kb deletion in the gene encoding the human beta-hexosaminidase beta-chain. **1990**.

(144) Neote K1, B. B., Dumbrille-Ross A, Troxel C, Schuster SM, Mahuran DJ, Gravel RA. Characterization of the human HEXB gene encoding lysosomal beta-hexosaminidase. **1990**.

- (145) Neote, K.; McInnes, B.; Mahuran, D. J.; Gravel, R. A. Structure and distribution of an Alu-type deletion mutation in Sandhoff disease. *Journal of Clinical Investigation* **1990**, *86*, 1524-1531.
- (146) Mahuran, D. J. Personal Communication. . **1994**.
- (147) McInnes, B.; Potier, M.; Wakamatsu, N.; Melancon, S. B.; Klavins, M. H.; Tsuji, S.; Mahuran, D. J. An unusual splicing mutation in the HEXB gene is associated with dramatically different phenotypes in patients from different racial backgrounds. *Journal of Clinical Investigation* **1992**, *90*, 306-314.
- (148) Hara Y1, I. P., Drousiotou A, Stylianidou G, Anastasiadou V, Suzuki K. Mutation analysis of a Sandhoff disease patient in the Maronite community in Cyprus. **1994**.
- (149) Drousiotou, A.; Stylianidou, G.; Anastasiadou, V.; Christopoulos, G.; Mavrikiou, E.; Georgiou, T.; Kalakoutis, G.; Oladimeji, A.; Hara, Y.; Suzuki, K.; Furihata, K.; Ueno, I.; Ioannou, P. A.; Fensom, A. H. Sandhoff disease in Cyprus: population screening by biochemical and DNA analysis indicates a high frequency of carriers in the Maronite community. *Hum Genet* **2000**, *107*, 12-17.
- (150) Fitterer, B.; Hall, P.; Antonishyn, N.; Desikan, R.; Gelb, M.; Lehotay, D. Incidence and carrier frequency of Sandhoff disease in Saskatchewan determined using a novel substrate with detection by tandem mass spectrometry and molecular genetic analysis. *Molecular Genetics and Metabolism* **2014**, *111*, 382-389.
- (151) Fitterer, B. B.; Antonishyn, N. A.; Hall, P. L.; Lehotay, D. C. A polymerase chain reaction-based genotyping assay for detecting a novel sandhoff disease-causing mutation. *Genetic Testing and Molecular Biomarkers* **2012**, *16*, 401-405.
- (152) Kleiman FE1, d. K. R., de Ramirez AO, Gravel RA, Argaraña CE. Sandhoff disease in Argentina: high frequency of a splice site mutation in the HEXB gene and correlation between enzyme and DNA-based tests for heterozygote detection. **1994**.
- (153) Dreyfus, J. C.; Poenaru, L.; Vibert, M.; Ravise, N.; Boue, J. Characterization of a variant of beta-hexosaminidase: "hexosaminidase Paris". *American Journal of Human Genetics* **1977**, *29*, 287-293.
- (154) Bolhuis PA1, P. N., Bikker H, Baas F, Vianney de Jong JM. Molecular basis of an adult form of Sandhoff disease: substitution of glutamine for arginine at position 505 of the beta-chain of beta-hexosaminidase results in a labile enzyme. **1993**.
- (155) De Gasperi R1, G. S. M., Grebner EE, Mansfield D, Battistini S, Sartorato EL, Raghavan SS, Davis JG, Kolodny EH. Substitution of alanine543 with a threonine residue at the carboxy terminal end of the beta-chain is

associated with thermolabile hexosaminidase B in a Jewish family of Oriental ancestry. **1995**.

(156) Gomez-Lira M1, S. A., Mottes M, Perusi C, Pignatti PF, Rizzuto N, Salviati A. A common beta hexosaminidase gene mutation in adult Sandhoff disease patients. **1995**.

(157) Schröder, M.; Schnabel, D.; Suzuki, K.; Sandhoff, K. A mutation in the gene of a glycolipid-binding protein (GM2 activator) that causes GM2-gangliosidosis variant AB. *FEBS Letters* **1991**, 290, 1-3.

(158) Schröder M1, S. D., Hurwitz R, Young E, Suzuki K, Sandhoff K. Molecular genetics of GM2-gangliosidosis AB variant: a novel mutation and expression in BHK cells. **1993**.

(159) Xie, B.; Wang, W.; Mahuran, D. J. A Cys138-to-Arg substitution in the GM2 activator protein is associated with the AB variant form of GM2 gangliosidosis. *American Journal of Human Genetics* **1992**, 50, 1046-1052.

(160) Chen, B.; Rigat, B.; Curry, C.; Mahuran, D. J. Structure of the GM2A gene: identification of an exon 2 nonsense mutation and a naturally occurring transcript with an in-frame deletion of exon 2. *American Journal of Human Genetics* **1999**, 65, 77-87.

(161) Yamanaka, S.; Johnson, M. D.; Grinberg, A.; Westphal, H.; Crawley, J. N.; Taniike, M.; Suzuki, K.; Proia, R. L. Targeted disruption of the Hexa gene results in mice with biochemical and pathologic features of Tay-Sachs disease. *Proceedings of the National Academy of Sciences of the United States of America* **1994**, 91, 9975-9979.

(162) Phaneuf, D.; Wakamatsu, N.; Huang, J.-Q.; Borowski, A.; Peterson, A. C.; Fortunato, S. R.; Ritter, G.; Igdoura, S. A.; Morales, C. R.; Benoit, G.; Akerman, B. R.; Leclerc, D.; Hanai, N.; Marth, J. D.; Trasler, J. M.; Gravel, R. A. Dramatically Different Phenotypes in Mouse Models of Human Tay-Sachs and Sandhoff Diseases. *Human Molecular Genetics* **1996**, 5, 1-14.

(163) Jeyakumar, M.; Smith, D.; Elliott-Smith, E.; Cortina-Borja, M.; Reinkensmeier, G.; Butters, T. D.; Lemm, T.; Sandhoff, K.; Perry, V. H.; Dwek, R. A.; Platt, F. M. An Inducible Mouse Model of Late Onset Tay-Sachs Disease. *Neurobiology of Disease* **2002**, 10, 201-210.

(164) Sango, K.; McDonald, M. P.; Crawley, J. N.; Mack, M. L.; Tifft, C. J.; Skop, E.; Starr, C. M.; Hoffmann, A.; Sandhoff, K.; Suzuki, K.; Proia, R. L. Mice lacking both subunits of lysosomal [beta]-hexosaminidase display gangliosidosis and mucopolysaccharidosis. *Nat Genet* **1996**, 14, 348-352.

(165) Liu, Y.; Hoffmann, A.; Grinberg, A.; Westphal, H.; McDonald, M. P.; Miller, K. M.; Crawley, J. N.; Sandhoff, K.; Suzuki, K.; Proia, R. L. Mouse model of G(M2)activator deficiency manifests cerebellar pathology and

motor impairment. *Proceedings of the National Academy of Sciences of the United States of America* **1997**, 94, 8138-8143.

(166) Yuzyuk, J. A.; Bertoni, C.; Beccari, T.; Orlacchio, A.; Wu, Y.-Y.; Li, S.-C.; Li, Y.-T. Specificity of Mouse GM2 Activator Protein and β -N-Acetylhexosaminidases A and B: SIMILARITIES AND DIFFERENCES WITH THEIR HUMAN COUNTERPARTS IN THE CATABOLISM OF GM2. *Journal of Biological Chemistry* **1998**, 273, 66-72.

(167) Jeyakumar, M.; Butters, T. D.; Cortina-Borja, M.; Hunnam, V.; Proia, R. L.; Perry, V. H.; Dwek, R. A.; Platt, F. M. Delayed symptom onset and increased life expectancy in Sandhoff disease mice treated with N-butyldeoxynojirimycin. *Proceedings of the National Academy of Sciences of the United States of America* **1999**, 96, 6388-6393.

(168) Wada, R.; Tifft, C. J.; Proia, R. L. Microglial activation precedes acute neurodegeneration in Sandhoff disease and is suppressed by bone marrow transplantation. *Proceedings of the National Academy of Sciences of the United States of America* **2000**, 97, 10954-10959.

(169) Norflus, F.; Tifft, C. J.; McDonald, M. P.; Goldstein, G.; Crawley, J. N.; Hoffmann, A.; Sandhoff, K.; Suzuki, K.; Proia, R. L. Bone marrow transplantation prolongs life span and ameliorates neurologic manifestations in Sandhoff disease mice. *Journal of Clinical Investigation* **1998**, 101, 1881-1888.

(170) Neufeld, E. F. From serendipity to therapy. *Annual review of biochemistry* **2011**, 80, 1-15.

(171) Figura, K. V.; Hasilik, A. Lysosomal Enzymes and their Receptors. *Annual Review of Biochemistry* **1986**, 55, 167-193.

(172) Neufeld, E. B.; Stonik, J. A.; Demosky, S. J.; Knapper, C. L.; Combs, C. A.; Cooney, A.; Comly, M.; Dwyer, N.; Blanchette-Mackie, J.; Remaley, A. T.; Santamarina-Fojo, S.; Brewer, H. B. The ABCA1 Transporter Modulates Late Endocytic Trafficking: INSIGHTS FROM THE CORRECTION OF THE GENETIC DEFECT IN TANGIER DISEASE. *Journal of Biological Chemistry* **2004**, 279, 15571-15578.

(173) Parenti, G.; Pignata, C.; Vajro, P.; Salerno, M. New strategies for the treatment of lysosomal storage diseases (Review). *International journal of molecular medicine* **2013**, 31, 11-20.

(174) de Ru, M. H.; Boelens, J. J.; Das, A. M.; Jones, S. A.; van der Lee, J. H.; Mahlaoui, N.; Mengel, E.; Offringa, M.; O'Meara, A.; Parini, R. Enzyme replacement therapy and/or hematopoietic stem cell transplantation at diagnosis in patients with mucopolysaccharidosis type I: results of a European consensus procedure. *Orphanet J Rare Dis* **2011**, 6, 55.

- (175) Valayannopoulos, V.; Wijburg, F. A. Therapy for the mucopolysaccharidoses. *Rheumatology* **2011**, *50*, v49-v59.
- (176) Orchard, P. J.; Blazar, B. R.; Wagner, J.; Charnas, L.; Krivit, W.; Tolar, J. Hematopoietic Cell Therapy for Metabolic Disease. *The Journal of Pediatrics* **2007**, *151*, 340-346.
- (177) Orchard, P. J.; Tolar, J. In *Tilte*2010; Elsevier.
- (178) Platt, F. M. Sphingolipid lysosomal storage disorders. *Nature* **2014**, *510*, 68-75.
- (179) Barton, N. W.; Brady, R. O.; Dambrosia, J. M.; Di Bisceglie, A. M.; Doppelt, S. H.; Hill, S. C.; Mankin, H. J.; Murray, G. J.; Parker, R. I.; Argoff, C. E.; Grewal, R. P.; Yu, K.-T. Replacement Therapy for Inherited Enzyme Deficiency – Macrophage-Targeted Glucocerebrosidase for Gaucher's Disease. *New England Journal of Medicine* **1991**, *324*, 1464-1470.
- (180) Barton, N. W.; Furbish, F. S.; Murray, G. J.; Garfield, M.; Brady, R. O. Therapeutic response to intravenous infusions of glucocerebrosidase in a patient with Gaucher disease. *Proceedings of the National Academy of Sciences of the United States of America* **1990**, *87*, 1913-1916.
- (181) Mehta, A.; Beck, M.; Elliott, P.; Giugliani, R.; Linhart, A.; Sunder-Plassmann, G.; Schiffmann, R.; Barbey, F.; Ries, M.; Clarke, J. T. R. Enzyme replacement therapy with agalsidase alfa in patients with Fabry's disease: an analysis of registry data. *The Lancet*, *374*, 1986-1996.
- (182) Lidove, O.; West, M. L.; Pintos-Morell, G.; Reisin, R.; Nicholls, K.; Figuera, L. E.; Parini, R.; Carvalho, L. R.; Kampmann, C.; Pastores, G. M.; Mehta, A. Effects of enzyme replacement therapy in Fabry disease[mdash]A comprehensive review of the medical literature. *Genet Med* **2010**, *12*, 668-679.
- (183) Feriozzi, S.; Torras, J.; Cybulla, M.; Nicholls, K.; Sunder-Plassmann, G.; West, M.; on behalf of the, F. O. S. I. The Effectiveness of Long-Term Agalsidase Alfa Therapy in the Treatment of Fabry Nephropathy. *Clinical Journal of the American Society of Nephrology : CJASN* **2012**, *7*, 60-69.
- (184) Van der Beek, N. A. M. E.; Hagemans, M. L. C.; Reuser, A. J. J.; Hop, W. C. J.; Van der Ploeg, A. T.; Van Doorn, P. A.; Wokke, J. H. J. Rate of disease progression during long-term follow-up of patients with late-onset Pompe disease. *Neuromuscular Disorders* **2009**, *19*, 113-117.
- (185) van der Ploeg, A. T. Where do we stand in enzyme replacement therapy in Pompe's disease? *Neuromuscular Disorders* **2010**, *20*, 773-774.
- (186) Kirkegaard, T. Emerging therapies and therapeutic concepts for lysosomal storage diseases. *Expert Opinion on Orphan Drugs* **2013**, *1*, 385-404.

- (187) Rattazzi, M. C.; Dobrenis, K.: 25. Treatment of GM2 gangliosidosis: Past experiences, implications, and future prospects. In *Advances in Genetics*; Academic Press, 2001; Vol. Volume 44; pp 317-339.
- (188) Platt, F. M.; Neises, G. R.; Dwek, R. A.; Butters, T. D. N-butyldeoxynojirimycin is a novel inhibitor of glycolipid biosynthesis. *Journal of Biological Chemistry* **1994**, 269, 8362-8365.
- (189) Platt, F. M.; Neises, G. R.; Reinkensmeier, G.; Townsend, M. J.; Perry, V. H.; Proia, R. L.; Winchester, B.; Dwek, R. A.; Butters, T. D. Prevention of Lysosomal Storage in Tay-Sachs Mice Treated with N-Butyldeoxynojirimycin. *Science* **1997**, 276, 428-431.
- (190) Platt, F. M.; Lachmann, R. H. Treating lysosomal storage disorders: Current practice and future prospects. *Biochimica et Biophysica Acta (BBA) - Molecular Cell Research* **2009**, 1793, 737-745.
- (191) Cox, T.; Lachmann, R.; Hollak, C.; Aerts, J.; van Weely, S.; Hrebíček, M.; Platt, F.; Butters, T.; Dwek, R.; Moyses, C.; Gow, I.; Elstein, D.; Zimran, A. Novel oral treatment of Gaucher's disease with N-butyldeoxynojirimycin (OGT 918) to decrease substrate biosynthesis. *The Lancet* **2000**, 355, 1481-1485.
- (192) Fan, J.-Q.; Ishii, S.; Asano, N.; Suzuki, Y. Accelerated transport and maturation of lysosomal [alpha]-galactosidase A in Fabry lymphoblasts by an enzyme inhibitor. *Nat Med* **1999**, 5, 112-115.
- (193) Fan, J.-Q.; Ishii, S. Active-site-specific chaperone therapy for Fabry disease. *FEBS Journal* **2007**, 274, 4962-4971.
- (194) Frustaci, A.; Chimenti, C.; Ricci, R.; Natale, L.; Russo, M. A.; Pieroni, M.; Eng, C. M.; Desnick, R. J. Improvement in Cardiac Function in the Cardiac Variant of Fabry's Disease with Galactose-Infusion Therapy. *New England Journal of Medicine* **2001**, 345, 25-32.
- (195) Ingemann, L.; Kirkegaard, T. Lysosomal storage diseases and the heat shock response: convergences and therapeutic opportunities. *Journal of Lipid Research* **2014**, 55, 2198-2210.
- (196) Suzuki, Y. Emerging novel concept of chaperone therapies for protein misfolding diseases. *Proceedings of the Japan Academy. Series B, Physical and Biological Sciences* **2014**, 90, 145-162.
- (197) Wirth, T.; Parker, N.; Ylä-Herttuala, S. History of gene therapy. *Gene* **2013**, 525, 162-169.
- (198) Blaese, R. M.; Culver, K. W.; Miller, A. D.; Carter, C. S.; Fleisher, T.; Clerici, M.; Shearer, G.; Chang, L.; Chiang, Y.; Tolstoshev, P.; Greenblatt, J. J.; Rosenberg, S. A.; Klein, H.; Berber, M.; Mullen, C. A.; Ramsey, W. J.; Muul, L.; Morgan, R. A.; Anderson, W. F. T lymphocyte-directed gene therapy for ADA-SCID: initial trial results after 4 years. *Science* **1995**, 270, 475+.

- (199) Gaspar, H. B.; Thrasher, A. J. Gene therapy for severe combined immunodeficiencies. *Expert Opinion on Biological Therapy* **2005**, *5*, 1175-1182.
- (200) Pearson, S.; Jia, H.; Kandachi, K. China approves first gene therapy. *Nat Biotech* **2004**, *22*, 3-4.
- (201) Lentz, T. B.; Gray, S. J.; Samulski, R. J. Viral vectors for gene delivery to the central nervous system. *Neurobiology of Disease* **2012**, *48*, 179-188.
- (202) Simonato, M.; Bennett, J.; Boulis, N. M.; Castro, M. G.; Fink, D. J.; Goins, W. F.; Gray, S. J.; Lowenstein, P. R.; Vandenberghe, L. H.; Wilson, T. J.; Wolfe, J. H.; Glorioso, J. C. Progress in gene therapy for neurological disorders. *Nature reviews. Neurology* **2013**, *9*, 277-291.
- (203) Hoggan, M. D.; Blacklow, N. R.; Rowe, W. P. Studies of small DNA viruses found in various adenovirus preparations: physical, biological, and immunological characteristics. *Proceedings of the National Academy of Sciences of the United States of America* **1966**, *55*, 1467-1474.
- (204) Atchison, R. W.; Casto, B. C.; Hammon, W. M. Adenovirus-Associated Defective Virus Particles. *Science* **1965**, *149*, 754-756.
- (205) Myers, M. W.; Laughlin, C. A.; Jay, F. T.; Carter, B. J. Adenovirus helper function for growth of adeno-associated virus: effect of temperature-sensitive mutations in adenovirus early gene region 2. *Journal of virology* **1980**, *35*, 65-75.
- (206) Rose, J. A.; Berns, K. I.; Hoggan, M. D.; Koczot, F. J. EVIDENCE FOR A SINGLE-STRANDED ADENOVIRUS-ASSOCIATED VIRUS GENOME: FORMATION OF A DNA DENSITY HYBRID ON RELEASE OF VIRAL DNA. *Proceedings of the National Academy of Sciences* **1969**, *64*, 863-869.
- (207) Lusby, E.; Bohenzky, R.; Berns, K. I. Inverted terminal repetition in adeno-associated virus DNA: independence of the orientation at either end of the genome. *Journal of Virology* **1981**, *37*, 1083-1086.
- (208) Mendelson, E.; Smith, M. G.; Miller, I. L.; Carter, B. J. Effect of a viral rep gene on transformation of cells by an adeno-associated virus vector. *Virology* **1988**, *166*, 612-615.
- (209) Frank, J. K.; Barrie, J. C.; Claude, F. G.; James, A. R. Self-Complementarity of Terminal Sequences Within Plus or Minus Strands of Adenovirus-Associated Virus DNA. *Proceedings of the National Academy of Sciences* **1973**, *70*, 215-219.
- (210) Hauswirth, W. W.; Berns, K. I. Adeno-associated virus DNA replication: Nonunit-length molecules. *Virology* **1979**, *93*, 57-68.
- (211) Hoggan, G. F. T., F.B. Johnson. Continuous "carriage" of adeno-associated virus genome in cell cultures in the absence of helper adenovirus. **1972**.

- (212) Kotin, R. M.; Berns, K. I. Organization of adeno-associated virus DNA in latently infected detroit 6 cells. *Virology* **1989**, *170*, 460-467.
- (213) Cheung, A. K.; Hoggan, M. D.; Hauswirth, W. W.; Berns, K. I. Integration of the adeno-associated virus genome into cellular DNA in latently infected human Detroit 6 cells. *Journal of Virology* **1980**, *33*, 739-748.
- (214) Kotin, R. M.; Siniscalco, M.; Samulski, R. J.; Zhu, X. D.; Hunter, L.; Laughlin, C. A.; McLaughlin, S.; Muzyczka, N.; Rocchi, M.; Berns, K. I. Site-specific integration by adeno-associated virus. *Proceedings of the National Academy of Sciences of the United States of America* **1990**, *87*, 2211-2215.
- (215) McCarty, D. M.; Young, S. M.; Samulski, R. J. INTEGRATION OF ADENO-ASSOCIATED VIRUS (AAV) AND RECOMBINANT AAV VECTORS. *Annual Review of Genetics* **2004**, *38*, 819-845.
- (216) Daya, S.; Berns, K. I. Gene Therapy Using Adeno-Associated Virus Vectors. *Clinical Microbiology Reviews* **2008**, *21*, 583-593.
- (217) Wu, Z.; Asokan, A.; Samulski, R. J. Adeno-associated Virus Serotypes: Vector Toolkit for Human Gene Therapy. *Mol Ther* **2006**, *14*, 316-327.
- (218) Bartel, M. A.; Weinstein, J. R.; Schaffer, D. V. Directed evolution of novel adeno-associated viruses for therapeutic gene delivery. *Gene Ther* **2012**, *19*, 694-700.
- (219) Boutin, S.; Monteilhet, V.; Veron, P.; Leborgne, C.; Benveniste, O.; Montus, M.; Masurier, C. Prevalence of serum IgG and neutralizing factors against adeno-associated virus (AAV) types 1, 2, 5, 6, 8, and 9 in the healthy population: implications for gene therapy using AAV vectors. *Human Gene Therapy* **2010**, *21*, 704-712.
- (220) Calcedo, R.; Vandenberghe, L. H.; Gao, G.; Lin, J.; Wilson, J. M. Worldwide Epidemiology of Neutralizing Antibodies to Adeno-Associated Viruses. *Journal of Infectious Diseases* **2009**, *199*, 381-390.
- (221) Kotterman, M. A.; Schaffer, D. V. Engineering adeno-associated viruses for clinical gene therapy. *Nat Rev Genet* **2014**, *15*, 445-451.
- (222) Carter, B. J. Adeno-associated Virus and the Development of Adeno-associated Virus Vectors: A Historical Perspective. *Mol Ther* **2004**, *10*, 981-989.
- (223) Samulski, R. J.; Muzyczka, N. AAV-Mediated Gene Therapy for Research and Therapeutic Purposes. *Annual Review of Virology* **2014**, *1*, 427-451.
- (224) Terence Flotte, C.-I. B. C., Carol Conrad, William Guggino, Thomas Reynolds, Beryl Rosenstein, George Taylor, Sandra Walden, and Randall Wetzel. . A Phase I Study of an Adeno-Associated Virus-CFTR Gene Vector in Adult CF Patients with Mild Lung Disease. Johns Hopkins Children's Center, Baltimore, Maryland. **1996**.

(225) Fraites, T. J.; Schleissing, M. R.; Shanely, R. A.; Walter, G. A.; Cloutier, D. A.; Zolotukhin, I.; Pauly, D. F.; Raben, N.; Plotz, P. H.; Powers, S. K.; Kessler, P. D.; Byrne, B. J. Correction of the Enzymatic and Functional Deficits in a Model of Pompe Disease Using Adeno-associated Virus Vectors. *Mol Ther* **2002**, *5*, 571-578.

(226) Kaplitt, M. G.; Feigin, A.; Tang, C.; Fitzsimons, H. L.; Mattis, P.; Lawlor, P. A.; Bland, R. J.; Young, D.; Strybing, K.; Eidelberg, D.; During, M. J. Safety and tolerability of gene therapy with an adeno-associated virus (AAV) borne GAD gene for Parkinson's disease: an open label, phase I trial. *The Lancet*, *369*, 2097-2105.

(227) Bainbridge, J. W. B.; Smith, A. J.; Barker, S. S.; Robbie, S.; Henderson, R.; Balaggan, K.; Viswanathan, A.; Holder, G. E.; Stockman, A.; Tyler, N.; Petersen-Jones, S.; Bhattacharya, S. S.; Thrasher, A. J.; Fitzke, F. W.; Carter, B. J.; Rubin, G. S.; Moore, A. T.; Ali, R. R. Effect of Gene Therapy on Visual Function in Leber's Congenital Amaurosis. *New England Journal of Medicine* **2008**, *358*, 2231-2239.

(228) Hauswirth, W. W.; Aleman, T. S.; Kaushal, S.; Cideciyan, A. V.; Schwartz, S. B.; Wang, L.; Conlon, T. J.; Boye, S. L.; Flotte, T. R.; Byrne, B. J.; Jacobson, S. G. Treatment of Leber Congenital Amaurosis Due to RPE65 Mutations by Ocular Subretinal Injection of Adeno-Associated Virus Gene Vector: Short-Term Results of a Phase I Trial. *Human Gene Therapy* **2008**, *19*, 979-990.

(229) Maguire, A. M.; High, K. A.; Auricchio, A.; Wright, J. F.; Pierce, E. A.; Testa, F.; Mingozzi, F.; Bennicelli, J. L.; Ying, G.-s.; Rossi, S.; Fulton, A.; Marshall, K. A.; Banfi, S.; Chung, D. C.; Morgan, J. I. W.; Hauck, B.; Zeleniaia, O.; Zhu, X.; Raffini, L.; Coppieters, F.; De Baere, E.; Shindler, K. S.; Volpe, N. J.; Surace, E. M.; Acerra, C.; Lyubarsky, A.; Redmond, T. M.; Stone, E.; Sun, J.; McDonnell, J. W.; Leroy, B. P.; Simonelli, F.; Bennett, J. Age-dependent effects of RPE65 gene therapy for Leber's congenital amaurosis: a phase 1 dose-escalation trial. *The Lancet*, *374*, 1597-1605.

(230) Nathwani, A. C.; Tuddenham, E. G. D.; Rangarajan, S.; Rosales, C.; McIntosh, J.; Linch, D. C.; Chowdary, P.; Riddell, A.; Pie, A. J.; Harrington, C.; O'Beirne, J.; Smith, K.; Pasi, J.; Glader, B.; Rustagi, P.; Ng, C. Y. C.; Kay, M. A.; Zhou, J.; Spence, Y.; Morton, C. L.; Allay, J.; Coleman, J.; Sleep, S.; Cunningham, J. M.; Srivastava, D.; Basner-Tschakarjan, E.; Mingozzi, F.; High, K. A.; Gray, J. T.; Reiss, U. M.; Nienhuis, A. W.; Davidoff, A. M. Adenovirus-Associated Virus Vector-Mediated Gene Transfer in Hemophilia B. *New England Journal of Medicine* **2011**, *365*, 2357-2365.

- (231) Rafii, M. S.; Baumann, T. L.; Bakay, R. A. E.; Ostrove, J. M.; Siffert, J.; Fleisher, A. S.; Herzog, C. D.; Barba, D.; Pay, M.; Salmon, D. P.; Chu, Y.; Kordower, J. H.; Bishop, K.; Keator, D.; Potkin, S.; Bartus, R. T. A phase1 study of stereotactic gene delivery of AAV2-NGF for Alzheimer's disease. *Alzheimer's & Dementia* **2014**, *10*, 571-581.
- (232) Bowles, D. E.; McPhee, S. W. J.; Li, C.; Gray, S. J.; Samulski, J. J.; Camp, A. S.; Li, J.; Wang, B.; Monahan, P. E.; Rabinowitz, J. E.; Grieger, J. C.; Govindasamy, L.; Agbandje-McKenna, M.; Xiao, X.; Samulski, R. J. Phase 1 Gene Therapy for Duchenne Muscular Dystrophy Using a Translational Optimized AAV Vector. *Mol Ther* **2012**, *20*, 443-455.
- (233) Leone, P.; Shera, D.; McPhee, S. W. J.; Francis, J. S.; Kolodny, E. H.; Bilaniuk, L. T.; Wang, D.-J.; Assadi, M.; Goldfarb, O.; Goldman, H. W.; Freese, A.; Young, D.; During, M. J.; Samulski, R. J.; Janson, C. G. Long-Term Follow-Up After Gene Therapy for Canavan Disease. *Science translational medicine* **2012**, *4*, 165ra163-165ra163.
- (234) Gonçalves, M. A. F. V. Adeno-associated virus: from defective virus to effective vector. *Virology Journal* **2005**, *2*, 43-43.
- (235) Salmon, F.; Grosios, K.; Petry, H. Safety profile of recombinant adeno-associated viral vectors: focus on alipogene tiparvovec (Glybera®). *Expert Review of Clinical Pharmacology* **2013**, *7*, 53-65.
- (236) Gao, G.; Vandenberghe, L. H.; Alvira, M. R.; Lu, Y.; Calcedo, R.; Zhou, X.; Wilson, J. M. Clades of Adeno-Associated Viruses Are Widely Disseminated in Human Tissues. *Journal of Virology* **2004**, *78*, 6381-6388.
- (237) Zincarelli, C.; Soltys, S.; Rengo, G.; Rabinowitz, J. E. Analysis of AAV Serotypes 1-9 Mediated Gene Expression and Tropism in Mice After Systemic Injection. *Mol Ther* **2008**, *16*, 1073-1080.
- (238) Asokan, A.; Schaffer, D. V.; Jude Samulski, R. The AAV Vector Toolkit: Poised at the Clinical Crossroads. *Mol Ther* **2012**, *20*, 699-708.
- (239) Bish, L. T.; Morine, K.; Sleeper, M. M.; Sanmiguel, J.; Wu, D.; Gao, G.; Wilson, J. M.; Sweeney, H. L. Adeno-Associated Virus (AAV) Serotype 9 Provides Global Cardiac Gene Transfer Superior to AAV1, AAV6, AAV7, and AAV8 in the Mouse and Rat. *Human Gene Therapy* **2008**, *19*, 1359-1368.
- (240) Burger, C.; Gorbatyuk, O. S.; Velardo, M. J.; Peden, C. S.; Williams, P.; Zolotukhin, S.; Reier, P. J.; Mandel, R. J.; Muzyczka, N. Recombinant AAV Viral Vectors Pseudotyped with Viral Capsids from Serotypes 1, 2, and 5 Display Differential Efficiency and Cell Tropism after Delivery to Different Regions of the Central Nervous System. *Mol Ther* **2004**, *10*, 302-317.

- (241) Cearley, C. N.; Wolfe, J. H. Transduction Characteristics of Adeno-associated Virus Vectors Expressing Cap Serotypes 7, 8, 9, and Rh10 in the Mouse Brain. *Mol Ther* **2006**, *13*, 528-537.
- (242) Davidson, B. L.; Stein, C. S.; Heth, J. A.; Martins, I.; Kotin, R. M.; Derksen, T. A.; Zabner, J.; Ghodsi, A.; Chiorini, J. A. Recombinant adeno-associated virus type 2, 4, and 5 vectors: Transduction of variant cell types and regions in the mammalian central nervous system. *Proceedings of the National Academy of Sciences of the United States of America* **2000**, *97*, 3428-3432.
- (243) Duque, S.; Joussemet, B.; Riviere, C.; Marais, T.; Dubreil, L.; Douar, A.-M.; Fyfe, J.; Moullier, P.; Colle, M.-A.; Barkats, M. Intravenous Administration of Self-complementary AAV9 Enables Transgene Delivery to Adult Motor Neurons. *Mol Ther* **2009**, *17*, 1187-1196.
- (244) Foust, K. D.; Nurre, E.; Montgomery, C. L.; Hernandez, A.; Chan, C. M.; Kaspar, B. K. Intravascular AAV9 preferentially targets neonatal-neurons and adult-astrocytes in CNS. *Nature biotechnology* **2009**, *27*, 59-65.
- (245) Gray, S. J.; Foti, S. B.; Schwartz, J. W.; Bachaboina, L.; Taylor-Blake, B.; Coleman, J.; Ehlers, M. D.; Zylka, M. J.; McCown, T. J.; Samulski, R. J. Optimizing Promoters for Recombinant Adeno-Associated Virus-Mediated Gene Expression in the Peripheral and Central Nervous System Using Self-Complementary Vectors. *Human Gene Therapy* **2011**, *22*, 1143-1153.
- (246) Rahim, A. A.; Wong, A. M. S.; Hoefer, K.; Buckley, S. M. K.; Mattar, C. N.; Cheng, S. H.; Chan, J. K. Y.; Cooper, J. D.; Waddington, S. N. Intravenous administration of AAV2/9 to the fetal and neonatal mouse leads to differential targeting of CNS cell types and extensive transduction of the nervous system. *The FASEB Journal* **2011**, *25*, 3505-3518.
- (247) Foust, K. D.; Wang, X.; McGovern, V. L.; Braun, L.; Bevan, A. K.; Haidet, A. M.; Le, T. T.; Morales, P. R.; Rich, M. M.; Burghes, A. H. M.; Kaspar, B. K. Rescue of the spinal muscular atrophy phenotype in a mouse model by early postnatal delivery of SMN. *Nature biotechnology* **2010**, *28*, 271-274.
- (248) Wang, Z.; Tapscott, S. J.; Chamberlain, J. S.; Storb, R. Immunity and AAV-Mediated Gene Therapy for Muscular Dystrophies in Large Animal Models and Human Trials. *Frontiers in Microbiology* **2011**, *2*, 201.
- (249) Bevan, A. K.; Duque, S.; Foust, K. D.; Morales, P. R.; Braun, L.; Schmelzer, L.; Chan, C. M.; McCrate, M.; Chicoine, L. G.; Coley, B. D.; Porensky, P. N.; Kolb, S. J.; Mendell, J. R.; Burghes, A. H. M.; Kaspar, B. K. Systemic Gene Delivery in Large Species for Targeting Spinal Cord, Brain, and Peripheral Tissues for Pediatric Disorders. *Molecular Therapy* **2011**, *19*, 1971-1980.
- (250) Samaranch, L.; Salegio, E. A.; San Sebastian, W.; Kells, A. P.; Foust, K. D.; Bringas, J. R.; Lamarre, C.; Forsayeth, J.; Kaspar, B. K.; Bankiewicz, K. S.

Adeno-Associated Virus Serotype 9 Transduction in the Central Nervous System of Nonhuman Primates. *Human Gene Therapy* **2012**, 23, 382-389.

(251) Passini, M. A.; Bu, J.; Roskelley, E. M.; Richards, A. M.; Sardi, S. P.; O'Riordan, C. R.; Klinger, K. W.; Shihabuddin, L. S.; Cheng, S. H. CNS-targeted gene therapy improves survival and motor function in a mouse model of spinal muscular atrophy. *The Journal of Clinical Investigation* **2010**, 120, 1253-1264.

(252) Federici, T.; Taub, J. S.; Baum, G. R.; Gray, S. J.; Grieger, J. C.; Matthews, K. A.; Handy, C. R.; Passini, M. A.; Samulski, R. J.; Boulis, N. M. Robust spinal motor neuron transduction following intrathecal delivery of AAV9 in pigs. *Gene Ther* **2012**, 19, 852-859.

(253) Benkhelifa-Ziyyat, S.; Besse, A.; Roda, M.; Duque, S.; Astord, S.; Carcenac, R.; Marais, T.; Barkats, M. Intramuscular scAAV9-SMN Injection Mediates Widespread Gene Delivery to the Spinal Cord and Decreases Disease Severity in SMA Mice. *Mol Ther* **2013**, 21, 282-290.

(254) Henriques, A.; Pitzer, C.; Dittgen, T.; Klugmann, M.; Dupuis, L.; Schneider, A. CNS-targeted Viral Delivery of G-CSF in an Animal Model for ALS: Improved Efficacy and Preservation of the Neuromuscular Unit. *Molecular Therapy* **2011**, 19, 284-292.

(255) Xue, Y. Q.; Ma, B. F.; Zhao, L. R.; Tatom, J. B.; Li, B.; Jiang, L. X.; Klein, R. L.; Duan, W. M. AAV9-mediated erythropoietin gene delivery into the brain protects nigral dopaminergic neurons in a rat model of Parkinson's disease. *Gene Ther* **2009**, 17, 83-94.

(256) Hinderer, C.; Bell, P.; Gurda, B. L.; Wang, Q.; Louboutin, J.-P.; Zhu, Y.; Bagel, J.; O'Donnell, P.; Sikora, T.; Ruane, T.; Wang, P.; Haskins, M. E.; Wilson, J. M. Intrathecal Gene Therapy Corrects CNS Pathology in a Feline Model of Mucopolysaccharidosis I. *Mol Ther* **2014**.

(257) Fu, H.; DiRosario, J.; Killedar, S.; Zaraspe, K.; McCarty, D. M. Correction of Neurological Disease of Mucopolysaccharidosis IIIB in Adult Mice by rAAV9 Trans-Blood-Brain Barrier Gene Delivery. *Molecular Therapy* **2011**, 19, 1025-1033.

(258) Aronovich, E. L.; Hackett, P. B. Lysosomal storage disease: Gene therapy on both sides of the blood-brain barrier. *Molecular Genetics and Metabolism*.

(259) Dayton, R. D.; Wang, D. B.; Klein, R. L. The advent of AAV9 expands applications for brain and spinal cord gene delivery. *Expert Opinion on Biological Therapy* **2012**, 12, 757-766.

(260) Bapat, B.; Ethier, M.; Neote, K.; Mahuran, D.; Gravel, R. A. Cloning and sequence analysis of a cDNA encoding the β -subunit of mouse β -hexosaminidase. *FEBS Lett.* **1988**, 237, 191-195.

(261) Bello, A.; Tran, K.; Chand, A.; Doria, M.; Allocca, M.; Hildinger, M.; Beniac, D.; Kranendonk, C.; Auricchio, A.; Kobinger, G. P. Isolation and evaluation of novel adeno-associated virus sequences from porcine tissues. *Gene Ther.* **2009**, *16*, 1320-1328.

(262) Kaback, M. M.; Shapiro, L. J.; Hirsch, P.: Tay-Sachs disease heterozygote detection: a quality control study. In *Tay-Sachs disease: screening and prevention*; 18 ed.; Kaback, M. M., Rimoin, D. L., O'Brien, J. L., Eds.; Progress in Clinical and Biological Research; A.R. Liss: New York, 1977; pp 267-279.

(263) Varshney, G. K.; Lu, J.; Gildea, D. E.; Huang, H.; Pei, W.; Yang, Z.; Huang, S. C.; Schoenfeld, D.; Pho, N. H.; Casero, D.; Hirase, T.; Mosbrook-Davis, D.; Zhang, S.; Jao, L. E.; Zhang, B.; Woods, I. G.; Zimmerman, S.; Schier, A. F.; Wolfsberg, T. G.; Pellegrini, M.; Burgess, S. M.; Lin, S. A large-scale zebrafish gene knockout resource for the genome-wide study of gene function. *Genome Res.* **2013**, *23*, 727-735.

(264) LaFave, M. C.; Varshney, G. K.; Gildea, D. E.; Wolfsberg, T. G.; Baxevanis, A. D.; Burgess, S. M. MLV integration site selection is driven by strong enhancers and active promoters. *Nucleic Acids Res.* **2014**, *42*, 4257-4269.

(265) Barnett, D. W.; Garrison, E. K.; Quinlan, A. R.; Stromberg, M. P.; Marth, G. T. BamTools: a C++ API and toolkit for analyzing and managing BAM files. *Bioinformatics* **2011**, *27*, 1691-1692.

(266) Langmead, B.; Trapnell, C.; Pop, M.; Salzberg, S. L. Ultrafast and memory-efficient alignment of short DNA sequences to the human genome. *Genome Biol.* **2009**, *10*, R25.

(267) Martin, M. Cutadapt removes adapter sequences from high-throughput sequencing reads. *EMBnet.journal* **2011**, *17*, 10-12.

(268) Quinlan, A. R.; Hall, I. M. BEDTools: a flexible suite of utilities for comparing genomic features. *Bioinformatics* **2010**, *26*, 841-842.

(269) Flicek, P.; Amode, M. R.; Barrell, D.; Beal, K.; Billis, K.; Brent, S.; Carvalho-Silva, D.; Clapham, P.; Coates, G.; Fitzgerald, S.; Gil, L.; Giron, C. G.; Gordon, L.; Hourlier, T.; Hunt, S.; Johnson, N.; Juettemann, T.; Kahari, A. K.; Keenan, S.; Kulesha, E.; Martin, F. J.; Maurel, T.; McLaren, W. M.; Murphy, D. N.; Nag, R.; Overduin, B.; Pignatelli, M.; Pritchard, B.; Pritchard, E.; Riat, H. S.; Ruffier, M.; Sheppard, D.; Taylor, K.; Thormann, A.; Trevanion, S. J.; Vullo, A.; Wilder, S. P.; Wilson, M.; Zadissa, A.; Aken, B. L.; Birney, E.; Cunningham, F.; Harrow, J.; Herrero, J.; Hubbard, T. J.; Kinsella, R.; Muffato, M.; Parker, A.; Spudich, G.; Yates, A.; Zerbino, D. R.; Searle, S. M. Ensembl 2014. *Nucleic Acids Res.* **2014**, *42*, D749-755.

(270) Kinsella, R. J.; Kahari, A.; Haider, S.; Zamora, J.; Proctor, G.; Spudich, G.; Almeida-King, J.; Staines, D.; Derwent, P.; Kerhornou, A.; Kersey, P.

Flicek, P. Ensembl BioMarts: a hub for data retrieval across taxonomic space. *Database (Oxford)* **2011**, 2011, bar030.

(271) Phaneuf, D.; Wakamatsu, N.; Huang, J. Q.; Borowski, A.; Peterson, A. C.; Fortunato, S. R.; Ritter, G.; Igdoura, S. A.; Morales, C. R.; Benoit, G.; Akerman, B. R.; Leclerc, D.; Hanai, N.; Marth, J. D.; Trasler, J. M.; Gravel, R. A. Dramatically different phenotypes in mouse models of human Tay-Sachs and Sandhoff diseases. *Hum. Mol. Genet.* **1996**, 5, 1-14.

(272) Drew, T.; Prentice, S.; Schepens, B.: Cortical and brainstem control of locomotion. In *Prog. Brain Res.*; Shigemori, D. G. S., Mario, W., Eds.; Elsevier, 2004; Vol. Volume 143; pp 251-261.

(273) M. Ito, T. S., N. Yagi, M. Yamamoto. The cerebellar modification of rabbit's horizontal vestibulo-ocular reflex induced by sustained head rotation combined with visual stimulation. *Proc. Jap. Acad. Sci.*, 50 (1974), pp. 85–89 **1974**.

(274) Ito, M. New concepts in cerebellar function. *Rev. Neurol.*, 149, pp. 596–599 **1993**.

(275) Perry, V. H.; Holmes, C. Microglial priming in neurodegenerative disease. *Nat Rev Neurol* **2014**, 10, 217-224.

(276) Perry, V. H.; Teeling, J. Microglia and macrophages of the central nervous system: the contribution of microglia priming and systemic inflammation to chronic neurodegeneration. *Seminars in Immunopathology* **2013**, 35, 601-612.

(277) Begolka, W. S.; Vanderlugt, C. L.; Rahbe, S. M.; Miller, S. D. Differential Expression of Inflammatory Cytokines Parallels Progression of Central Nervous System Pathology in Two Clinically Distinct Models of Multiple Sclerosis. *The Journal of Immunology* **1998**, 161, 4437-4446.

(278) Wang, P. R.; Xu, M.; Toffanin, S.; Li, Y.; Llovet, J. M.; Russell, D. W. Induction of hepatocellular carcinoma by in vivo gene targeting. *Proc. Natl. Acad. Sci. U. S. A.* **2012**, 109, 11264-11269.

(279) Katoh, M. Cancer genomics and genetics of FGFR2 (Review). *Int. J. Oncol.* **2008**, 33, 233-237.

(280) Brooks, A. I.; Stein, C. S.; Hughes, S. M.; Heth, J.; McCray, P. M.; Sauter, S. L.; Johnston, J. C.; Cory-Slechta, D. A.; Federoff, H. J.; Davidson, B. L. Functional correction of established central nervous system deficits in an animal model of lysosomal storage disease with feline immunodeficiency virus-based vectors. *Proceedings of the National Academy of Sciences of the United States of America* **2002**, 99, 6216-6221.

(281) Chen, Y. H.; Claflin, K.; Geoghegan, J. C.; Davidson, B. L. Sialic Acid Deposition Impairs the Utility of AAV9, but Not Peptide-modified AAVs

for Brain Gene Therapy in a Mouse Model of Lysosomal Storage Disease. *Molecular Therapy* **2012**, 20, 1393-1399.

(282) Lowenstein, P. R. Crossing the Rubicon. *Nat Biotech* **2009**, 27, 42-44.

(283) Caley, D. W.; Maxwell, D. S. Development of the blood vessels and extracellular spaces during postnatal maturation of rat cerebral cortex. *The Journal of Comparative Neurology* **1970**, 138, 31-47.

(284) Sargeant, T. J.; Drage, D. J.; Wang, S.; Apostolakis, A. A.; Cox, T. M.; Cachón-González, M. B. Characterization of Inducible Models of Tay-Sachs and Related Disease. *PLoS Genetics* **2012**, 8, e1002943.

(285) Gulinello, M.; Chen, F.; Dobrenis, K. Early deficits in motor coordination and cognitive dysfunction in a mouse model of the neurodegenerative lysosomal storage disorder, Sandhoff disease. *Behavioural brain research* **2008**, 193, 315-319.

(286) Hu, L.; Sun, Y.; Villasana, L. E.; Paylor, R.; Klann, E.; Pautler, R. G. Early Changes in the Apparent Diffusion Coefficient (ADC) in a Mouse Model of Sandhoff's Disease Occur Prior to Disease Symptoms and Behavioral Deficits. *Magnetic resonance in medicine : official journal of the Society of Magnetic Resonance in Medicine / Society of Magnetic Resonance in Medicine* **2009**, 62, 1175-1184.

(287) Cappe, C.; Morel, A.; Barone, P.; Rouiller, E. M. The Thalamocortical Projection Associated Virus Vectors. *Journal of Virology* **2002**, 76, 4580-4590.

(312) Calcedo, R.; Morizono, H.; Wang, L.; McCarter, R.; He, J.; Jones, D.; Batshaw, M. L.; Wilson, J. M. Adeno-n Systems in Primate: An Anatomical Support for Multisensory and Sensorimotor Interplay. *Cerebral Cortex (New York, NY)* **2009**, 19, 2025-2037.

(288) Rogove, A.; Lu, W.; Tsirka, S. Microglial activation and recruitment, but not proliferation, suffice to mediate neurodegeneration. *Cell death and differentiation* **2002**, 9, 801-806.

(289) Cachon-Gonzalez, M. B.; Wang, S. Z.; Ziegler, R.; Cheng, S. H.; Cox, T. M. Reversibility of neuropathology in Tay-Sachs-related diseases. *Hum. Mol. Genet.* **2014**, 23, 730-748.

(290) Cabrera-Salazar, M. A.; Roskelley, E. M.; Bu, J.; Hodges, B. L.; Yew, N.; Dodge, J. C.; Shihabuddin, L. S.; Sohar, I.; Sleat, D. E.; Scheule, R. K.; Davidson, B. L.; Cheng, S. H.; Lobel, P.; Passini, M. A. Timing of Therapeutic Intervention Determines Functional and Survival Outcomes in a Mouse Model of Late Infantile Batten Disease. *Mol Ther* **2007**, 15, 1782-1788.

(291) Cachón-González, M. B.; Wang, S. Z.; McNair, R.; Bradley, J.; Lunn, D.; Ziegler, R.; Cheng, S. H.; Cox, T. M. Gene Transfer Corrects Acute GM2

Gangliosidosis—Potential Therapeutic Contribution of Perivascular Enzyme Flow. *Molecular Therapy* **2012**, *20*, 1489-1500.

(292) Donsante, A.; Vogler, C.; Muzyczka, N.; Crawford, J. M.; Barker, J.; Flotte, T.; Campbell-Thompson, M.; Daly, T.; Sands, M. S. Observed incidence of tumorigenesis in long-term rodent studies of rAAV vectors. *Gene Ther.* **2001**, *8*, 1343-1346.

(293) Zhong, L.; Malani, N.; Li, M.; Brady, T.; Xie, J.; Bell, P.; Li, S.; Jones, H.; Wilson, J. M.; Flotte, T. R.; Bushman, F. D.; Gao, G.: Recombinant adeno-associated virus integration sites in murine liver after ornithine transcarbamylase gene correction. In *Hum. Gene Ther.*, 2013; Vol. 24; pp 520-525.

(294) Bell, P.; Moscioni, A. D.; McCarter, R. J.; Wu, D.; Gao, G.; Hoang, A.; Sanmiguel, J. C.; Sun, X.; Wivel, N. A.; Raper, S. E.; Furth, E. E.; Batshaw, M. L.; Wilson, J. M. Analysis of Tumors Arising in Male B6C3F1 Mice with and without AAV Vector Delivery to Liver. *Mol Ther* **2006**, *14*, 34-44.

(295) Moscioni, D.; Morizono, H.; McCarter, R. J.; Stern, A.; Cabrera-Luque, J.; Hoang, A.; Sanmiguel, J.; Wu, D.; Bell, P.; Gao, G. P.; Raper, S. E.; Wilson, J. M.; Batshaw, M. L. Long-term correction of ammonia metabolism and prolonged survival in ornithine transcarbamylase-deficient mice following liver-directed treatment with adeno-associated viral vectors. *Mol. Ther.* **2006**, *14*, 25-33.

(296) Masat E1, P. G., Mingozi F. Humoral immunity to AAV vectors in gene therapy: challenges and potential solutions. **2013**.

(297) Monteilhet, V.; Saheb, S.; Boutin, S.; Leborgne, C.; Veron, P.; Montus, M.-F.; Moullier, P.; Benveniste, O.; Masurier, C. A 10 Patient Case Report on the Impact of Plasmapheresis Upon Neutralizing Factors Against Adeno-associated Virus (AAV) Types 1, 2, 6, and 8. *Mol Ther* **2011**, *19*, 2084-2091.

(298) Mingozi, F.; Chen, Y.; Edmonson, S. C.; Zhou, S.; Thurlings, R. M.; Tak, P. P.; High, K. A.; Vervoordeldonk, M. J. Prevalence and pharmacological modulation of humoral immunity to AAV vectors in gene transfer to synovial tissue. *Gene Ther* **2013**, *20*, 417-424.

(299) Karman, J.; Gumlaw, N. K.; Zhang, J.; Jiang, J.-L.; Cheng, S. H.; Zhu, Y. Proteasome Inhibition Is Partially Effective in Attenuating Pre-Existing Immunity against Recombinant Adeno-Associated Viral Vectors. *PLoS ONE* **2012**, *7*, e34684.

(300) Finn, J. D.; Hui, D.; Downey, H. D.; Dunn, D.; Pien, G. C.; Mingozi, F.; Zhou, S.; High, K. A. Proteasome Inhibitors Decrease AAV2 Capsid derived Peptide Epitope Presentation on MHC Class I Following Transduction. *Mol Ther* **2009**, *18*, 135-142.

(301) Neubert, K.; Meister, S.; Moser, K.; Weisel, F.; Maseda, D.; Amann, K.; Wiethe, C.; Winkler, T. H.; Kalden, J. R.; Manz, R. A.; Voll, R. E. The

proteasome inhibitor bortezomib depletes plasma cells and protects mice with lupus-like disease from nephritis. *Nat Med* **2008**, *14*, 748-755.

(302) Monahan, P. E.; Lothrop, C. D.; Sun, J.; Hirsch, M. L.; Kafri, T.; Kantor, B.; Sarkar, R.; Tillson, D. M.; Elia, J. R.; Samulski, R. J. Proteasome Inhibitors Enhance Gene Delivery by AAV Virus Vectors Expressing Large Genomes in Hemophilia Mouse and Dog Models: A Strategy for Broad Clinical Application. *Mol Ther* **2010**, *18*, 1907-1916.

(303) Chicoine, L. G.; Montgomery, C. L.; Bremer, W. G.; Shontz, K. M.; Griffin, D. A.; Heller, K. N.; Lewis, S.; Malik, V.; Grose, W. E.; Shilling, C. J.; Campbell, K. J.; Preston, T. J.; Coley, B. D.; Martin, P. T.; Walker, C. M.; Clark, K. R.; Sahenk, Z.; Mendell, J. R.; Rodino-Klapac, L. R. Plasmapheresis Eliminates the Negative Impact of AAV Antibodies on Microdystrophin Gene Expression Following Vascular Delivery. *Mol Ther* **2014**, *22*, 338-347.

(304) Corti, M.; Elder, M. E.; Falk, D. J.; Lawson, L.; Smith, B. K.; Nayak, S.; Conlon, T. J.; Clément, N.; Erger, K.; Lavassani, E.; Green, M. M.; Doerfler, P. A.; Herzog, R. W.; Byrne, B. J. B-cell depletion is protective against anti-AAV capsid immune response: a human subject case study. *Molecular Therapy – Methods & Clinical Development* **2014**, *1*.

(305) Mingozi, F.; Anguela, X. M.; Pavani, G.; Chen, Y.; Davidson, R. J.; Hui, D. J.; Yazicioglu, M.; Elkouby, L.; Hinderer, C. J.; Faella, A.; Howard, C.; Tai, A.; Podsakoff, G. M.; Zhou, S.; Basner-Tschakarjan, E.; Wright, J. F.; High, K. A. Overcoming Preexisting Humoral Immunity to AAV Using Capsid Decoys. *Science Translational Medicine* **2013**, *5*, 194ra192.

(306) Tseng, Y.-S.; Agbandje-Mckenna, M. Mapping the AAV capsid host antibody response towards the development of second generation gene delivery vectors. *Frontiers in Immunology* **2014**, *5*.

(307) Gurda, B. L.; Raupp, C.; Popa-Wagner, R.; Naumer, M.; Olson, N. H.; Ng, R.; McKenna, R.; Baker, T. S.; Kleinschmidt, J. A.; Agbandje-McKenna, M. Mapping a Neutralizing Epitope onto the Capsid of Adeno-Associated Virus Serotype 8. *Journal of Virology* **2012**, *86*, 7739-7751.

(308) Bartel, M.; Schaffer, D.; Büning, H. Enhancing the Clinical Potential of AAV Vectors by Capsid Engineering to Evade Pre-Existing Immunity. *Frontiers in Microbiology* **2011**, *2*, 204.

(309) Jeyakumar, M.; Thomas, R.; Elliot-Smith, E.; Smith, D. A.; van der Spoel, A. C.; d'Azzo, A.; Hugh Perry, V.; Butters, T. D.; Dwek, R. A.; Platt, F. M. Central nervous system inflammation is a hallmark of pathogenesis in mouse models of GM1 and GM2 gangliosidosis. *Brain* **2003**, *126*, 974-987.

(310) Abo-Ouf, H.; Hooper, A. W.; White, E. J.; van Rensburg, H. J.; Trigatti, B. L.; Igdoura, S. A. Deletion of tumor necrosis factor- α ameliorates

neurodegeneration in Sandhoff disease mice. *Hum. Mol. Genet.* **2013**, *22*, 3960-3975.

(311) Zaiss, A.-K.; Liu, Q.; Bowen, G. P.; Wong, N. C. W.; Bartlett, J. S.; Muruve, D. A. Differential Activation of Innate Immune Responses by Adenovirus and Adeno-AAAssociated Virus Antibody Profiles in Newborns, Children, and Adolescents. *Clinical and Vaccine Immunology : CVI* **2011**, *18*, 1586-1588.

(313) Hu, C.; Lipshutz, G. S. AAV-based neonatal gene therapy for hemophilia A: long-term correction and avoidance of immune responses in mice. *Gene Ther* **2012**, *19*, 1166-1176.

(314) Bostick, B.; Ghosh, A.; Yue, Y.; Long, C.; Duan, D. Systemic AAV-9 transduction in mice is influenced by animal age but not by the route of administration. *Gene Ther* **2007**, *14*, 1605-1609.

(315) Banachlocha, M. A. M. Neuromagnetic dialogue between neuronal minicolumns and astroglial network: A new approach for memory and cerebral computation. *Brain Research Bulletin* **2007**, *73*, 21-27.

(316) Swain, G. P.; Prociuk, M.; Bagel, J. H.; O'Donnell, P.; Berger, K.; Drobatz, K.; Gurda, B. L.; Haskins, M. E.; Sands, M. S.; Vite, C. H. Adeno-associated virus serotypes 9 and rh10 mediate strong neuronal transduction of the dog brain. *Gene Ther* **2014**, *21*, 28-36.

(317) McCarty, D.; Monahan, P.; Samulski, R. Self-complementary recombinant adeno-associated virus (scAAV) vectors promote efficient transduction independently of DNA synthesis. *Gene therapy* **2001**, *8*, 1248-1254.

(318) Gray, S. J.; Foti, S. B.; Schwartz, J. W.; Bachaboina, L.; Taylor-Blake, B.; Coleman, J.; Ehlers, M. D.; Zylka, M. J.; McCown, T. J.; Samulski, R. J. Optimizing promoters for recombinant adeno-associated virus-mediated gene expression in the peripheral and central nervous system using self-complementary vectors. *Hum. Gene Ther.* **2011**, *22*, 1143-1153.

(319) Dayton, R. D.; Wang, D. B.; Klein, R. L. The advent of AAV9 expands applications for brain and spinal cord gene delivery. *Expert Opin. Biol. Ther.* **2012**, *12*, 757-766.

(320) Xie, J.; Xie, Q.; Zhang, H.; Ameres, S. L.; Hung, J.-H.; Su, Q.; He, R.; Mu, X.; Ahmed, S.; Park, S.; Kato, H.; Li, C.; Mueller, C.; Mello, C. C.; Weng, Z.; Flotte, T. R.; Zamore, P. D.; Gao, G. MicroRNA-regulated, systemically delivered rAAV9: a step closer to CNS-restricted transgene expression. *Molecular therapy : the journal of the American Society of Gene Therapy* **2011**, *19*, 526-535.

(321) Gray, S. J.; Blake, B. L.; Criswell, H. E.; Nicolson, S. C.; Samulski, R. J.; McCown, T. J. Directed Evolution of a Novel Adeno-associated Virus (AAV)

Vector That Crosses the Seizure-compromised Blood–Brain Barrier (BBB). *Molecular Therapy* **2010**, *18*, 570-578.

(322) Petrs-Silva, H.; Dinculescu, A.; Li, Q.; Min, S.-H.; Chiodo, V.; Pang, J.-J.; Zhong, L.; Zolotukhin, S.; Srivastava, A.; Lewin, A. S.; Hauswirth, W. W. High-efficiency Transduction of the Mouse Retina by Tyrosine-mutant AAV Serotype Vectors. *Mol Ther* **2008**, *17*, 463-471.

(323) Dalkara, D.; Byrne, L. C.; Klimczak, R. R.; Visel, M.; Yin, L.; Merigan, W. H.; Flannery, J. G.; Schaffer, D. V. In Vivo–Directed Evolution of a New Adeno-Associated Virus for Therapeutic Outer Retinal Gene Delivery from the Vitreous. *Science Translational Medicine* **2013**, *5*, 189ra176.

(324) Zhong, L.; Li, B.; Mah, C. S.; Govindasamy, L.; Agbandje-McKenna, M.; Cooper, M.; Herzog, R. W.; Zolotukhin, I.; Warrington, K. H.; Weigel-Van Aken, K. A.; Hobbs, J. A.; Zolotukhin, S.; Muzyczka, N.; Srivastava, A. Next generation of adeno-associated virus 2 vectors: Point mutations in tyrosines lead to high-efficiency transduction at lower doses. *Proceedings of the National Academy of Sciences of the United States of America* **2008**, *105*, 7827-7832.

(325) Pulicherla, N.; Shen, S.; Yadav, S.; Debbink, K.; Govindasamy, L.; Agbandje-McKenna, M.; Asokan, A. Engineering Liver-detargeted AAV9 Vectors for Cardiac and Musculoskeletal Gene Transfer. *Mol Ther* **2011**, *19*, 1070-1078.

(326) Muller, O. J.; Kaul, F.; Weitzman, M. D.; Pasqualini, R.; Arap, W.; Kleinschmidt, J. A.; Trepel, M. Random peptide libraries displayed on adeno-associated virus to select for targeted gene therapy vectors. *Nat Biotech* **2003**, *21*, 1040-1046.

(327) Cachon-Gonzalez, M. B.; Wang, S. Z.; Lynch, A.; Ziegler, R.; Cheng, S. H.; Cox, T. M. Effective gene therapy in an authentic model of Tay-Sachs-related diseases. *Proc. Natl. Acad. Sci. U.S.A* **2006**, *103*, 10373-10378.

(328) Sinici, I.; Yonekawa, S.; Tkachyova, I.; Gray, S. J.; Samulski, R. J.; Wakarchuk, W.; Mark, B. L.; Mahuran, D. J. In cellulo examination of a beta-alpha hybrid construct of beta-hexosaminidase A subunits, reported to interact with the GM2 activator protein and hydrolyze GM2 ganglioside. *PLoS One* **2013**, *8*, e57908.

(329) Ghosh, A.; Yue, Y.; Duan, D. Efficient Transgene Reconstitution with Hybrid Dual AAV Vectors Carrying the Minimized Bridging Sequences. *Human Gene Therapy* **2011**, *22*, 77-83.

(330) Yla-Herttuala, S. Endgame: Glybera Finally Recommended for Approval as the First Gene Therapy Drug in the European Union. *Mol Ther* **2012**, *20*, 1831-1832.

- (331) Valdmanis, P. N.; Lisowski, L.; Kay, M. A. rAAV-Mediated Tumorigenesis: Still Unresolved After an AAV Assault. *Mol Ther* **2012**, *20*, 2014-2017.
- (332) Rosas, L. E.; Grieves, J. L.; Zaraspe, K.; La Perle, K. M. D.; Fu, H.; McCarty, D. M. Patterns of scAAV Vector Insertion Associated With Oncogenic Events in a Mouse Model for Genotoxicity. *Mol Ther* **2012**, *20*, 2098-2110.
- (333) Koeberl, D. D. Vector-related Tumorigenesis Not Found in Ornithine Transcarbamylase-deficient Mice. *Mol Ther* **2006**, *14*, 1-2.
- (334) Kay, M. A. AAV vectors and tumorigenicity. *Nat Biotech* **2007**, *25*, 1111-1113.
- (335) Zhong, L.; Malani, N.; Li, M.; Brady, T.; Xie, J.; Bell, P.; Li, S.; Jones, H.; Wilson, J. M.; Flotte, T. R.; Bushman, F. D.; Gao, G. Recombinant Adeno-Associated Virus Integration Sites in Murine Liver After Ornithine Transcarbamylase Gene Correction. *Human Gene Therapy* **2013**, *24*, 520-525.
- (336) Russell, D. W. AAV Vectors, Insertional Mutagenesis, and Cancer. *Mol Ther* **2007**, *15*, 1740-1743.
- (337) Chandler, R. J.; LaFave, M. C.; Varshney, G. K.; Trivedi, N. S.; Carrillo-Carrasco, N.; Senac, J. S.; Wu, W.; Hoffmann, V.; Elkahloun, A. G.; Burgess, S. M.; Venditti, C. P. Vector design influences hepatic genotoxicity after adeno-associated virus gene therapy. *The Journal of Clinical Investigation* **2015**, *125*, 0-0.
- (338) Asokan, A.; Pulicherla, N.: Viral vectors with modified transduction profiles and methods of making and using the same. Google Patents, 2014.
- (339) von Kalle, C.; Deichmann, A.; Schmidt, M. Vector Integration and Tumorigenesis. *Human gene therapy* **2014**, *25*, 475-481.
- (340) Wang, Z.; Lisowski, L.; Finegold, M. J.; Nakai, H.; Kay, M. A.; Grompe, M. AAV Vectors Containing rDNA Homology Display Increased Chromosomal Integration and Transgene Persistence. *Mol Ther* **2012**, *20*, 1902-1911.